Departament d'Ecologia

Universitat de Barcelona

CLIMATE and ATMOSPHERIC CO_2 EFFECTS on IBERIAN PINE FORESTS assessed by TREE-RING CHRONOLOGIES and their potential for CLIMATIC RECONSTRUCTIONS

Efectes del clima i del CO_2 atmosfèric en pinedes ibèriques avaluats mitjançant cronologies d'anells dels arbres i el seu potencial per reconstruir el clima

Laia Andreu Hayles

PhD DISSERTATION

RESULTS

CHAPTER 1

Paper published in:

Global Change Biology (2007) **13**, 804–815, doi: 10.1111/j.1365-2486.2007.01322.x

Title: **CLIMATE INCREASES REGIONAL TREE-GROWTH VARIABILITY IN IBERIAN PINE FORESTS**

Authors: Laia Andreu*, Emilia Gutiérrez*, Marc Macias*[†], Montse Ribas*, Oriol Bosch* and J. Julio Camarero[‡]

*Departament d'Ecologia, Universitat de Barcelona, Avinguda Diagonal 645, 08028 Barcelona, Spain; [†]Department of Geology, Faculty of Science, University of Helsinki, Gustaf Hällströminkatu, 2, 00014 Finland; [‡]ARAID, Instituto Pirenaico de Ecología, CSIC Avda. Montañana, 1005 Zaragoza 50192, Spain.

Global Change Biology (2007) **13,** 804–815, doi: 10.1111/j.1365-2486.2007.01322.x

Climate increases regional tree-growth variability in Iberian pine forests

LAIA ANDREU*, EMILIA GUTIÉRREZ*, MARC MACIAS*†, MONTSE RIBAS*, ORIOL BOSCH* and J. JULIO CAMARERO‡

*Departament d'Ecologia, Universitat de Barcelona, Avinguda Diagonal 645, 08028 Barcelona, Spain, †Department of Geology, Faculty of Science, University of Helsinki, Gustaf Hällströminkatu, 2, 00014 Finland, ‡ARAID, Instituto Pirenaico de Ecología, CSIC Avda. Montañana, 1005 Zaragoza 50192, Spain

Abstract

Tree populations located at the geographical distribution limit of the species may provide valuable information about tree-growth response to changes on climatic conditions. We established nine *Pinus nigra*, 12 *P. sylvestris* and 17 *P. uncinata* tree-ring width chronologies along the eastern and northern Iberian Peninsula, where these species are found at the edge of their natural range. Tree-growth variability was analyzed using principal component analysis (PCA) for the period 1885–1992. Despite the diversity of species, habitats and climatic regimes, a common macroclimatic signal expressed by the first principal component (PC1) was found. Moreover, considering the PC1 scores as a regional chronology, significant relations were established with Spanish meteorological data. The shared variance held by the tree chronologies, the frequency of narrow rings and the interannual growth variability (sensitivity) increased markedly during the studied period. This shows an enhancement of growth synchrony among forests indicating that climate might have become more limiting to growth. Noticeably, an upward abrupt shift in common variability at the end of the first half of the 20th century was detected. On the other hand, moving-interval response functions showed a change in the growth–climate relationships during the same period. The relationship between growth and late summer/autumn temperatures of the year before growth (August–September, negative correlation, and November, positive correlation) became stronger. Hence, water stress increase during late summer previous to tree growth could be linked to the larger growth synchrony among sites, suggesting that climate was driving the growth pattern changes. This agrees with the upward trend in temperature observed in these months. Moreover, the higher occurrence of extreme years and the sensitivity increase in the second half of the 20th century were in agreement with an increment in precipitation variability during the growing period. Precipitation variability was positively related to tree-growth variability, but negatively to radial growth. In conclusion, a change in tree-growth pattern and in the climatic response of the studied forests was detected since the mid-20th century and linked to an increase in water stress. These temporal trends were in agreement with the observed increase in warmer conditions and in precipitation variability.

Keywords: climatic variability, dendroclimatology, global warming, growth pattern change, Iberian peninsula, *Pinus nigra*, *P. sylvestris*, *P. uncinata*, species distribution limit, water stress

Received 13 February 2006; revised version received 14 June 2006 and accepted 28 August 2006

Introduction

Climate exerts a strong influence on the geographical distribution of plants through specific physiological thresholds of temperatures and water availability (Woodward, 1987). At the end of the 20th century many changes in phenology, distribution areas, ecological amplitude, community composition and dynamics were observed (Menzel & Fabian, 1999; Chapin *et al*., 2000; Peñuelas & Filella, 2001; Walther *et al*., 2002; Peñuelas & Boada, 2003). Significant links between

Correspondence: Laia Andreu Hayles, tel. +34 93 402 15 08, fax +34 93 411 14 38, e-mail: laiandreu@ub.edu

these phenomena and the current climatic change have been established (Parmesan & Yohe, 2003; Root *et al*., 2003). Modeling efforts have been made to assess the impacts of global change on species distribution. Some calculations pointed out Spain as one of the regions with the most dramatic future species losses (Bakkenes *et al*., 2002). Moreover, special caution was recommended for species growing close to their distribution limits due to the failure of models to collect the complete suitable environmental range (Thuiller, 2003).

Frequently, climate becomes highly limiting to physiological processes for tree species at the edge of their natural range, because trees on these sites are particularly susceptible to climatic variations (Fritts, 1976). Our study was carried out in the Iberian Peninsula with three species located at the edge of their phytogeographical distribution area: *Pinus sylvestris* L., *P. uncinata* Ramond ex. DC and *P. nigra* Arnold subsp. *salzmannii*. The first two species, which are Eurosiberian, find in the Iberian Peninsula their southern and western distribution limit; while the latter, a typical Mediterranean pine, finds its western boundary. Distribution of the forests in the Iberian Peninsula is highly determined by the Atlantic and Mediterranean climatic influences. However, most forests are restricted to the mountainous areas where relief causes important variations to the regional climate (Blanco *et al*., 1997; Barbéro *et al*., 1998).

Annual temperatures over Europe have increased about 0.8 °C during the 20th century. A larger warming has been observed over the Iberian Peninsula (IPCC, 2001), where the 1980–1995 period was characterized by intense droughts, which produced severe damage to several woody species (Peñuelas *et al*., 2001). There has also been an increment in the mean of fire hazard indices and in the number of very high-risk days (Piñol *et al*., 1998). In general terms, exceptionally high temperatures and a great interannual climatic variability have characterized climate in the Iberian Peninsula during the second half of 20th century (Font Tullot, 1988; Romero *et al*., 1998; De Luis *et al*., 2000; IPCC, 2001; Giorgi *et al*., 2004).

We hypothesized that warming and climatic variability produced changes in tree-growth patterns, as well as in the climate response of Iberian pine forests. To answer this question, we established a network of 38 pine ring-width chronologies along eastern and northern Iberian Peninsula. Climate research generally encompasses much larger spatial and temporal scales than most ecological research studies which are local and short-term (Walther *et al*., 2002). In this context, dendroecological studies are valuable for examining long-term natural responses of plants because the length of tree-ring series provides an extended context to assess changes in tree growth (Knapp *et al*., 2001). The aims of this study were: (a) to detect the macroclimatic signal shared by all the chronologies; (b) to analyze temporal variability of radial growth and the possible climatic drivers; and (c) to assess growth–climate relationships and their stability throughout time.

Material and methods

Sampling sites and procedures

Sixty-one forest stands were initially sampled. At each site, a minimum of 15 trees were cored with an increment borer at 1.30 m high. At least two cores were taken from each tree. Sampling was focused on the oldest natural forest stands in the area. Isolated trees or trees growing in open forests were preferred to trees from dense forests. Site characteristics of the 38 selected sites (see below, chronology selection criteria) are described in Table 1A.

Chronology building

Cores were mounted and sanded until cells were clearly visible under a binocular microscope (Stokes & Smiley, 1968). All samples were visually cross-dated to avoid miscounting by missing (locally absent) or false (double) rings with the procedures described by Yamaguchi (1991). Afterwards, ring widths were measured with an accuracy of 0.01 mm using an ANIOL measuring device (Dendroware ANIOL, Schleswig, Germany) (Aniol, 1983). The resulting measured series underwent a cross-dating quality control with the statistical program COFECHA (Holmes, 1983).

The best series from each stand were selected after discarding: (a) series with abrupt growth changes in the raw data and (b) series poorly correlated with the master chronology. Then, individual series were standardized applying a spline function with a 50% frequency response of 32 years (Cook & Peters, 1981). Standardization involved transforming the ring-width value into a dimensionless index by dividing the observed by the expected values given by the spline function (Fritts, 1976). An autoregressive model was applied to remove the autocorrelation related to the previous year growth. A robust mean, which reduces the variance and bias caused by extreme values, was computed. As a result, an estimation of the common signal of all the series was obtained: the ring width chronology. Sixty-one residual chronologies were developed following this procedure using the program ARSTAN (Cook, 1985).

Chronology selection was based on two criteria: (1) reliability based on the expressed population signal criteria (EPS > 0.85, Wigley *et al*., 1984); and (2) lack of

Table 1 (A) Geographic features of the study sites. (B) Chronology characteristics*

(A) Sites				(B) Chronologies							
Site ID	Latitude	Longitude	Altitude (m)	Time span	Mean years	No. trees	No. radii	ms_x	r	Reliable time span	EPS 1885–1992
Pinus nigra											
n1	42°32′N	00°09′E	700	1819–1999	130.2	15	30	0.348	0.678	1862–1999	0.927
n2	40°07′N	01°05′W	1450	1585–1993	262	25	28	0.275	0.498	1751–1993	0.916
n3	37°48′N	02°57′W	1800	1331–2002	299.8	20	31	0.262	0.682	1602–2002	0.943
n4	40°35′N	01°47′W	1500	1817–1999	158.4	15	24	0.329	0.771	1822–1999	0.964
n5	40°17′N	00°32′W	1150	1856–1999	128.1	15	29	0.302	0.646	1866–1999	0.908
n6	37°15′N	02°30′W	1850	1653–1999	142.4	9	16	0.286	0.59	1884–1999	0.851
n7	40°40′N	00°03′W	1250	1844–1999	134.9	12	20	0.297	0.69	1853–1999	0.926
n8†	38°08′N	02°41′W	1620	1609–1994	282.4	16	23	0.292	0.514	1777–1994	0.832
n9	40°20′N	01°55′W	1370	1637–1995	260.5	16	20	0.269	0.569	1766–1995	0.879
P. sylvestris											
s1†	42°19′N	00°26′W	1450	1830–1999	102.8	16	32	0.317	0.647	1889–1999	0.801
s2†	40°48′N	00°21′E	1250	1800–2000	130.8	13	25	0.234	0.508	1897–1998	0.829
s3	42°28′N	00°29′E	1540	1786–1999	163.1	7	14	0.312	0.645	1885–1999	0.856
s4	42°48′N	00°22′W	1890	1713–1993	220.8	17	24	0.201	0.578	1798–1993	0.887
s5	43°04′N	05°15′W	1650	1633–2002	252.6	16	30	0.267	0.62	1767–2002	0.913
s6	40°14′N	00°20′W	1500	1844–2000	135.8	15	29	0.279	0.65	1855–2000	0.923
s7	41°20′N	01°01′E	950	1861–1999	78.1	18	31	0.35	0.682	1885–1992	0.857
s8	42°33′N	00°54′E	1888	1747–1995	141.6	17	36	0.27	0.624	1855–1995	0.902
s9	40°28′N	01°34′W	1645	1824–1999	123.3	14	26	0.34	0.723	1843–1999	0.917
s10	42°36′N	01°06′E	1450	1772–1999	113.2	15	37	0.294	0.643	1825–1999	0.853
s11	41°58′N	02°49′W	1750	1677–1999	196.3	14	24	0.21	0.571	1801–1999	0.865
s12	42°43′N	00°29′W	1750	1676–1993	242.3	12	16	0.257	0.578	1780–1993	0.853
P. uncinata											
u1	42°42′N	01°02′E	2390	1677–1996	170.1	14	24	0.177	0.638	1771–1996	0.921
u2	42°36′N	00°59′E	2334	1663–1995	206.7	13	25	0.186	0.616	1782–1995	0.899
u3	42°43′N	00°11′E	1890	1707–1996	197.8	9	18	0.265	0.632	1826–1996	0.862
u4	42°38′N	00°45′E	2160	1537–1994	213.8	19	32	0.192	0.546	1861–1994	0.864
u5	42°34′N	00°57′E	2210	1509–1995	252.2	21	42	0.198	0.575	1721–1995	0.923
u6	42°33′N	01°04′E	2078	1447–1996	344.5	11	20	0.182	0.533	1831–1996	0.851
u7	42°41′N	00°05′E	2000	1653–1993	218.5	17	24	0.202	0.55	1751–1992	0.885
u8	42°57′N	00°47′W	1750	1572–1999	266	16	31	0.235	0.558	1756–1999	0.899
u9	42°32′N	00°55′E	2135	1338–1997	249.7	31	59	0.167	0.581	1700–1995	0.929
u10	42°38′N	00°04′W	1900	1795–1998	156	17	34	0.22	0.583	1845–1998	0.891
u11	42°23′N	02°08′E	2075	1681–2001	177.5	20	37	0.176	0.541	1875–2001	0.884
u12	42°27′N	01°37′E	2350	1677–1997	195.5	20	39	0.193	0.602	1787–1997	0.916
u13	42°24′N	02°17′E	2080	1764–1999	150.5	11	19	0.199	0.568	1877–1998	0.851
u14	42°35′N	01°00′E	1933	1811–1996	163.7	20	40	0.221	0.7	1821–1996	0.946
u15	40°30′N	00°25′W	1890	1642–1996	242.4	22	33	0.214	0.588	1779–1996	0.897
u16	42°36′N	01°03′E	2290	1716–1995	187.2	17	19	0.17	0.537	1818–1995	0.911
u17	42°00′N	02°45′W	1950	1752–1999	189.9	17	32	0.177	0.571	1794–1994	0.896

*Time span; mean years is the average of the number of years measured in each core and gives an underestimated value of the mean age of the trees; number of trees; number of radii; interannual variability or mean sensitivity index (ms_x); mean correlation of all series with the master chronology (r); reliable time span (EPS > 0.85); and EPS value for the studied period (1885–1992).
†See 'Methodology'.
EPS, expressed population signal.

evidence of past management practices. The EPS is a statistic that quantifies the common variability present in all tree-ring series at a particular site. It expresses the proportion between the common variance of the trees (signal) and the total variance (signal + noise). All the trees in a stand are affected by the same set of climatic variables, so common information could be regarded as climatic information (Cook & Briffa, 1990). Eventually,

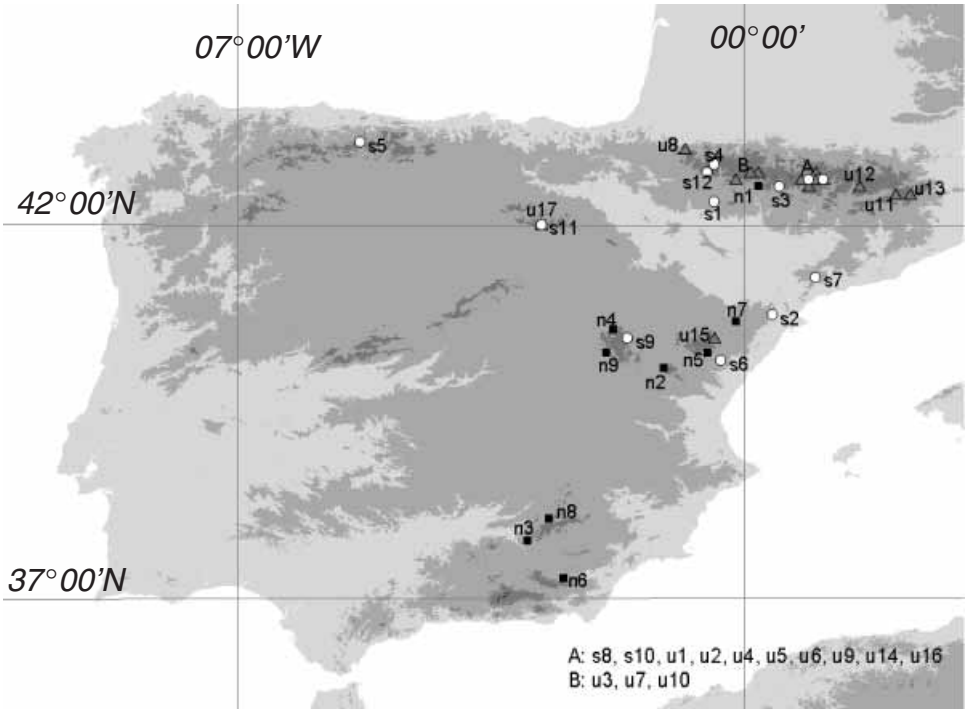

Fig. 1 Geographical position of the selected sites in the Iberian Peninsula. *Pinus nigra* stands are represented by black squares, *P. sylvestris* by white circles and *P. uncinata* by gray triangles. The A and B letters represent groups of chronology geographically closed.

38 chronologies were selected with a common time-span from 1885 to 1992 (Fig. 1). Three of them were chosen with an EPS between 0.80 and 0.85 because their quality was still good enough and all were reliable at least from 1897. These chronologies were kept due to the singularity of their location in order to achieve a better and more representative coverage of *P. nigra* and *P. sylvestris* distribution area. Descriptive statistics are presented (Table 1B) to allow comparisons among sites with other dendroclimatic data sets (Fritts, 1976; Cook & Briffa, 1990). A possible age effect was discarded in the temporal analyses of tree-growth variability and in the study of the radial growth–climate relationship stability following Carrer & Urbinati (2004) analyses procedures (results not shown).

Tree-growth variability

A principal component analysis (PCA) based on the correlation matrix was calculated for the common period 1885–1992 to evaluate the shared variance of the chronology network. PCAs also were computed separately by species: 9, 12 and 17 chronologies of *P. nigra*, *P. sylvestris* and *P. uncinata*, respectively. The broken stick test was performed to determine the significance of the components (Holmes, 1992). PCAs with all chronologies were computed for successive periods of 38 years lagged 5 years from 1885 to 1992 in order to evaluate the temporal changes of this shared variability. The use of 38-year periods was necessary because the number of observations (years) must be greater or equal to the number of variables (chronologies). The variance explained by the first principal component (PC1) was used as indicator of the similarity among the chronologies.

In order to analyze tree-growth variability, years with extreme growth values (± 1.645 SD, $P < 0.1$) were identified and the annual sensitivity (s_x) was also calculated for each chronology. The s_x constitutes the relative difference from one ring-width index to the next. Sensitivity was calculated based on the formula $s_x = |I_{t+1} - I_t| 2/(I_{t+1} + I_t)$, where I_t is the index value for the year t (Fritts, 1976). Next, all s_x series were averaged. To assess s_x trends, the mean (ms_x) and the standard deviation (SDs_x) were computed for 38-year periods 5 years lagged. The frequency of chronologies showing extremely low (<1.645 SD) and high (>1.645 SD) indices and the temporal trends of s_x will reveal periods of lower or higher climatic influence (Tardif *et al.*, 2003).

Meteorological data

The meteorological data used were the monthly average temperature and total precipitation of Spain from TYN

CY 1.1 data set (Mitchell *et al.*, 2003). The country aggregation is based on the CRU TS 2.0 gridded data set. The gridded data were aggregated into countries using political boundaries (Mitchell *et al.*, 2001). A complete analysis of climate trends in mean values and in variability [using the variation coefficient (VC)] was done. The VC, the ratio between 100 SD and the mean (Sokal & Rohlf, 1969), is a standardized measure of data variability. Monthly temperature and precipitation VC series were calculated yearly, as well as using intervals of 38 years lagged 5 years in order to make these series comparable to the tree-growth variability results.

Tree growth–climate relationship

Correlation and response function analyses were performed using the program Dendroclim2002 (Biondi & Waikul, 2004) to quantify the climate–growth relationships between the regional chronology (PC1) and the Spanish climate series (monthly mean temperature and precipitation data) from 1902 to 2000. The same analyses were done for the PC1 scores of each species PCA.

In order to avoid the problem of multicollinearity, commonly found in multivariable sets of meteorological data, a stepwise multiple regression was computed on principal components to assess climate–growth relationships (response function; Fritts, 1976). The significances of the calculated partial regression coefficients were estimated based on 1000 bootstrapped estimates obtained by random extraction with replacement from the initial data set (Guiot, 1991). Climate–growth relationships were analyzed from the previous July up to October of the growth year.

Response functions were performed considering a 38-year fixed interval, increasing the initial and final years of the analyses by one for each iteration (Biondi, 1997, 2000). Because we used intervals of 38 years, the moving response functions had to be done separately for precipitation and temperature due to a lack of degrees of freedom corresponding to such a short period. Consequently, changes in the growth–climate relationship throughout time had to be assessed using bootstrapped correlation values. However, response function analyses were performed for two periods (1902–1949 and 1945–1992) to check that the change in the significance of the correlations was in agreement with the significance of the response function coefficients.

Results

The common variance

The PC1 and the second PC (PC2) of the chronology network PCA were significant, representing 32.5% and 13.6% of the total variance, respectively. The scatter plot of the PCA loading coefficients displayed groups of chronologies with similar growth patterns (Fig. 2). Although the chronologies showed different loadings with the PC1, all of them had positive correlations with it, showing that they shared a common variance. *P. sylvestris* chronologies were scattered, covering nearly all the range of the first axis values, most of them being in an intermediate position between *P. nigra* and *P. uncinata*. On the other hand, *P. sylvestris* and *P. nigra* chronologies were mainly positively correlated with the second PC, while most of *P. uncinata* chronologies were negatively correlated with it. When PCA was computed by groups of chronologies depending on species (*P. nigra*, *P. sylvestris* and *P. uncinata*), the first axes appeared significant (41%, 39.4% and 53.4%). In contrast, the second eigenvectors were not significant (13.5%, 14.8% and 8.7%; graphs not shown).

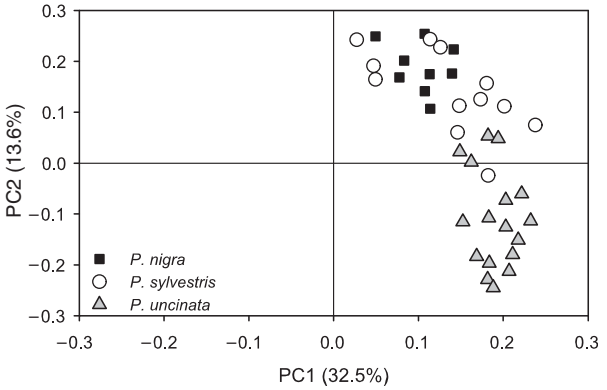

Fig. 2 Scatter plots of principal component analysis (PCA) loadings of the 38 chronologies for the period 1885–1992. Species symbols as in Fig. 1.

Temporal trends of the common variance

Figure 3 shows the evolution of the explained variance of the PC1 (i.e. the common variance among the chronologies involved in the PCA). The common variability of the chronologies showed a significant increase along the 20th century (as the fitted linear regression was highly significant, $P = 0.0001$). Moreover, an abrupt shift around the end of the first half of the century was observed. The variance explained by the PC1 increased from 28.73% in the '1925–1962' interval to 35.96% in the '1930–1967' interval (around 1949). This abrupt shift represented the maximum increment for all the studied period.

Tree-growth variability through time

The yearly relative frequency of chronologies with extreme growth indices is shown in Fig. 4. Since the

1950s, narrow tree-rings have been more frequently registered in comparison with the preceding period. This phenomenon was confirmed by sensitivity, which showed a sustained rise along the 20th century. Figure 5a shows a significant increase in ms_x and SDs_x trends along the 20th century, as the linear regressions fitted were significant. The SDs_x suffered an abrupt shift at the '1930–1967' period, showing a much greater variability of the sensitivity in the second half of the 20th century. The SDs_x shift occurred at the same period as the shift in the variance explained by PC1.

Trends in meteorological data

Figure 6 shows recent trends in monthly mean temperature and total precipitation, as well as in their VC. The slopes of the linear regressions fitted on the series (b in $y = a + bx$) were plotted to assess the significance of the trends. There were significant increases ($P < 0.01$) in annual and monthly mean temperature, but no significant trend in temperature VC series was detected (Fig. 6a). Concerning precipitation (Fig. 6b), although there was a significant ($P < 0.05$) decrement and increment in March and August precipitation, respectively, annual total precipitation did not present any trend. In contrast, significant increases in annual precipitation VC, as well as in September and October precipitation VC were found.

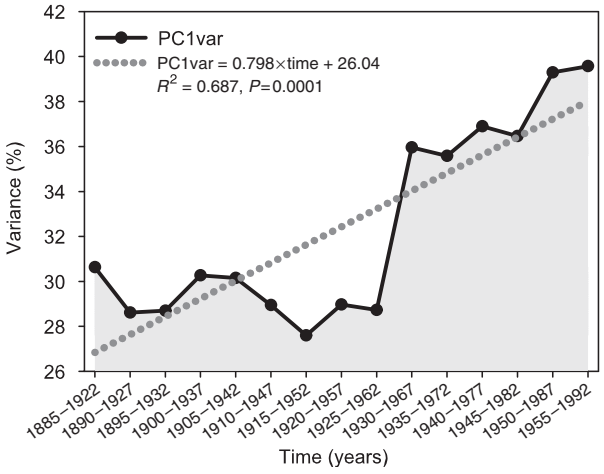

Fig. 3 Change of the variance explained by the first principal component (PC1var) using subintervals of 38 years lagged 5 years.

Radial growth response to climate

Considering the PC1 scores of the chronology network as a regional chronology for the studied area, climate–tree growth relationships were established between the PC1 and the Spanish climatic series (Fig. 7). The regional chronology showed significant responses to the climate conditions of the current summer, as well as to the late summer before the growth year. Tree growth showed significant ($P < 0.05$) response function coefficients to previous September (negative) and previous November (positive) temperatures. On the other hand, radial growth was positively correlated with July precipitation of current growth year. Correlation coefficients were also significantly negative and positive for prior August temperature and current June precipitation, respectively.

Correlation and response functions performed with the PC1 of each species showed that the three species shared the observed general pattern (Fig. 7), despite the own particular features of each one (results not shown). *P. sylvestris* and *P. uncinata* responded negatively to September and positively to November temperature. Although *P. nigra* also had the same significant correlation values with those

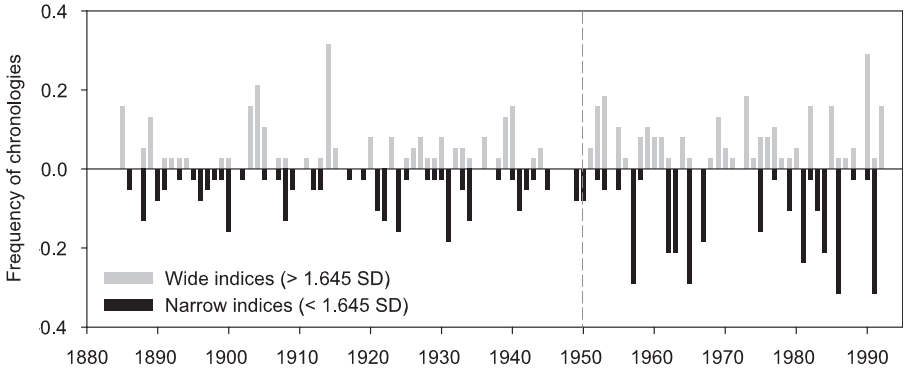

Fig. 4 Relative frequency of chronologies with wide (>1.65 SD) and narrow (<1.65 SD) ring-width residual chronology indices during the period 1885–1992.

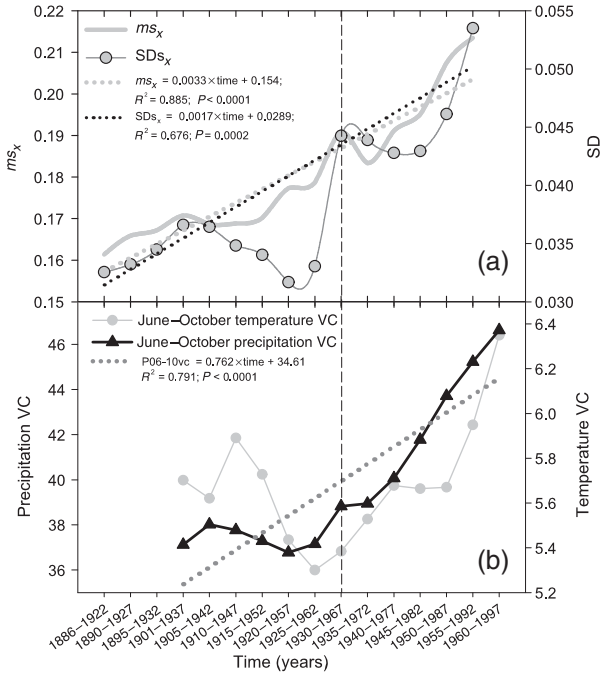

Fig. 5 (a) Temporal trends in the mean sensitivity (ms_x; gray line) and the standard deviation sensitivity (SDs_x; line with gray circles) using subintervals of 38 years lagged 5 years. (b) Temporal trends in precipitation variation coefficient (VC) from June to October (P06-10vc: black line with black triangles) and in temperature VC for the same period (gray line with gray circles).

months, the significant response function coefficients indicated that for this species growth was more affected by October temperature (negatively) and December and February temperature (positively). Concerning precipitation, July response function coefficients were significantly positive for the three species, while June was only significantly positive for *P. nigra* and *P. sylvestris*.

Radial growth response to climate through time

Figure 8 shows the evolution of the correlation values of three variables that were significant for both correlation and response function analyses (previous September and November temperature and current July precipitation). In addition, correlation values with prior August temperatures and current June precipitation (not significant for response function) are also displayed for a better understanding of changes in climate–growth relationship.

Our results indicate that the radial growth–climate relationship has varied across time. During the first half of the 20th century, correlation values between radial growth and September and November temperature previous to the growth year were negative and positive, respectively, but not significant. However, both became significant ($P<0.05$) at the '1930–1967' period (around 1949). Correlations with August temperatures became significant some years earlier than with September, but lost its significance at the end of the studied period. Conversely, radial growth correlation with current July precipitation remained stable throughout the century, while June precipitation was significant only at the beginning of the first half of the 20th century (Fig. 8c).

The three species shared the trends of prior August–September temperature and current July precipitation. However, positive correlation with summer precipitation (June and July) achieved higher values in the case of *P. nigra* and *P. sylvestris*. On the other hand, *P. uncinata* clearly showed the prior November temperature trend, while the other species did not (results not shown).

The change in the significance of the correlations along the 20th century (Fig. 8) was in agreement with the results of the response function analyses performed for two periods (1902–1949) and (1945–1992). Prior September and November temperature and current July precipitation only had significant response function values in the second period. In the first period, response coefficients of current July precipitation were also high, but very low values were found for prior September and November temperatures. In contrast, during the growth year high coefficients were found for June temperature and precipitation (results not shown).

Precipitation variability

Figure 5b shows the precipitation VC during the growing period (from June to October, according to the correlation and response function results, Fig. 7). A significant increase in the precipitation VC was detected along the 20th century, shown by the significance ($P<0.0001$) of a fitted linear regression. The temperature VC during the growing period, one order of magnitude below precipitation VC, presented a slight increase since the second half of the 20th century. However, this increase was not significant.

The relationship between the growing period precipitation VC and the annual sensitivity (s_x) is shown in Fig. 9a, whereas Fig. 9b shows its relationship with the regional chronology (PC1 scores). PC1 was significant and negatively related to June–October precipitation VC, while s_x was significant and positively related to it.

Discussion

The macroclimatic signal

Our chronologies were built from a wide range of forests considering that three different species were

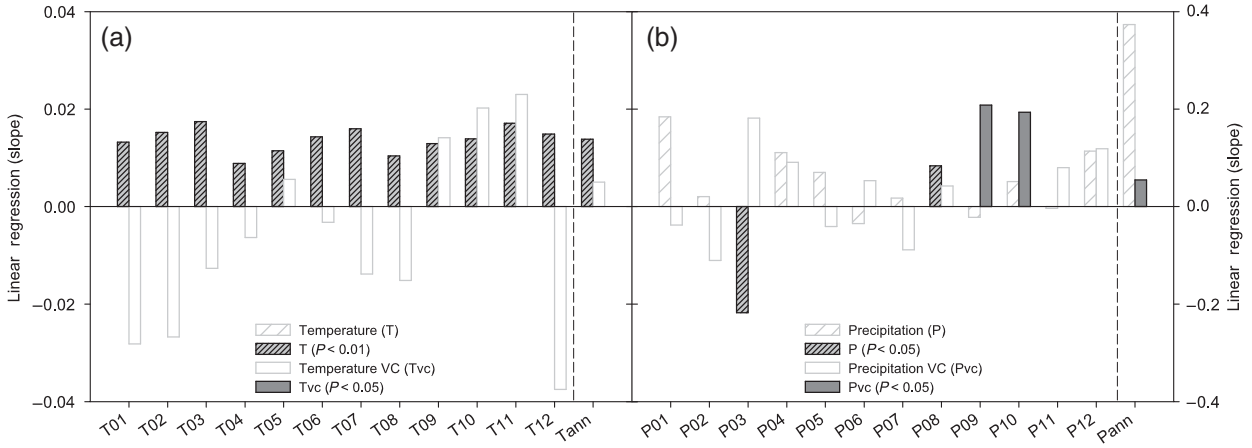

Fig. 6 Recent trends (slope of the linear regression; b in $y = a + bx$) in annual and monthly mean temperature and total precipitation, as well as in temperature variation coefficient (VC) and precipitation VC series.

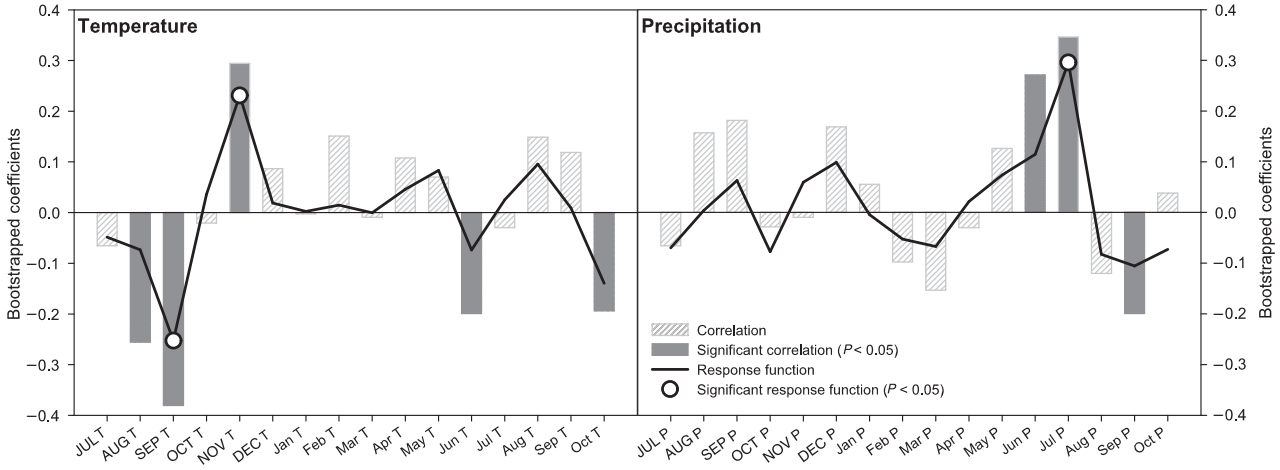

Fig. 7 Bootstrapped correlations (bars) and response functions (lines) performed between the first principal component (PC1) and monthly climate data from prior July to current October. Capitals: prior year months; lowercase: current year months. Significant correlation and response function coefficients ($P < 0.05$) are indicated with gray bars and white circles, respectively.

sampled in sites with different features and under different climatic influences. Despite all those factors, the PC1 contained a significant percentage of common variance shared by all the chronologies (Fig. 2). One of the main dendrochronological principles is the assumption that common information shared among trees in a stand could be regarded as climatic information. On a broader scale, the common variability shared by the 38 chronologies across the Iberian Peninsula should be caused by climate. Macroclimate seems the only reliable factor that could be influencing all these chronologies spread along the north and east of the Peninsula. Although our main result was the finding of a common climatic signal, tree-growth similarities among chronologies of the same species also were observed, as well as dissimilarities among chronologies of different species. Other authors have reported similar results (Gutiérrez, 1990; Schweingruber *et al*., 1991 in Tessier *et al*., 1997).

Temporal variability of radial growth

The variance held in common by the tree chronologies (macroclimatic signal) was not stable throughout time: it increased markedly during the studied period (Fig. 3). A maximum upward increment around the end of the first half of the 20th century ('1930–1967' interval) drew a clear shift between the two halves of the century. Up to a certain threshold, similarities among chronologies should increase under more limiting climatic conditions

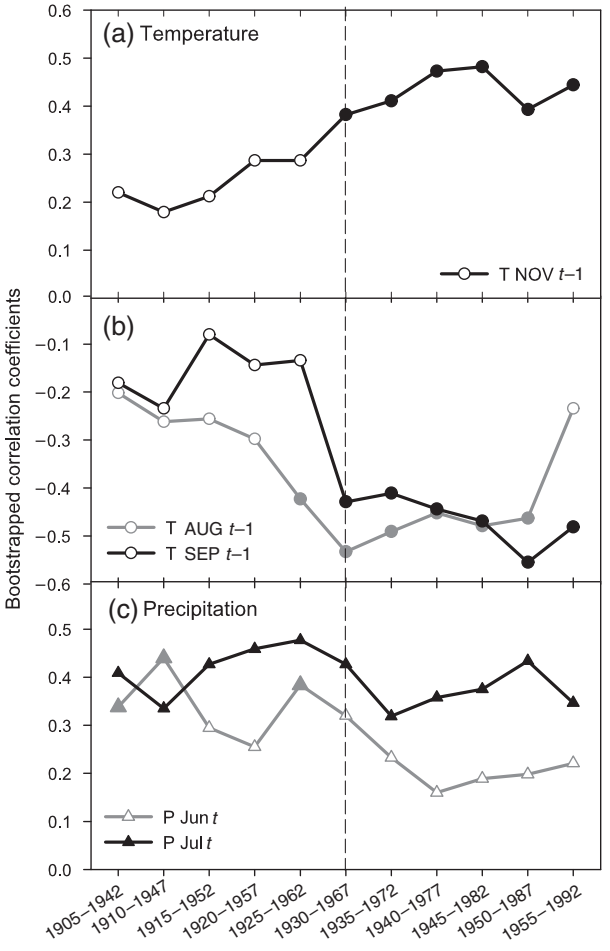

Fig. 8 Temporal changes in bootstrapped correlation coefficients using intervals of 38 years lagged 5 years of previous November temperature (a); August and September temperature before ring formation (b); and current June and July precipitation (c). Filled symbols: significant correlation coefficients ($P<0.05$).

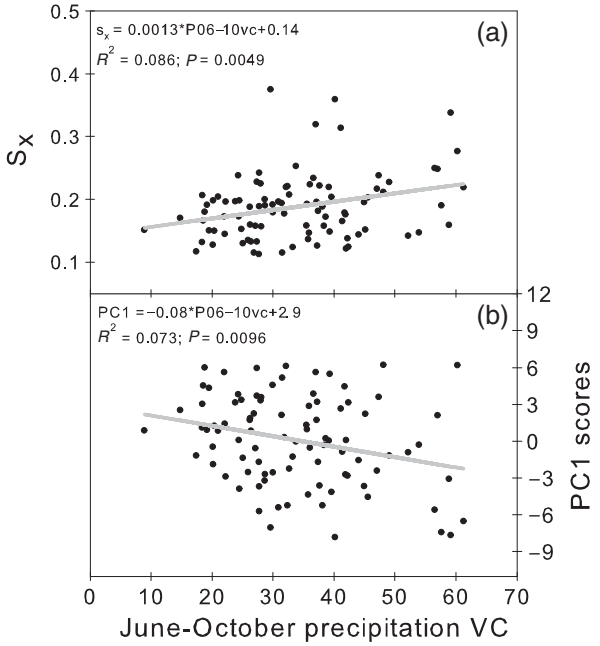

Fig. 9 (a) Relationship between annual sensitivity (s_x) and June to October precipitation variation coefficient (VC) (P06-10vc). (b) Relationship between PC1 scores and June to October precipitation VC (P06-10vc).

(Tardif *et al*., 2003). Shared growth variability can be interpreted as a common response to regional climatic signals (Tardif *et al*., 2003; Macias *et al*., 2004), and its changes along the 20th century as a signal of climatic changes which have affected the growth of the forests (Macias *et al*., 2006). Therefore, a higher common variance indicates that the sampled forests were growing more synchronously in the second half of the 20th century, suggesting that climate has become more limiting to growth.

Similarly, the frequency of narrow rings (Fig. 4), as well as interannual growth variability (Fig. 5a) also rose along the 20th century. The increment in the frequency of extremely narrow rings suggests that during the second half of the 20th century there were more years in which climatic conditions limited tree growth. As a consequence, narrower rings were produced in more forests during these years of unfavorable growing conditions. The dramatic increment of the SDs_x in the '1930–1967' period denotes that not only the ms_x stepped up along the 20th century, but also its variability in the second half was appreciably superior.

Climate conditions might have become more limiting to growth since the mid-20th century, as suggested by increasing similarity among the tree chronologies. Yearly climatic variability has also increased as illustrated by the higher sensitivity and extreme growth indices recorded by the trees. Thus, growth pattern changes of three different species have been detected in the Iberian Peninsula supporting the idea that climate is the main cause because nonclimatic explanations decline at increasing spatial scale and species number (Parmesan & Yohe, 2003). The significant increases observed in monthly mean temperatures and in annual precipitation variability (Fig. 6) could have been some of the climatic factors limiting growth in the second half of the 20th century. However, the establishment of climate–growth relationships is essential to set up a significant link between the growth pattern change and climate.

Climate–growth relationship

Pine forests response to summer drought seems to be general for the three species as inferred from the

response functions. Radial growth was constrained by water stress during summer previous to growth, as suggested by the negative relationship with previous September temperature, and to a lesser degree, by a positive relationship with precipitation at the end of the summer (Fig. 7). Our results reveal that warm late summers can prolong the growing season, limiting the formation of metabolic reserves and consequently affecting radial growth in the following year (Fritts, 1976). These results have been corroborated by a previous study of tree-ring phenology and structure in Pyrenees (Camarero *et al*., 1998). On the other hand, July precipitation of current year was positively associated with radial growth, showing that precipitation is crucial during the year of ring formation. *P. sylvestris* and *P. nigra* presented a stronger positive relationship with current June–July precipitation than *P. uncinata*, suggesting that they may be more susceptible to deficits in the water balance. In agreement with these findings, the former species are located in drier sites than *P. uncinata*, which lives at higher elevations, where evapotranspiration is lower. The obtained climate–growth relationships using regional climate series agree with those performed using local climatic series in the Pyrenees (Camarero, 1999; Tardif *et al*., 2003) and the east of Spain (Gutiérrez, 1989; Richter & Eckstein, 1991).

Change in climatic response

Moving interval response functions suggest an extension of the water-stress period from mid-summer to late summer (from August to September temperature) and a strengthening of the climate–growth relationship. Tree-growth has increased its negative correlation with prior September temperature and its positive correlation with prior November temperature along the 20th century (Fig. 8). Moreover, the most remarkable result was that correlation values became significant in the '1930–1967' period (around 1949). This change in the climatic response was produced at the same time that the change in the tree-growth pattern described above. While the evolution of the correlation coefficients with prior August–September temperature was common for the three species, the November temperature correlation trend was particular for *P. uncinata*. Therefore, excluding November temperature, late summer temperatures previous to growth may be the climatic driver of the observed tree-growth pattern change among forests in the Iberian Peninsula, indicating an increase in water stress effects on radial growth during the last half of the 20th century. These findings were in agreement with the significant temperature increases observed in these months (Fig. 6a). Similarly, enhanced *Abies alba* water stress has been reported in northern Spain (Macias *et al*., 2006). Another study in Alaska also pointed out that temperature explained more variability in white spruce radial growth after 1950, suggesting that a true climatic control was involved (Wilmking *et al*., 2004).

Precipitation variability

In agreement with the observed tree-growth pattern (Figs 3, 4 and 5a), precipitation variability during the growing period presented an increasing trend along the 20th century (Fig. 5b). Consistent with our results, Font Tullot (1988) reported in the Iberian Peninsula an increase in the frequency of extreme climatic events (high temperatures, frosts, droughts) in the second half of the 20th century. Other authors have found an increase in climatic anomalies during the last 50 years (Manrique & Fernández-Cancio, 2000). The increment in precipitation variability may induce an increase in common tree-growth variation among the forests, as well as in the tree-growth variability through time. According to this, s_x values were positively related to the precipitation VC of the growing period (Fig. 9a). On the other hand, it is noteworthy the negative effect that precipitation variability may have over tree growth (Fig. 9b), suggesting that climatic variability could also be a factor limiting tree growth. Therefore, our results highlight that two factors could have been limiting radial growth during the second half of the 20th century: (1) an underlying upward trend of mean temperatures that enhances water stress during previous late summer; and (2) an increase in precipitation variability during the growing period. These results agree with the increase in warmer conditions (IPCC, 2001; Giorgi *et al*., 2004) and climatic variability (Font Tullot, 1988; Romero *et al*., 1998; De Luis *et al*., 2000) described in Spain.

Increases in temperature and in the frequency of extreme climatic events are expected in Europe (IPCC, 2001). In this context, the intensification of warming in a longer term could lead to the elimination of drought-susceptible trees (Barber *et al*., 2000) through stress-related mortality (Wilmking *et al*., 2004). On the other hand, extreme weather and climate events have been linked to biological changes (Easterling *et al*., 2000), like for example, a severe drought in 1994 that caused important damages and even mortality in Spanish forests (Martínez-Vilalta & Piñol, 2002; Lloret *et al*., 2004). Considering that we showed that our forests are highly sensitive to warming and climatic variability, new climatic conditions could bring serious consequences for Iberian forests growth dynamics.

Finally, the stability of the significant relationship between current July precipitation and growth highlights the possibility of realistic reconstructions of summer precipitation in Iberian Peninsula using a network

of tree-ring width chronologies. However, special caution is recommended for temperature reconstruction due to the instability of its relationship with radial growth. Similarly, other authors also pointed out that some climate reconstructions based on ring width could miscalibrate past climate (Tardif *et al.*, 2003; Wilmking *et al.*, 2004).

Conclusions

Despite the diversity of species, habitats and climatic regimes, our chronologies shared a common macroclimatic signal expressed by the first PC. The shared variance held by the tree chronologies and the interannual growth variability increased markedly during the studied period. This enhancement of growth synchrony among forests indicates that climate might have become more limiting to tree ring formation. Noticeably, the upward abrupt shift in common variability at the end of the first half of the 20th century happened at the same time as an enhancement of the prior August–September temperature influence over radial growth. Consequently, the greater similarity in tree-growth may be linked to a strengthening of water stress during late summer previous to the ring formation that agrees with the temperature increasing trend observed in these months. Moreover, the higher occurrence of extremely narrow rings and the sensitivity increase coincided with an increment of the precipitation variability during the growing period. Precipitation variability was positively related to tree-growth variability, but negatively to radial growth. Therefore, at least two climatic factors could have been limiting tree growth and driving the observed changes in growth pattern and in climatic response of the studied forest during the second half of the 20th century: the increasing trends observed in mean temperatures and the increment detected in precipitation variability during the growing period.

The absence of temporal stability in some growth–climate relationships may be critical and should be considered for reconstructions of past climatic conditions using tree-ring widths. The analysis of the temporal trends of shared variance among chronologies, as well as other tree ring characteristics should be taken into account to improve the reliability of the reconstructions.

Acknowledgements

We are very grateful to Octavi Planells, Pete Fulé and Salvador Pueyo for the constructive and critical comments; to Elena Muntán for their help during fieldwork and chronology building and to José Creus for his contribution to the ForMAT database. Data were collected during the CICyT Spanish project (Contract AMB95-0160); EU ForMAT project (Contract ENV4-CT97-0641) and EU ISONET project (Contract EV K2-2001-00237). The authors acknowledge two anonymous referees for their suggestions that helped to improve the original version of the paper.

References

Aniol RW (1983) Tree-ring analysis using CATRAS. *Dendrochronolgia*, **1**, 45–53.

Bakkenes M, Alkemade JRM, Ihle F, Leemans R, Latour JB (2002) Assessing effects of forecasted climate change on the diversity and distribution of European higher plants for 2050. *Global Change Biology*, **8**, 390–407.

Barber VA, Juday GP, Finney BP (2000) Reduced growth of Alaskan white spruce in the twentieth century from temperature-induced drought stress. *Nature*, **405**, 668–673.

Barbéro M, Losiel R, Quézel P, Richardson DM, Romane F (1998) Pines of the mediterranean basin. In: *Ecology and Biogeography of Pinus* (ed. Richardson DM), pp. 153–170. Cambridge University Press, Cambridge.

Biondi F (1997) Evolutionary and moving response functions in dendroclimatology. *Dendrochronologia*, **15**, 139–150.

Biondi F (2000) Are climate–tree growth relationships changing in North-Central Idaho, USA? *Arctic, Antarctic and Alpine Research*, **32**, 111–116.

Biondi F, Waikul K (2004) DENDROCLIM2002: a C++ program for statistical calibration of climate signals in tree-ring chronologies. *Computers and Geosciences*, **30**, 303–311.

Blanco E, Casado MA, Costa M *et al.* (1997) *Los Bosques Ibéricos*. Planeta, Barcelona.

Camarero JJ (1999). *Growth and regeneration patterns and processes in 'Pinus uncinata' Ram: treeline ecotones in the Pyrenees and in an isolated population in the Western distribution limit in Spain*. DS Thesis, University of Barcelona, Barcelona, 527 pp.

Camarero JJ, Guerrero-Campo J, Gutiérrez E (1998) Tree-ring growth and structure of *Pinus uncinata* and *Pinus sylvestris* in the central Spanish Pyrenees. *Artic and Alpine Research*, **30**, 1–10.

Carrer M, Urbinati C (2004) Age-dependent tree-ring growth responses to climate in *Larix decidua* and *Pinus cembra*. *Ecology*, **85**, 730–740.

Chapin FS, Zavaleta ES, Eviner VT *et al.* (2000) Consequences of changing biodiversity. *Nature*, **405**, 234–242.

Cook ER (1985). *A time series analysis approach to tree-ring standardization*. DS Thesis, University of Arizona, Tucson.

Cook ER, Briffa KR (1990) Data analysis. In: *Methods of Dendrochronology* (eds Cook ER, Kairiukstis LA), pp. 97–162. Kluwer, Boston.

Cook ER, Peters K (1981) The smoothing spline: a new approach to standardizing forest interior tree-ring width series for dendroclimatic studies. *Tree-Ring Bulletin*, **41**, 45–53.

De Luis M, Raventós J, González-Hidalgo JC, Sanchez JR, Cortina J (2000) Spatial analysis of rainfall trends in the region of Valencia (East Spain). *International Journal of Climatology*, **20**, 1451–1469.

Easterling DR, Meehl GA, Parmesan C, Changnon SA, Karl TR, Mearns LO (2000) Climate extremes: observations, modeling, and impacts. *Science*, **289**, 2068–2074.

Font Tullot I (1988) *Historia Del Clima de España. Cambios Climáticos y Sus Causas*. Instituto Nacional de Meteorología, Madrid.

Fritts HC (1976) *Tree Rings and Climate*. Academic Press, New York.

Giorgi F, Bi X, Pal JS (2004) Mean, interannual variability and trends in a regional climate change experiment over Europe. I. Present-day climate (1961–1990). *Climate Dynamics*, **22**, 733–756.

Guiot J (1991) The bootstrapped response function. *Tree-Ring Bulletin*, **51**, 39–41.

Gutiérrez E (1989) Dendroclimatological study of *Pinus sylvestris* L. in southern Catalonia (Spain). *Tree-ring Bulletin*, **49**, 1–9.

Gutiérrez E (1990) Heterogeneidad espacial y diversidad de habitats de tres especies de árboles en catalunya. *Studia Oecologica*, **7**, 49–62.

Holmes RL (1983) Computer-assisted quality control in tree-ring dating and measurement. *Tree-Ring Bulletin*, **43**, 68–78.

Holmes RL (1992). *Dendrochronology program library. Version 1992-1*. Laboratory of Tree-Ring Research, University of Arizona, Tucson.

IPCC (2001) Chapter 13. Europe. In: *Climate Change 2001: Impacts, Adaptation and Vulnerability. Contribution of Working Group II to the the Third Assessment Report of the Intergovernmental Panel on Climate Change* (eds McCarthy JJ, Canziani OF, Leary NA *et al*.), Cambridge University Press, Cambridge.

Knapp PA, Soulé PT, Grissino-Mayer HD (2001) Detecting potential regional effects of increased atmospheric CO_2 on growth rates of western juniper. *Global Change Biology*, **7**, 903–917.

Lloret F, Siscart D, Dalmases C (2004) Canopy recovery after drought dieback in holm-oak Mediterranean forests of Catalonia (NE Spain). *Global Change Biology*, **10**, 2092–2099.

Macias M, Andreu L, Bosch O *et al*. (2006) Increasing aridity is enhancing silver fir (*Abies alba* Mill.) water stress in its southwestern distribution limit. *Climatic change*, **79**, 289–313.

Macias M, Timonen M, Kirchhefer AJ, Lindholm M, Eronen M, Gutiérrez E (2004) Growth variability of scots pine along a West–East gradient across Northern Fennoscandia: a dendroclimatic approach. *Artic, Antartic and Apline Research*, **36**, 565–574.

Manrique E, Fernández-Cancio A (2000) Extreme climatic events in dendroclimatic reconstructions from Spain. *Climatic Change*, **44**, 123–138.

Martínez-Vilalta J, Piñol J (2002) Drought-induced mortality and hydraulic architecture in pine populations of the NE Iberian Peninsula. *Forest Ecology and Management*, **161**, 247–256.

Menzel A, Fabian P (1999) Growing season extended in Europe. *Nature*, **397**, 659.

Mitchell TD, Carter TR, Jones PD, Hulme M, New M (2003) *A comprehensive set of high-resolution grids of monthly climate for Europe and the globe*: *the observed record (1901–2000) and 16 scenarios (2001–2100)*. Tyndall Working Paper 55, Tyndall Centre, UEA, Norwich, UK. ⟨http://www.tyndall.ac.uk⟩

Mitchell TD, Hulme M, New M (2001) Climate data for political areas. *Area*, **34**, 109–112.

Parmesan C, Yohe G (2003) A globally coherent fingerprint of climate change impacts across natural systems. *Nature*, **421**, 37–42.

Peñuelas J, Boada M (2003) A global change-induced biome shift in the Montseny mountains (NE Spain). *Global Change Biology*, **9**, 131–140.

Peñuelas J, Filella I (2001) Responses to warming world. *Science*, **294**, 793–795.

Peñuelas J, Lloret F, Montoya R (2001) Severe drought effects on Mediterranean woody flora in Spain. *Forest Science*, **47**, 214–218.

Piñol J, Terradas J, Lloret F (1998) Climate warming, wildfire hazard, and wildfire occurrence in coastal eastern Spain. *Climatic Change*, **38**, 345–357.

Richter K, Eckstein D (1991) The dendrochronological signal of pine trees (*Pinus* spp.) in Spain. *Tree-Ring Bulletin*, **51**, 1–13.

Romero R, Guijarro JA, Ramis C, Alonso S (1998) A 30-year (1964–1993) daily rainfall data base for the Spanish Mediterranean regions: first exploratory study. *International Journal of Climatology*, **18**, 541–560.

Root TL, Price JT, Hall KR, Schneider SH, Rosenzweig C, Pounds JA (2003) Fingerprints of global warming on wild animals and plants. *Nature*, **421**, 57–60.

Sokal RR, Rohlf FJ (1969) *Biometry: The Principles and Practice of Statistics in Biological Research*. Freeman, San Francisco.

Stokes MA, Smiley TL (1968) *An Introduction to Tree-Ring Dating*. University of Chicago Press, Chicago.

Schweingruber FH, Wehrli U, Aellen-Rumo K (1991) Weiserjahre als zeiger extremer standortseinflüsse. *Schweiz. Z. Forstwes*, **142**, 33–52.

Tardif J, Camarero JJ, Ribas M, Gutiérrez E (2003) Spatiotemporal variability in tree growth in the central Pyrenees: climatic and site influences. *Ecological Monographs*, **73**, 241–257.

Tessier L, Guibal F, Schweingruber FH (1997) Research strategies in dendroecology and dendroclimatology in mountain environments. *Climatic Change*, **36**, 499–517.

Thuiller W (2003) BIOMOD – optimizing predictions of species distributions and projecting potential future shifts under global change. *Global Change Biology*, **9**, 1353–1362.

Walther G-R, Post E, Convey P *et al*. (2002) Ecological responses to recent climate change. *Nature*, **416**, 389–395.

Wigley TML, Briffa KR, Jones PD (1984) On the average value of correlated time series, with applications in Dendroclimatology and Hydrometeorology. *Journal of Climate and Applied Meterology*, **23**, 201–213.

Wilmking M, Juday GP, Barber VA, Zald HSJ (2004) Recent climate warming forces contrasting growth responses of white spruce at treeline in Alaska through temperature thresholds. *Global Change Biology*, **10**, 1724–1736.

Woodward FI (1987) *Climate and Plant Distribution*. Cambridge University Press, Cambridge.

Yamaguchi DK (1991) A simple method for cross-dating increment cores from living trees. *Canadian Journal of Forest Research*, **21**, 414–416.

CHAPTER 2

Paper submitted to *Oecologia*

Manuscript ID: OEC-CHK-2007-0405

Title: **INCREASING ATMOSPHERIC CO_2 CONCENTRATION IS ENHANCING WATER-USE EFFICIENCY IN FIVE SPANISH PINE FORESTS**

Authors: Laia Andreu[1], Octavi Planells[1], Emilia Gutiérrez[1], Gerhard Helle[2] and Gerhard H. Schleser[2]

(1) Departament d'Ecologia, Universitat de Barcelona. Avinguda Diagonal, 645. 08028. Barcelona. Spain. (2) Institute for Chemistry and Dynamics of the Geosphere, Institute 5: Sedimentary Systems, Forschungszentrum Jülich GmbH (FZJ), Leo-Brandt Strasse, D-52425 Jülich, Germany.

INCREASING ATMOSPHERIC CO_2 CONCENTRATION IS ENHANCING WATER-USE EFFICIENCY IN FIVE SPANISH PINE FORESTS

Laia Andreu[1], Octavi Planells[1], Emilia Gutiérrez[1], Gerhard Helle[2] and Gerhard H. Schleser[2]

(1) Departament d'Ecologia, Universitat de Barcelona. Avinguda Diagonal, 645. 08028. Barcelona. Spain. (2) Institute for Chemistry and Dynamics of the Geosphere, Institute 5: Sedimentary Systems, Forschungszentrum Jülich GmbH (FZJ), Leo-Brandt Strasse, D-52425 Jülich, Germany.

Correspondence author: Name: Laia Andreu Hayles. Departament d'Ecologia, Universitat de Barcelona. Avinguda Diagonal, 645. 08028. Barcelona. Spain. Phone: +34.93.402.15.08 Fax number: ++34.93.411.14.38 E-mail: laiandreu@ub.edu

Abstract

How plants will respond to changes in atmospheric CO_2 and climate is still an open question. The increase in the atmospheric CO_2 concentration (c_a) is linked to a decrease of its isotopic signature ($\delta^{13}C_{atm}$), caused by the rise of ^{13}C-depleted CO_2 due to fossil fuel burning and deforestation since the industrial revolution (ca. AD1800). This paper describes the low frequency fluctuations of $\delta^{13}C$ tree-ring cellulose chronologies from five Iberian pine forests since AD1800. In analogy to the declining $\delta^{13}C_{atm}$ trend, all $\delta^{13}C$ tree-ring series decreased, most pronouncedly since 1960. ^{13}C discrimination (Δ), leaf intercellular concentration (c_i) and water-use efficiency (W_i) of plants through time were inferred from $\delta^{13}C$ data of tree-ring cellulose. Significant differences among Δ values of the chronologies were found probably due to different site conditions and/or species-specific characteristics. Changes in time were estimated by using time intervals of 40-years. The Δ ($\approx c_i/c_a$) trends remained more or less constant throughout time until the period 1960-99, for which a high variability in Δ was observed. An increase in c_i and W_i was observed at all sites, reaching mean increases of 14% (± 5.8%) and 18% (± 6%) for the 1960-99 period, respectively. With the rise in c_a, the ratio of c_i/c_a remained more or less constant, resulting in an enhancement of W_i. Neither temperature increase, nor precipitation decrease or vapour pressure deficit (VPD) increase detected during winter seem to be responsible for the W_i enhancement observed at all sites during the 1960-99 period. The results point towards c_a as being the main driving force for the W_i improvement observed during the cited period.

Keywords: Tree-rings, $\delta^{13}C$ isotope signature, ^{13}C discrimination (Δ), intercellular CO_2 concentration (c_i), temperature, precipitation and vapour pressure deficit (VPD) trends.

Introduction

Patterns of carbon exchange by terrestrial ecosystems may be changing as a consequence of land-use modifications and climatic changes (Schimel et al. 2001). How the terrestrial carbon reservoir responded to rising atmospheric CO_2 concentrations (c_a), requires the study of plant physiological adaptations (Feng 1998). By using carbon isotope signatures ($\delta^{13}C$) of tree-ring cellulose, changes in discrimination (Δ) through time can be assessed for natural forests (Saurer et al. 2004). This provides the possibility for analyzing changes of intrinsic water-use efficiency (W_i) because Δ ($\approx c_i/c_a$) is linked to W_i through the effects of assimilation and stomatal conductance via intercellular CO_2 (c_i). Zhang et al. (1994) found a highly significant negative correlation between Δ and W_i measured *in situ*. Different responses in Δ and W_i have been found in several regions and ecosystems of the world (Marshall and Monserud 1996; Bert et al. 1997; Duquesnay et al. 1998), however, studies on $\delta^{13}C$ in conifers of semi-arid environments are still scarce (Williams and Ehleringer 1996; Ferrio et al. 2003; Klein et al. 2005).

Since tree-rings are a valuable source of long term information on environmental change, our study was carried out using chronologies of three pine species *Pinus sylvestris* L., *P. uncinata* Ramond ex. DC and *P. nigra* Arnold subsp. *salzmannii* from the Iberian Peninsula. Additionally, $^{13}C/^{12}C$ ratios of tree-ring cellulose are a useful parameter for assessing past climate variability (e.g. Hemming et al. 1998; McCarroll and Pawellek 2001; Helle et al. 2002; Helle and Schleser 2004), soil water content (e.g. Panek and Goldstein 2001), water-use efficiency (e.g. Matzner et al. 2001; Ponton et al. 2001) or hydraulic properties of the water-conducting system of stems and branches (Panek 1996).

Low frequency variations in $\delta^{13}C$ of tree-ring series from the 19th and 20th centuries are generally linked with physiological responses to increasing atmospheric CO_2 concentration (c_a) in conjunction with its declining $\delta^{13}C$ values ($\delta^{13}C_{atm}$). As stomata tend to reduce their aperture under elevated CO_2 concentration, this mechanism often results in an improvement of W_i. Though this was already demonstrated by controlled experiments (Ceulemans and Mousseau 1994), extrapolations to natural ecosystems are complicated. More research in natural forests of different regions of the world is necessary to assess the reactions under natural conditions. Changes in tree-growth variability among conifer forests related to the changing climatic conditions have been reported for Spain (e.g. Tardif et al. 2003; Macias et al. 2006; Andreu et al. 2007). However, stable isotope studies using dendrochronological methods are particularly scant in the Iberian Peninsula (Ferrio et al. 2003; Ferrio and Voltas, 2005; Planells et al. 2007). Here, we present 200 years long $\delta^{13}C$ chronologies from five Spanish pine forests to study their responses to rising c_a, mainly in

terms of their carbon isotope composition and water relations.

Material and methods

Five forest stands were sampled in the Iberian Peninsula (Fig. 1). One *Pinus nigra* stand is located in the south-east (*pn*Caz), while in the north, two *P. sylvestris* forests (*ps*Lil and *ps*Tej) and two *P. uncinata* forests (*pu*Ped and *pu*Vin) were sampled. *Ps*Tej and *pu*Vin are located only 10 Km away from each other, allowing a better assessment of species-specific responses to similar climatic conditions, previously discussed by Planells et al. (2007). Sampling focused on the oldest natural forest stands in the area. Site characteristics are described in Table 1. At each site, more than fifteen trees were cored with an increment borer at around 1.30 m stem height. At least four cores were taken from each tree: two for ring-width chronology building and the rest for isotope analyses.

Isotope chronologies

For *pn*Caz, *ps*Lil and *pu*Ped eight to ten cross-dated cores from four different trees were selected, while for *ps*Tej and *pu*Vin eight cores from eight trees were chosen (Table 2). These cores were dated with an absolute precision using reliable ring-width chronologies established at each site. For each location, tree-rings were dissected and pooled year by year (Leavitt and Long 1984; Treydte et al. 2001). α-cellulose was extracted to avoid isotope variations caused by varying contents of other wood fractions such as lignin (Wilson and Grinsted 1977) or resins that have a systematically different isotopic signature. The extraction method was based on the use of sodium hydroxide, sodium chlorite and acetic acid to remove the extractives (Loader et al. 1997). The α-cellulose was homogenized in two different ways: *ps*Tej and *pu*Vin samples were ground with an ultra centrifugation mill (Retsch ZM1, mesh size of 0.5 mm); samples from *pn*Caz, *ps*Lil and *pu*Ped were homogenized with an ultrasonic device developed at the Forschungszentrum Jülich GmbH, Germany. ^{12}C and ^{13}C were measured as CO_2 by combusting the α-cellulose samples in an elemental analyzer (Fisons NA 1500 NC) coupled via an open split to an isotope ratio mass spectrometer (Micromass Optima) operating in continuous flow mode. The reproducibility was better than 0.1‰. The isotope signature is expressed in the delta notation, relative to the standard VPDB (IAEA 1995):

$$\delta^{13}C_{sample} = \left[\frac{(^{13}C/^{12}C)_{sample}}{(^{13}C/^{12}C)_{PDB}} - 1 \right] x1000 \quad (1)$$

c_i/c_a, c_i and W_i calculations

Smoothing 50-year spline curves were fitted to the raw $\delta^{13}C$ chronologies in order to extract the long-term variations of these series, similarly to the method used by Feng (1998). The fitted values were used to calculate carbon isotope discrimination (Δ). The Δ, the net discrimination against ^{13}C, expresses the

isotope shift between air ($\delta^{13}C_{air}$) and plant organic matter ($\delta^{13}C_{tree}$) in ‰:

$$\Delta = \frac{\delta^{13}C_{air} - \delta^{13}C_{tree}}{1 + \delta^{13}C_{tree}/1000} \quad (2)$$

Qualitatively the fractionation by C3 plants can be described as a two step process. In the first step CO_2 diffuses through the stomata, the intercellular air spaces and the liquid phase of the mesophyll cells towards the carboxylation sites. In the second step CO_2 reacts with ribulose-1.5bis-phosphate (RuBP carboxylase). For C3 plants, the relationship between carbon isotope discrimination and leaf gas exchange can be described by the following equation (Farquhar et al. 1982, 1989):

$$\Delta = a + (b - a)\frac{c_i}{c_a}, \quad (3)$$

where a is the fractionation between $^{13}CO_2$ and $^{12}CO_2$ during diffusion of CO_2 through the stomata (4.4‰); b is the discrimination against $^{13}CO_2$ due to RuBP carboxylase (~27‰, Farquhar and Richards 1984); c_i and c_a are the needle intercellular spaces and ambient concentrations (µmol·mol^{-1}) of CO_2, respectively.

High precision records of $\delta^{13}C_{atm}$ obtained from Antarctic ice core data and direct measurements (Francey et al. 1999), summarized by McCarroll and Loader (2004), were used to calculate Δ using equation 3. It was assumed that the $\delta^{13}C_{air}$ at the experimental site equalled the $\delta^{13}C_{air}$ of the ambient atmosphere. Knowing Δ, c_i/c_a can be calculated by rearranging equation 3:

$$\frac{c_i}{c_a} = \frac{\Delta - a}{b - a}, \quad (4)$$

c_i was determined using the data of the atmospheric CO_2 concentration (Robertson et al. 2001) summarized by McCarroll and Loader (2004). The intrinsic water-use efficiency W_i, is the ratio of the fluxes of net photosynthesis A and conductance for water vapour gH_2O (Feng 1999, citing Ehleringer et al. 1993):

$$W_i = \frac{A}{g_{H_2O}} = (c_a - c_i)\frac{1}{1.6} \quad (5)$$

Although the Francey and Farquhar (1982) model was developed for whole-leaf tissue, which differs isotopically from stem cellulose, many authors (e.g. Bert et al. 1997) have used $\delta^{13}C$ tree-ring cellulose to calculate this set of equations considering a constant isotopic difference between wood and leaves (Feng 1998). In addition, intra-seasonal investigations revealed identical trends in leaf cellulose and tree-ring cellulose, where tree-ring cellulose was found to be generally enriched in ^{13}C as compared to leaf cellulose (Helle and Schleser 2004). The use of cellulose from tree-ring instead of needle organic matter allows precise annual dating and does not affect the conclusions of this work focused on long term variations.

Differences in ‰ of $\delta^{13}C_{atm}$ and $\delta^{13}C$ tree-ring series were calculated for time periods of 40-years (1800-39, 1840-79, 1880-1919, 1920-59 and 1960-99) using the spline curve values fitted to the raw $\delta^{13}C$ chronologies. Changes in c_i/c_a, c_i, c_a and W_i given as % were calculated using

the same proceeding. The last period (1960-1999) allows comparisons with other studies (Zhao et al. 2001; Saurer et al. 2004).

Meteorological data

The meteorological data was a set of monthly mean temperature and total precipitation from 1960 to 1999. These data, made by the Spanish *Instituto Nacional de Meteorologia* (INM), belong to a homogenised grid composed by cells of 25 x 25 km. The nearest data were selected for each site, choosing the same grid (which corresponds to Urbión range) for *ps*Tej and *pu*Vin.

Vapour pressure deficit (VPD) was computed by vapour pressure (VP) subtraction from day-time saturation vapour pressure (VPsat), using the equations proposed by Ferrio and Voltas (2005) for the Mediterranean region:

$$\ln(\mathrm{VP}) = 6.34 + 0.047Tm + 0.93\left(\frac{Pm}{1000}\right) - 0.22\left(\frac{Z}{1000}\right)$$

$$\mathrm{VPsat} = 613.75\exp\left(17.502\frac{Tday}{240.97 + Tday}\right),$$

where *Tm* is monthly mean temperature (ºC), *Pm* is monthly precipitation (mm), and Z is altitude (m a.s.l.). *Tday* (day-time temperature) is calculated summing 1/3 average minimum temperature and 2/3 average maximum temperature. As minimum and maximum temperature data were not available, *Tm* was used instead of *Tday* considering that these variables follow similar trends.

Results

Comparison among $\delta^{13}C$ and Δ chronologies

Figure 2 shows the decreasing trend of the five $\delta^{13}C$ chronologies. Mean (± standard deviation, SD), minimum and maximum $\delta^{13}C$ values of each chronology for the 19th and 20th centuries are shown in Table 2. These periods were chosen due to the shorter length of the *ps*Tej chronology that started in 1900.

Box-plots were represented to allow comparisons among Δ data (Fig. 3). *Pn*Caz shows the lowest Δ values, according to be the southernmost and driest site: highest mean temperature and lowest precipitation (Table 1). *Pn*Caz is followed by *pu*Vin, *pu*Ped and *ps*Lil (with very similar values), and *ps*Tej showing the highest Δ values. One-factor Anova between each pair of chronologies resulted in significant differences at the 99% level ($p<0.01$) among the Δ values of all studied sites for the 19th century. Only *pu*Ped versus *ps*Lil was not significant (Table 3). The same holds for the 20th century, with the unique exception of *pu*Ped versus *pu*Vin, which showed a significant difference at a lower confidence level ($p<0.05$).

Variations in $\delta^{13}C$, Δ ($\approx c_i/c_a$), c_i and W_i with time

All raw $\delta^{13}C$ chronologies decreased with time (Fig. 2). The fitted spline curves reflect these decreasing trends (Fig. 2 and Fig. 4a). The strongest

decrements in all $\delta^{13}C$ chronologies were observed from 1960 to 1999 (Fig. 5a). During this period, the mean decline among all the sites was -0.86‰ (± 0.55‰) which is similar to the decline of $\delta^{13}C_{atm}$ of -1.1‰ (Table 4). As is indicated by the large SD (± 0.55‰), the downward trends do, however, differ quite strongly from each other. The performed Anova with the decrements of all the preceding periods results in a heterogeneous picture, which indicates the rather different behaviour of the declining trends (Table 5).

Δ, and hence c_i/c_a, slightly increased or decreased during the two centuries depending on sites (Fig. 4b, Fig. 5b) and time periods (Table 4). No distinct common pattern was found, all trends remained vague and only during the very last decades a downward trend was developed for *pn*Caz, *ps*Lil and *pu*Ped, while *ps*Tej and *pu*Vin showed no changes and an increment, respectively. However, the observed changes in Δ among time periods were not significant (Table 5).

C_i increased at all sites (Fig. 4c) with the exception of the 1800-39 period (Fig. 5c). The highest increment of the mean value of c_i (14% ± 5.8%) was observed for the 1960-99 period, being significantly different from the other increments (Table 5). The mean c_i increment seems to be almost proportional to the change in c_a, with the exception of 1880-1919 period, when the percentage of the c_a increment was slightly weaker than the mean percentage of the c_i increment (Table 4). Though the mean c_i increment for 1960-99 was similar to the c_a increase (15.8%), higher or lower c_i changes in comparison with c_a were observed for each chronology separately (Fig. 5c).

Similarly, trees of all sites showed an increase in W_i independent of species (Fig. 4d). Again, the largest increment was found in 1960-99 (Fig. 5d and Table 4). There were highly significant differences ($p<0.01$) between the increments in 1960-99 and the other periods (Table 5).

Trends in meteorological data

Figure 6 depicts the trends of the monthly mean temperature, precipitation and VPD from 1960 to 1999 for the four sites: Cazorla, Pedraforca, Lillo and Urbión range. The bars represent the slopes (rates of changes) of the linear regressions (b in $y = a + bx$) fitted to the meteorological series to assess their trend significance.

In the case of Cazorla and Urbión, significant mean temperature increases in January, February ($p<0.05$) were observed, as well as in March, December and annually ($p<0.01$). Urbión mean temperature also showed a significant increase in August (99% level) and in November (95% level). At Lillo and Pedraforca, December mean temperatures also increased ($p<0.05$), while June and September decreased ($p<0.05$), respectively.

A significant precipitation decrease was observed for January ($p<0.05$), February,

March and annually ($p<0.01$) at Cazorla and Urbión. Similarly, Pedraforca showed a decrease in precipitation for February ($p<0.01$), March and on an annual basis ($p<0.05$). Precipitation at Cazorla site increased in August and decreased in December ($p<0.05$).

VPD at the site of Cazorla showed significant increments (99% level) in January, February, March, December and annually, as well as in April and November (95% level). Similarly, for the Urbión site, VPD showed significant increments in January, February, March and on an annual basis ($p<0.01$), but also in August, November and December ($p<0.05$). VPD at the site of Lillo decreased in June and increased in December (95% level). No monthly trend in VPD was detected at Pedraforca site.

Discussion

Species-specific, site and climate factors affecting Δ values

As expected, the southernmost forest (*pn*Caz) had the lowest Δ values reflecting the driest conditions of all sites (Fig. 3). On the other hand, the different levels of Δ values between the two forests of *ps*Tej and *pu*Vin growing under similar conditions (i.e. separated only by 10 Km) suggest different ^{13}C fractionation patterns presumably due to different site conditions and/or difference in species. Although other factors like aspect or stand density were taken into account, they could not be related to the Δ differences observed among the sites.

The declining trend in tree-ring $\delta^{13}C$ values

The decreasing trend shown by all raw $\delta^{13}C$ chronologies is attributed to the rise of ^{13}C-depleted CO_2 due to fossil fuel burning and deforestation since industrialization (Fig. 2 and Fig. 4a). However, it should be noted that the decline pattern is particular at each forest stand. The $\delta^{13}C_{atm}$ decrease and the corresponding c_a increase are the largest in the 1960-99 period (Table 4). This is clearly reflected in our $\delta^{13}C$ tree-ring series and simply mirrors, at least to a certain degree the change in the source value, namely $^{13}C_{atm}$. In accordance with the downward trend of the $\delta^{13}C_{atm}$, the $\delta^{13}C$ content in the tree-ring series shows a similar trend that became steeper after 1960 (Fig. 4a and Table 4). Interestingly, Zhao et al. (2001) reported a faster decrease of wheat $\delta^{13}C$ values after 1960, which however appeared to be more rapid than the $\delta^{13}C_{atm}$ fall. In contrast to the results of Zhao et al. (2001), the decrease in our tree-ring $\delta^{13}C$ values was similar to the decrease in $\delta^{13}C_{atm}$ (Fig. 5a), being slightly lower in three series. A lower decrease in $\delta^{13}C$ tree-ring values was also found by Saurer et al. (2004) in an investigation with conifer trees in northern Eurasia, suggesting a similar response to c_a by the studied Iberian pines as those of Boreal forests.

The stability of c_i/c_a ($\approx\Delta$)

The c_i/c_a behaviour was more or less constant throughout time until the last interval of the studied period. During the 1960-99 period, a high variability in the c_i/c_a of the chronologies was detected. At three sites falling trends were observed, positive at one site and stable at the other (Fig. 5b), in agreement with range of trend described by Feng (1998). The wide range in the Δ response observed depending on sites and/or species showed non stability in c_i/c_a trends, at least in four of the forests. Saurer et al. (2004) proposed three different scenarios that mainly differ in the degree to which the increase in c_i follows the increase in c_a: (1) c_i constant → c_i/c_a decreases → W_i increases; (2) c_i increases proportional to c_a → c_i/c_a constant → W_i increases; (3) c_i increases at the same amount than c_a → c_i/c_a increases → W_i constant. Considering only c_i/c_a, our results seem to illustrate the three scenarios, as we observed three decreasing trends, one constant behaviour and one increase in the c_i/c_a ratio during the 1960-99 period. However, taking into account that c_i and W_i increased in the five forests during this period, only scenario 2 complies with our results. Therefore, our results suggest a mechanism by which c_i/c_a stays more or less constant in the studied Spanish pine forests. Accordingly, Feng's studies (1998) pointed out that over the 20th century, even though c_i/c_a ratios decreased in most of the trees in response to c_a, the magnitude of these decrements was not sufficient to keep c_i constant. In contrast, Swanborough et al. (2003) reported an increasing c_i/c_a trend due to a decreasing photosynthetic rate associated with nutrient depletion.

A constant Δ pattern was also found in *P. edulis* from the southwestern United States along a summer monsoon gradient that differed in precipitation and evaporative humidity (Williams and Ehleringer 1996). In the way that c_i/c_a represents a set point in gas exchange to study how plants respond to environmental change (Ehleringer and Cerling 1995), this may be understood as a regulative adaptation of trees to rising CO_2 concentration. Constancy of c_i/c_a may be achieved by a concurrent reduction of both the stomatal conductance and the photosynthetic capacity in response to higher levels of CO_2 (Saurer et al. 2004). The reduced conductance may produce an overall warming contribution for land temperatures through reduction in the evaporative fraction. Reduction in plant transpiration could affect hydrological budgets, resulting in drier air and enhanced warming near surfaces (Betts et al. 2000). The observed physiological response in Spanish forests might cause a vegetation-climate feedback by modifying surface-atmosphere fluxes of energy and moisture. However, consequences of lower conductance are stronger in more continental areas (e.g. Siberia), where a high part of precipitation is generated by transpiration (Saurer et al. 2004).

The improvement of W_i

A significant increase in W_i from 1960 onwards was found for all the studied sites. The mean W_i increase amounts to about 18% ± 6% for the period from 1960 to 1999. This value is slightly higher than values described for *Pinus* by Saurer et al. (2004) (17.2% ± 2.7), calculated for the 20th century. However, in view of the SD the values are rather similar. Feng (1999) also described an improvement in W_i after 1900, reaching 5-25% in the 1980s. The constancy of c_i/c_a corresponding to an increase in W_i of those studies is consistent with our results. However, other investigations have reported a decrease in Δ with an even stronger improvement of W_i (Peñuelas and Azcón-Bieto 1992; Bert et al. 1997; Duquesnay et al. 1998; Hietz et al. 2005) or no change in W_i due to a Δ increase (Marshall and Monserud 1996).

Was the c_a increase enhancing W_i?

Considering that trees kept Δ (≈ c_i/c_a) more or less stable throughout the studied period, the increased c_a resulted in an enhancement of W_i (a reduction of leaf water loss per unit of carbon gain). Stomatal conductance is the main factor controlling water loss, while carbon gain depends on photosynthetic capacity. The trends of variables that affect stomatal conductance and carbon assimilation for the 1960-99 period were useful to assess if the c_a increase was the main driving force of the observed W_i improvement or if other factors were also playing an important role.

Two of the sites, Cazorla and Urbión, showed the highest increases in winter temperature, as well as significant decreases in winter precipitation. December temperature also increased in Lillo and Pedraforca, and precipitation also decreased in February and March at Pedraforca. A winter temperature increase could extend the growing period length. Changes in phenology linked to climate warming have already been reported (Menzel and Fabian, 1999; Peñuelas and Filella 2001). The prolongation of the growing season during spring and autumn will reduce or keep constant the W_i, as the trees would be growing under favourable climatic conditions and they do not need to be more efficient in the use of the water to produce assimilates. Since winter precipitation in the studied sites used to be snow due to the high altitude, a decrease in the amount of snow can also enhance an early beginning and a late end of the growing season.

Stomatal conductance is highly affected by the VPD that can be considered the driving force for transpiration. VPD increased significantly from November to March in Cazorla and Urbión. Moreover, April, August and December VPD increases were detected in Cazorla, Urbión and Lillo, respectively. In contrast, June VPD decreased in Lillo, while no trend in VPD was found in Pedraforca. In principle, a VPD increase during the growing season would produce a reduction in stomatal aperture, possibly but not necessarily enhancing W_i. The order of the chronologies listed

from the highest to the lowest W_i during the 1960-99 period (*ps*Lil, *pu*Ped, *pn*Caz, *ps*Tej and *pu*Vin) does not correspond to the highest VPD increments that were observed at the sites of Cazorla (*pn*Caz) and Urbión (*ps*Tej, *pu*Vin). Moreover, Urbión is the only location where a VPD increase was observed during summer (August), nevertheless the W_i of *ps*Tej and *pu*Vin showed the lowest values.

The temperature increase, precipitation decrease and VPD increase observed during winter do not seem to increase W_i. Moreover, these climatic trends did not develop equally at all sites, suggesting that these factors can not be responsible for the W_i enhancement detected in the five studied forest from 1960 to 1999. Therefore, these results strongly suggest that the c_a increase is the most feasible driving force leading to the W_i improvement observed during the 1960-99 period.

Acknowledgements

We are very grateful to Oriol Bosch, Elena Muntán, Montse Ribas, Pitter Ferrio, Mariano Barriendos, Carlos Almarza, Pedro Antonio Tíscar, Marc Filot, Markus Leuenberger and Heinz Vos for their help during sampling, laboratory work and manuscript preparation. This research was funded by EU project ForMAT (Contract ENV4-CT97-0641), EU project ISONET (Contract EV K2-2001-00237) and EU FP6 project Millennium (GOCE 017008).

References

Andreu L, Gutiérrez E, Macias M, Ribas M, Bosch O, Camarero JJ (2007) Climate increases regional tree growth variability in Iberian pine forests. Global Change Biol 13: 804-815, doi: 10.1111/j.1365-2486.2006.01322.x

Bert D, Leavitt SW, Dupouey JL (1997) Variations of wood $\delta^{13}C$ and water-use efficiency of *Abies alba* during the last century. Ecology 78(5): 1588-1596

Betts RA, Cox PM, Woodward FI (2000) Simulated responses of potential vegetation to doubled-CO_2 climate change and feedbacks on near-surface temperature. Global Ecol Biogeogr 9: 171-180

Ceulemans R, Mousseau M (1994) Effects of elevated atmospheric CO_2 on woody plants. Tansley Review no. 71. New Phytol 127: 425-446

Duquesnay A, Bréda N, Stievenard M, Dupouey JL (1998) Changes of tree-ring $\delta^{13}C$ and water-use efficiency of beech (*Fagus sylvatica* L.) in north-eastern France during the past century. Plant Cell Environ 21: 565-572

Ehleringer JR, Hall AE, Farquhar GD (eds) (1993) Stable isotopes and plant carbon-water relations. Academic Press, San Diego

Ehleringer JR, Cerling TE (1995) Atmospheric CO_2 and the ratio of intercellular to ambient CO_2 concentrations in plants. Tree Physiol 15: 105-111

Farquhar GD, O'Leary MH, Berry JA (1982) On the Relationship between Carbon Isotope Discrimination and the Intercellular Carbon Dioxide Concentration in Leaves. Aust J Plant Physiol 9: 121-137

Farquhar GD, Richards RA (1984) Isotope Composition of Plant Carbon Correlates with Water-use Efficiency of Wheat Genotypes. Aust J Plant Physiol 11: 539-552

Farquhar GD, Ehleringer FR, Hubick KT (1989) Carbon isotope discrimination and

photosynthesis. Ann Rev Plant Physiol Plant Mol Biol 40: 503-537

Feng X (1998) Long-term c_i/c_a response of trees in western North America to atmospheric CO_2 concentration derived from carbon isotope chronologies. Oecologia 117: 19-25

Feng X (1999) Trends in intrinsic water-use efficiency of natural trees for the past 100-200 years: A response to atmospheric CO_2 concentration. Geochim Cosmochim Acta 63 (13/14): 1891-1903

Ferrio JP, Florit A, Vega A, Serrano L, Voltas J (2003) $\Delta^{13}C$ and tree-ring width reflect different drought responses in *Quercus ilex* and *Pinus halepensis*. Oecologia 137: 512-518

Ferrio JP, Voltas J (2005) Carbon and oxygen isotope ratios in wood constituents of *Pinus halepensis* as indicators of precipitation, temperature and vapour pressure deficit. Tellus 57B: 164-173

Francey RJ, Farquhar GD (1982) An explanation of $^{13}C/^{12}C$ variations in tree-rings. Nature 297: 28-31

Francey RJ, Allison CE, Etheridge DM, Trudinger CM, Enting IG, Leuenberger M, Langenfels RL, Michel E, Steele LP (1999) A 1000-year high precision record of $\delta^{13}C$ in atmospheric CO_2. Tellus 51B: 170-193

Helle G, Schleser GH, Bräuning A (2002) Climate History of the Tibetan Plateau for the last 1500 years as inferred from stable carbon isotopes in tree-rings. IAEA CN-80-80: 301-311

Helle G, Schleser GH (2004) Interpreting climate proxies from tree-rings. In: Fischer H, Floeser G, Kumke T, Lohmann G, Miller H, Negendank JFW, von Storch H (Eds.): Towards a synthesis of Holocene proxy data and climate models. Springer Verlag Berlin

Hemming DL, Switsur VR, Waterhouse JS, Heaton THE, Carter AHC (1998) Climate variation and the stable carbon isotope composition of tree ring cellulose: an intercomparison of *Quercus robur*, *Fagus sylvatica* and *Pinus sylvestris*. Tellus 50B: 25-33

Hietz P, Wanek W, Dünisch O (2005) Long-term trends in cellulose $\delta^{13}C$ and water-use efficiency of tropical *Cedrela* and *Swietenia* from Brazil. Tree Physiol 25: 745-752.

IAEA (1995) TECDOC-825. Reference and Intercomparison Materials for Stable Isotopes of Light Elements, Proceedings of a Consultants Meeting, 1-3 December 1993, Vienna

Klein T, Hemming D, Lin T, Grünzweig JM, Maseyk K, Rotenberg E, Yakir D (2005) Association between tree-ring and needle $\delta^{13}C$ and leaf gas exchange in *Pinus halepensis* under semi-arid conditions. Oecologia 144: 45-54

Leavitt SW, Long A (1984) Sampling strategy for stable carbon isotope analysis of tree rings in pine. Nature 311: 145-147

Loader NJ, Robertson I, Barker AC, Switsur VR, Waterhouse JS (1997) An improved method for the batch processing of small wholewood samples to α-cellulose. Chem Geol 136(3-4): 313-317

Macias M, Andreu L, Bosch O, Camarero JJ, Gutiérrez E (2006) Increasing aridity is enhancing silver fir (*Abies alba* Mill.) water stress in its south-western distribution limit. Climatic change 79: 289-313, doi: 10.1007/s10584-006-9071-0

Marshall JD, Monserud RA (1996) Homeostatic gas-exchange parameters inferred from $^{13}C/^{12}C$ in tree rings of conifers. Oecologia 105: 13-21

Matzner SL, Rice KJ, Richards JH (2001) Factors affecting the relationship between carbon isotope discrimination and transpiration efficiency in blue oak (*Quercus douglasii*). Aust J Plant Physiol 28(1): 49-56

McCarroll D, Pawellek F (2001) Stable carbon isotope ratios of *Pinus sylvestris* from northern Finland and the potential for extracting a climate signal from long

Fennoscandian chronologies. Holocene 11(5): 517-526

McCarroll D, Loader NJ (2004) Stable isotopes in tree rings. Quaternary Sci Rev 23: 771-801

Menzel A, Fabian P (1999) Growing season extended in Europe. Nature 397: 659.

Panek JA (1996) Correlations between stable carbon-isotope abundance and hydraulic conductivity in Douglas-fir across a climate gradient in Oregon, USA. Tree Physiol 16: 747-755

Panek JA, Goldstein AH (2001) Response of stomatal conductance to drought in ponderosa pine: implications for carbon and ozone uptake. Tree Physiol 21(5): 337-344

Peñuelas J, Azcón-Bieto J (1992) Changes in leaf $\Delta^{13}C$ of herbarium plant species during the last 3 centuries of CO_2 increase. Plant Cell Environ 15: 485-489

Peñuelas J, Filella I (2001) Responses to Warming World. Science 294: 793-795.

Planells O, Gutiérrez E, Helle G, Schleser GH (2007) Assessment of 20th century ring width, $\delta^{13}C$ and $\delta^{18}O$ of two pine species from the Iberian System (Spain) as climate proxy series. Climatic change (submitted)

Ponton S, Dupouey JL, Bréda N, Feuillat F, Bodénès C, Dreyer E (2001) Carbon isotope discrimination and wood anatomy variations in mixed stands of *Quercus robur* and *Quercus petraea*. Plant Cell Environ 24(8): 861-868

Roberston A, Overpeck J, Rind D, Mosley-Thompson E, Zielinski G, Lean J, Koch D, Penner J, Tegen I, Healy R (2001) Hypothesized climate forcing time series for the last 500 years. J Geophys Res 106: 14783-14803.

Saurer M, Siegwolf RTW, Schweingruber FH (2004) Carbon isotope discrimination indicates improving water-use efficiency of trees in northern Eurasia over the last 100 years. Global Change Biol 10: 2109-2120

Schimel DS, House JI, Hibbard KA, Bousquet P, Ciais P, Peylin P, Braswell BH, Apps MJ, Baker D, Bondeau A, Canadell J, Churkina G, Cramer W, Denning AS, Field CB, Friedlingstein P, Goodale C, Heimann M, Houghton RA, Melillo JM, Moore III B, Murdiyarso D, Noble I, Pacala SW, Prentice IC, Raupach MR, Rayner PJ, Scholes RJ, Steffen WL, Wirth C (2001) Recent patterns and mechanisms of carbon exchange by terresterial ecosystems. Nature 414: 169-172

Swanborough PW, Lamont BB, February EC (2003) $\delta^{13}C$ and water-use efficiency in Australian grasstrees and South Africa conifers over the last century. Oecologia 136: 205-212

Tardif J, Camarero JJ, Ribas M, Gutiérrez E (2003) Spatiotemporal variability in tree growth in the central Pyrenees: climatic and site influences. Ecol Monogr 73(2): 241-257

Treydte K, Schleser GH, Schweingruber FH, Winiger M (2001) The climatic significance of $\delta^{13}C$ in subalpine spruces (Lötschental, Swiss Alps). Tellus 53B: 593-611

Williams DG, Ehleringer JR (1996) Carbon isotope discrimination in three semi-arid woodland species along a monsoon gradient. Oecologia 106: 455-460

Wilson AT, Grinsted MJ (1977) $^{12}C/^{13}C$ in cellulose and lignin as palaeothermometers. Nature 265: 133-135

Zhang J, Fins L, Marshall JD (1994) Stable carbon isotope discrimination, photosynthetic gas exchange, and growth differences among western larch families. Tree Physiol 14: 531-539

Zhao F, Spiro B, McGrath SP (2001) Trends in $^{13}C/^{12}C$ ratios and C isotope discrimination of wheat since 1845. Oecologia 128: 336-34

Table 1 Location and characteristics of the sites, as well as annual mean temperature (T), annual total precipitation (P) and annual vapour pressure deficit (VPD) obtained using the nearest points from the Spanish grid data set from 1931 to 2003.

Site	Species	Site ID	Range	Latitude	Longitude	Altitude (m a.s.l.)	Aspect	Annual mean T (ºC)	Annual total P (mm)	Annual VPD (Pa)
Cazorla	*Pinus nigra*	*pn*Caz	Baetic	37º 48' N	02º 57' W	1800	SW	14.19	757.1	953.0
Pinar de Lillo	*Pinus sylvestris*	*ps*Lil	Cantabrian	43º 03' N	05º 15' W	1600	NW	9.50	1495.5	574.5
Pedraforca	*Pinus uncinata*	*pu*Ped	Pre-Pyrenees	42º 14' N	01º 42' E	2100	E	9.46	855.2	616.0
Tejeros	*Pinus sylvestris*	*ps*Tej	Urbión	42° 00' N	02º 49' W	1750	NE	9.41	929.6	610.4
Vinuesa	*Pinus uncinata*	*pu*Vin	Urbión	41° 58' N	02º 45' W	1950	SW			

Table 2 Statistics of the raw $\delta^{13}C$ tree-ring chronologies.

Site ID	Time-span	Trees/ Cores	$\delta^{13}C$ (1800-1899) in ‰			$\delta^{13}C$ (1900-1999) in ‰		
			Mean ± SD	Minimum	Maximum	Mean ± SD	Minimum	Maximum
*pn*Caz	1800-2002	4/9	-20.95 ± 0.34	-21.92	-20.39	-21.77 ± 0.55	-22.85	-20.46
*ps*Lil	1800-2002	4/10	-22.12 ± 0.49	-23.62	-21.13	-22.91 ± 0.47	-24.18	-21.62
*pu*Ped	1800-2002	4/8	-22.07 ± 0.40	-23.04	-20.96	-22.62 ± 0.56	-24.28	-21.43
*ps*Tej	1900-1999	8/8	-	-	-	-23.55 ± 0.58	-24.87	-22.52
*pu*Vin	1800-1999	8/8	-21.42 ± 0.41	-22.59	-20.26	-22.40 ± 0.84	-24.53	-20.91

Table 3 Significance of the differences between Δ data from each site calculated for two different periods 1800-99 and 1900-99 (Fig. 3). The symbols ▲ and • are the significance at 99% and 95% level, respectively, and "ns" are non-significant differences.

1800-99 / **1900-99**	*pn*Caz	*ps*Lil	*pu*Ped	*ps*Tej	*pu*Vin
*pn*Caz	1	▲ ▲	▲ ▲	- ▲	▲ ▲
*ps*Lil		1	ns ▲	- ▲	▲ ▲
*pu*Ped			1	- ▲	▲ •
*ps*Tej				1	- ▲
*pu*Vin					1

Table 4 Change in $\delta^{13}C$, c_i/c_a, c_i and W_i of the tree-ring chronologies, as well as in $\delta^{13}C_{atm}$ and c_a, for 40-year periods since 1800.

		1800-39	1840-79	1880-1919	1920-59	1960-99
difference	$\delta^{13}C_{tree}$	0.04 ± 0.2	-0.21 ± 0.21	-0.35 ± 0.16	-0.25 ± 0.16	-0.86 ± 0.55
(‰)	$\delta^{13}C_{atm}$	-	-0.13	-0.17	-0.18	-1.1
	c_i/c_a	-0.44 ± 1.9	0.83 ± 2	1.6 ± 1.4	0.64 ± 1.5	-1.6 ± 5
change	c_i (ppm)	-0.44 ± 1.9	2.7 ± 2.1	5.9 ± 1.5	4.8 ± 1.5	14 ± 5.8
(%)	W_i (umol·mol^{-1})	0.33 ± 1.8	1.2 ± 1.9	2.4 ± 1.6	3.5 ± 1.5	18 ± 6
	c_a (ppm)	-	1.9	4.2	4.2	15.8

Table 5 Significance of the Anoves performed between periods. The symbols ▲ and • are the significance at 99% and 95% level, respectively, and "ns" are non-significant differences.

		1840-79	1880-1919	1920-59	1960-99
$\delta^{13}C$ (‰)	1800-39	ns	•	•	•
	1840-79		ns	ns	ns
	1880-1919			ns	ns
	1920-59				•
Δ	1800-39	ns	ns	ns	ns
	1840-79		ns	ns	ns
	1880-1919			ns	ns
	1920-59				ns
c_i (ppm)	1800-39	ns	▲	▲	▲
	1840-79		•	ns	▲
	1880-1919			ns	•
	1920-59				▲
W_i (umolmol-1)	1800-39	ns	ns	•	▲
	1840-79		ns	ns	▲
	1880-1919			ns	▲
	1920-59				▲

Figure 1

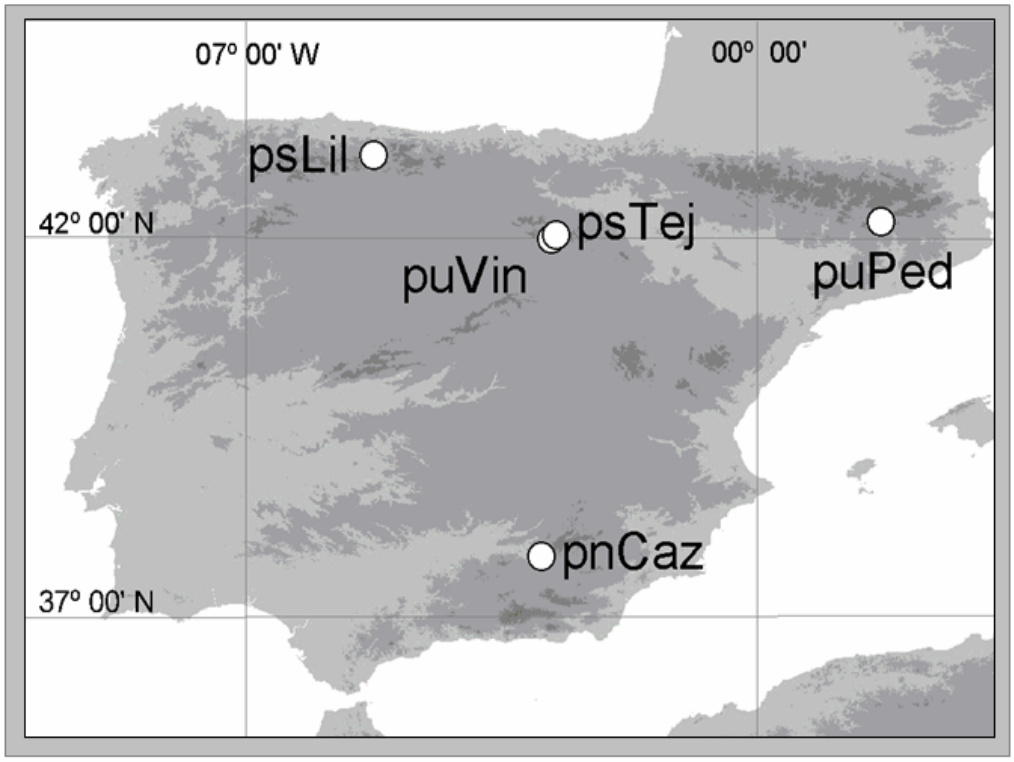

Geographical position of the selected sites in the Iberian Peninsula.

Figure 2

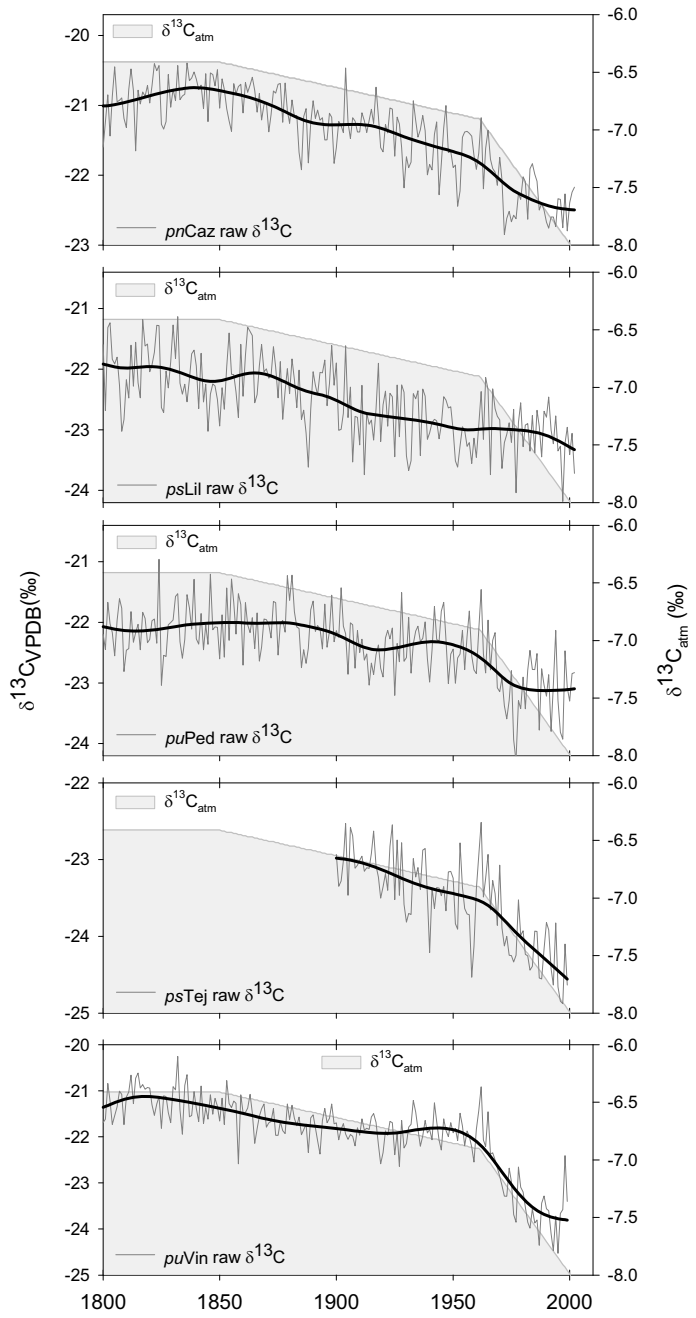

Raw $\delta^{13}C$ chronologies (grey lines). The 50-year smoothing splines (thick black lines) fitted to the raw $\delta^{13}C$ chronologies illustrate the long-term variations of these series. The $\delta^{13}C_{atm}$ decrease is shown by the grey area (right axis).

Figure 3

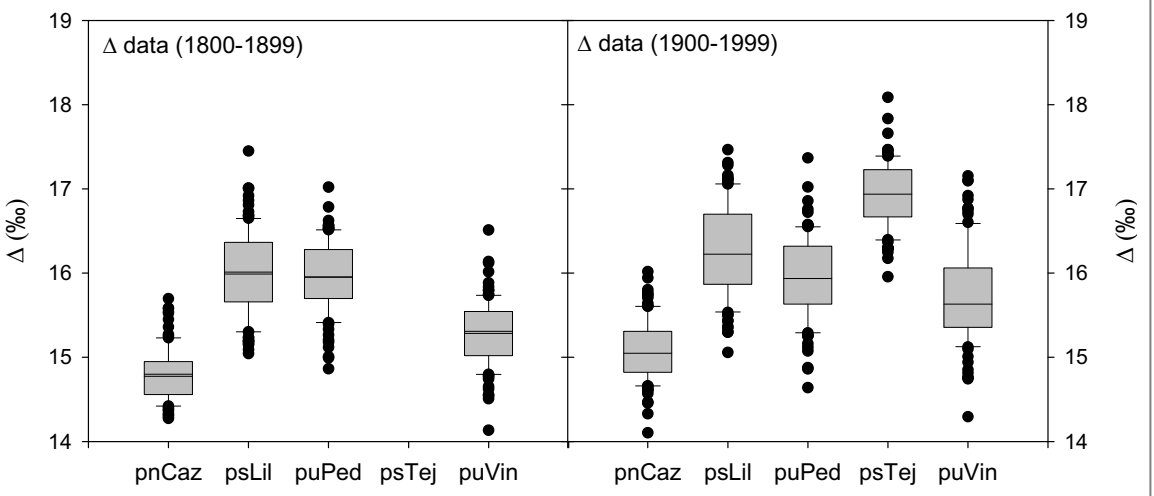

Box-plot of Δ data per each site calculated for two time periods. Significance of differences between the sites is shown in Table 3.

Figure 4

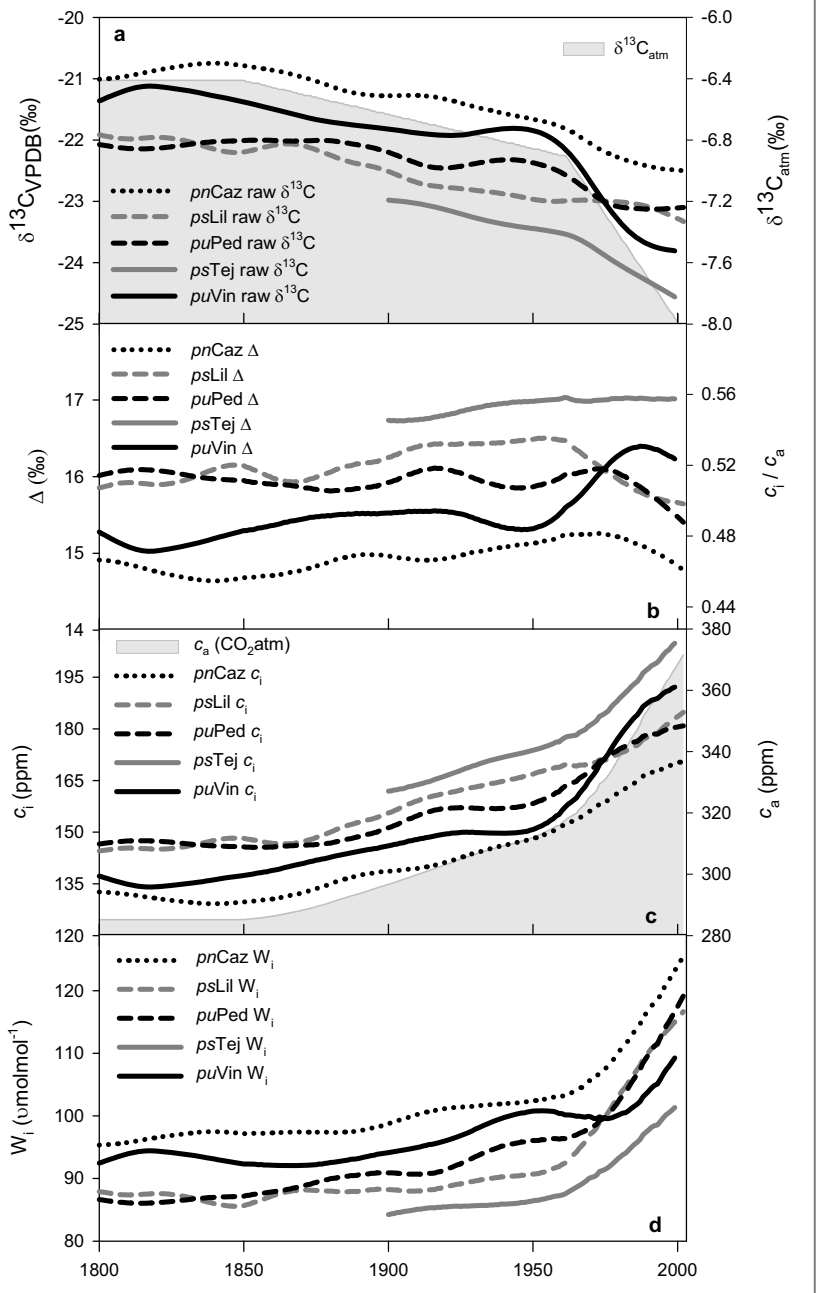

The 50-year smoothing spline fitted to: (a) $\delta^{13}C$ raw chronologies (left axis), as well as the $\delta^{13}C_{atm}$ decrease shown by the grey area (right axis); (b) Δ data (left axis) and to c_i/c_a data (right axis); (c) c_i data (left axis), as well as c_a trend shown by the grey area (right axis); (d) W_i data.

Figure 5

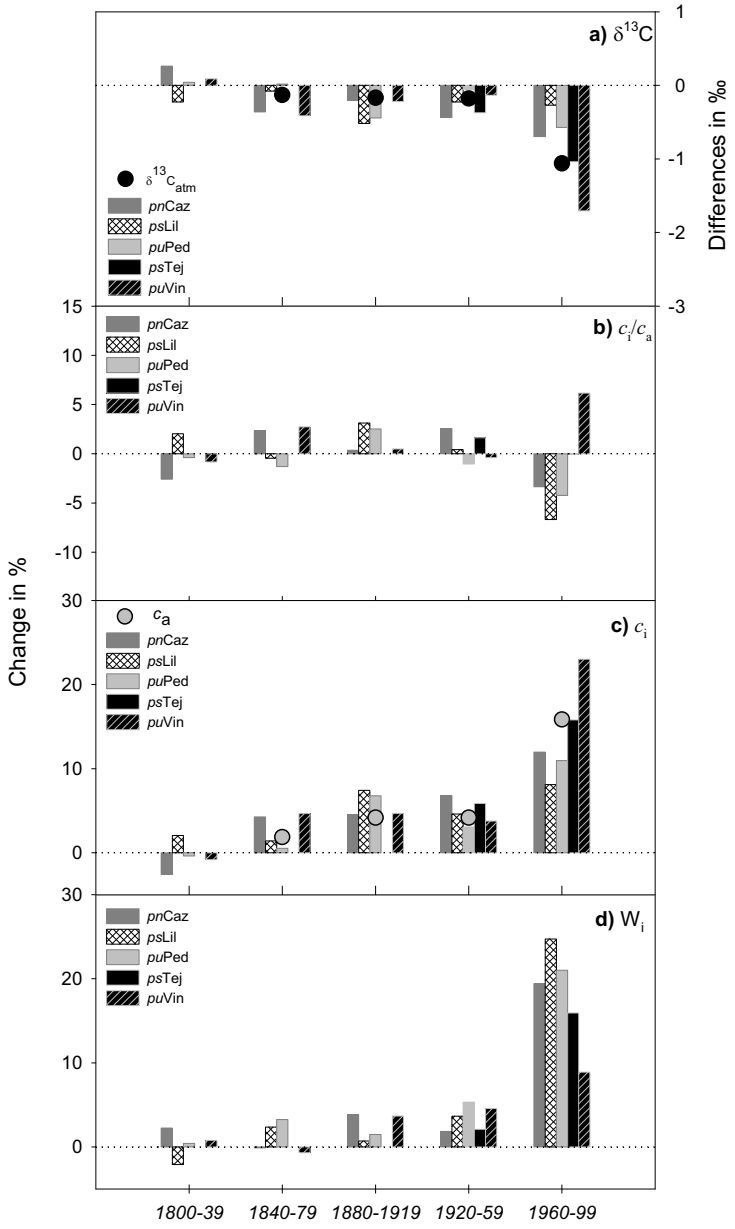

Differences in ‰ of $\delta^{13}C_{tree}$ and $\delta^{13}C_{atm}$ calculated for periods of 40-years. Changes in % using 40-year periods of: (b) Δ and c_i/c_a; (c) c_i and c_a; (d) W_i. Significance of differences between periods is shown in Table 5.

Figure 6

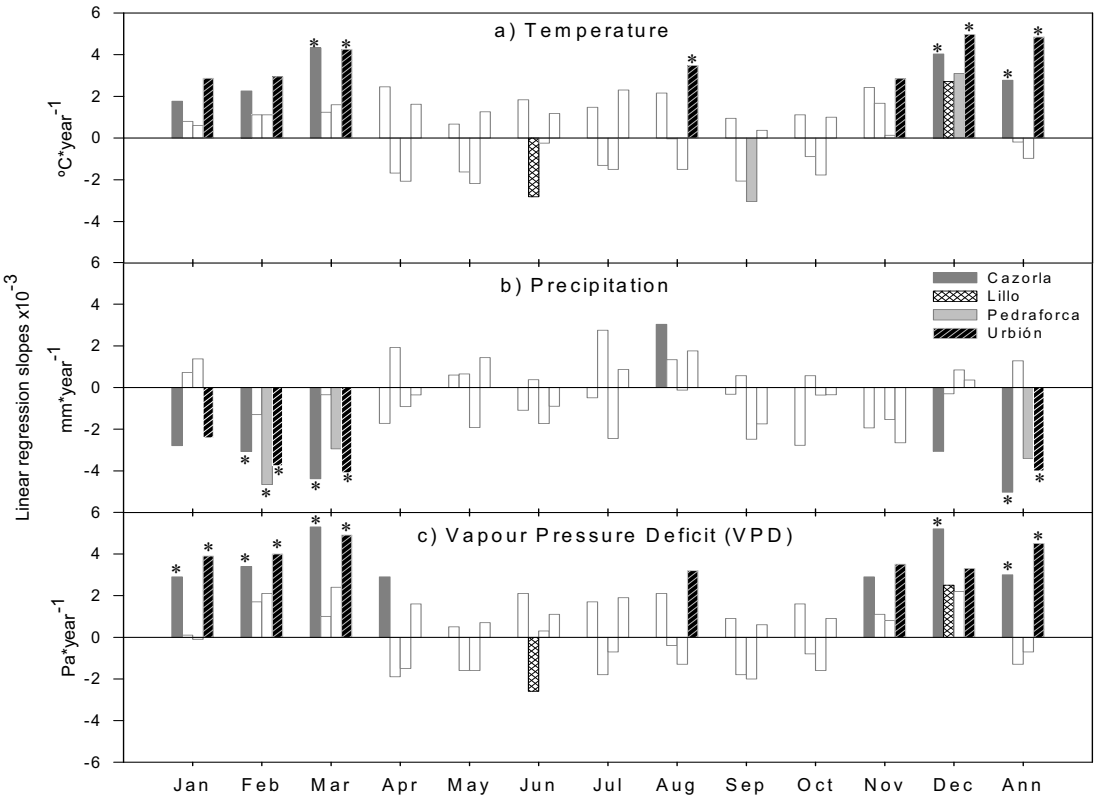

Monthly trends in: (a) mean temperature; (b) total precipitation; (c) vapour pressure deficit from 1960 to 1999. Significant trends at 99% and 95% level are shown by * and coloured bars, respectively.

CHAPTER 3

Paper submitted to *Tellus B*

Manuscript ID: TeB-07-07-0038

Title: **THE CLIMATIC SIGNIFICANCE OF TREE-RING WIDTH AND $\delta^{13}C$ IN SPANISH PINE FORESTS**

Authors: Laia Andreu[1,2], Octavi Planells[1], Emilia Gutiérrez[1], Gerhard Helle[2] and Gerhard H. Schleser[2]

(1) Departament d'Ecologia, Universitat de Barcelona. Avinguda Diagonal, 645. 08028. Barcelona. Spain. (2) Institute for Chemistry and Dynamics of the Geosphere, Institute 5: Sedimentary Systems, Forschungszentrum Jülich GmbH (FZJ), Leo-Brandt Strasse, D-52425 Jülich, Germany.

THE CLIMATIC SIGNIFICANCE OF TREE-RING WIDTH AND $\delta^{13}C$ IN SPANISH PINE FORESTS

Laia Andreu[1,2], Octavi Planells[1], Emilia Gutiérrez[1], Gerhard Helle[2] and Gerhard H. Schleser[2]

(1) Departament d'Ecologia, Universitat de Barcelona. Avinguda Diagonal, 645. 08028. Barcelona. Spain. (2) Institute for Chemistry and Dynamics of the Geosphere, Institute 5: Sedimentary Systems, Forschungszentrum Jülich GmbH (FZJ), Leo-Brandt Strasse, D-52425 Jülich, Germany.

Correspondence author: Name: Laia Andreu Hayles. Departament d'Ecologia, Universitat de Barcelona. Avinguda Diagonal, 645. 08028. Barcelona. Spain. Phone: +34.93.402.15.08 Fax number: ++34.93.411.14.38 E-mail: laiandreu@ub.edu

Abstract

This paper deals with tree-ring width and $\delta^{13}C$ chronologies from five Iberian forests and their sensitivity to climate. A better and more homogenous agreement was found among the carbon isotope records than among the ring widths series, suggesting that $\delta^{13}C$ ratios may preferentially record large scale climatic signals, while ring-width variations may reflect more local factors. A negative relationship was found between ring-width and $\delta^{13}C$. As inferred from response function analyses, ring-widths and $\delta^{13}C$ showed significant relationships with climate. The different sites and species revealed no uniform growth response to summer temperature and precipitation, while all $\delta^{13}C$ series were highly sensitive to summer precipitation and, to a lesser extent, to summer temperature. Hence, $\delta^{13}C$ values reflect drought stress during the summer season better than tree-ring widths. This demonstrates that isotopic ratios can be a useful tool for climatic reconstruction in case of weak relationships between climate and ring-width. Comparisons with other studies revealed a high influence of local conditions on $\delta^{13}C$ ratios. Nevertheless, a strong precipitation signal seems to be reflected in the $\delta^{13}C$ cellulose from trees growing under Mediterranean climate.

Introduction

Tree-rings are a valuable source of long-term information on environmental changes. As tree growth is affected by climate variations, past climate is frequently reconstructed from changes in annual ring widths or density. However, the $^{13}C/^{12}C$ ratio of tree-ring cellulose is also a useful parameter to assess past climate variability (e.g. Hemming et al., 1998;

McCarroll and Pawellek, 2001; Helle et al., 2002; Helle and Schleser, 2004), soil water content (e.g. Panek and Goldstein, 2001), water-use efficiency (e.g. Matzner et al., 2001; Ponton et al., 2001) or hydraulic properties of the water-conducting system of stems and branches (Panek, 1996). Up to now, there are not many studies comparing and combining environmental information from $\delta^{13}C$ of tree-ring cellulose and ring widths (Robertson et al., 1997a,b; Gagen et al., 2004, 2006; Planells et al., 2007).

Information relating $\delta^{13}C$ with water availability is still scarce for conifers from semi-arid environments (Williams and Ehleringer, 1996; Ferrio et al., 2003). Such studies can provide information on ecophysiological and climatic aspects of important areas in the current terrestrial biosphere (Klein et al., 2005). Our study was carried out in the Iberian Peninsula with three pine species located at the edge of their phytogeographical distribution area: *Pinus sylvestris* L., *P. uncinata* Ramond ex. DC and *P. nigra* Arnold subsp. *salzmannii* (Blanco et al., 1997). These sites were chosen because physiological processes become frequently limited by climate at the boundary of the geographical distribution of species due to their particular susceptibility to climatic variations (Fritts, 1976).

Mean annual temperature over Europe increased by about 0.8 ºC during the 20th century. Largest warming was observed over the Iberian Peninsula (IPCC, 2001), where the 1980-95 period was characterized by intense droughts, producing serious damage to several woody species (Peñuelas et al., 2001). Changes in the variability of tree-growth due to changing climatic conditions among conifer forests have been reported in Spain (e.g. Tardif et al., 2003; Macias et al., 2006; Andreu et al., 2007). Dendroclimatological studies using stable isotope are, however, particularly scant in the Iberian Peninsula (Ferrio et al., 2003; Ferrio and Voltas, 2005; Planells et al., 2007). In the literature, low frequency variations in $\delta^{13}C$ of tree-ring series from the late 19th and 20th century were generally linked with physiological responses to increasing atmospheric CO_2 concentrations in conjunction with declining atmospheric $\delta^{13}C$ (e.g. Feng, 1998), while high frequency fluctuations in $\delta^{13}C$ were related to climatic variables (Feng and Epstein, 1995; Hemming et al., 1998; Tang et al., 1999). Here, we present chronologies of tree-ring width and $\delta^{13}C$ of five Spanish forests for the last two centuries. The aim of this investigation was to assess the nature and strength of the climatic signal recorded in ring-width and $\delta^{13}C$ chronologies.

Material and methods

Five forest stands were sampled in the Iberian Peninsula (Fig 1). One *Pinus nigra* stand located in the southeast

(*pn*Caz), two *P. sylvestris* forests in the north and the northwest (*ps*Tej and *ps*Lil, respectively) and two *P. uncinata* forests in the north and northeast (*pu*Vin and *pu*Ped). *Ps*Tej and *pu*Vin are located only 10 km away from each other, allowing a better assessment of species-specific responses to similar climatic conditions previously discussed by Planells et al. (2007). Sampling focused on the oldest natural forest stands in the area. Site characteristics are described in Table 1. At each site, more than fifteen trees were cored with an increment borer at around 1.30 m stem height. At least four cores were taken from each tree: two for building ring-width chronologies and the rest for isotope analyses.

Ring-width chronologies

Cores were sanded until wood cells were clearly visible under the microscope (Stokes and Smiley, 1968). All samples were visually cross-dated following the procedures described by Yamaguchi (1991) to avoid miscounting by missing (locally absent) or false (multiple) rings. Afterwards, ring widths were measured with an accuracy of 0.01 mm using an ANIOL semi-automatic device (Aniol, 1983). The resulting series underwent a cross-dating quality control with the statistical program COFECHA (Holmes, 1983).

The individual ring width series were standardized to make them comparable (Fritts, 1976). Standardization was accomplished using the program TurboArstan, the windows version of Arstan (Cook, 1985). First, a power transformation of raw series was applied to stabilize variance (Cook and Peters, 1997; Helama et al., 2004). Second, the series were detrended by negative exponential or linear fitting. These conservative methods were applied to remove age related trends. Third, an autoregressive model was applied to remove autocorrelation leading to white-noise indices series. A robust mean, which reduces variance and bias caused by extreme values, was computed at the end of each step (Cook and Briffa, 1990). As a result, the standard chronologies "std_c" (detrended; Fig. 2), and the residual chronologies "res_c" (detrended without autocorrelation) were obtained. The reliable time span of the chronologies was determined by the Expressed Population Signal criteria (EPS > 0.85, Wigley et al., 1984). Descriptive statistics calculated using Cofecha and Arstan software are presented to allow comparisons among sites (Table 2). Since *ps*Tej std_c shows a lower EPS than 0.85, results of *ps*Tej std_c must be carefully interpreted.

Isotope chronologies

For *pn*Caz, *ps*Lil and *pu*Ped eight cross-dated samples from four different trees were selected (at least two cores per tree), while for *ps*Tej and *pu*Vin the chosen samples belonged to eight trees (one core per tree: Table 3).

For each site, tree-rings were separated and pooled year by year (Leavitt and Long, 1984; Treydte et al., 2001). α-cellulose was extracted to avoid isotope variations due to varying compositions of wood components such as lignin (Wilson and Grinsted, 1977) or resins which show a systematically different isotopic signature. The extraction of cellulose was based on the use of sodium hydroxide, sodium chlorite and acetic acid (Loader et al., 1997). The α-cellulose was homogenized in two different ways: *ps*Tej and *pu*Vin samples were ground with an ultra centrifugation mill (Retsch ZM1, mesh size of 0.5 mm), while samples from *pn*Caz, *ps*Lil and *pu*Ped were homogenized with an ultrasonic device developed at the Forschungszentrum Jülich GmbH, Germany. Carbon isotopes were measured by combusting α-cellulose to receive CO_2 in an elemental analyzer (Fisons NA 1500 NC) coupled via an open split to an isotope ratio mass spectrometer (Micromass Optima) operated in continuous flow mode. The precision was generally better than 0.1‰. The isotope signature expressed as $\delta^{13}C$ is given in the delta notation (‰), relative to the standard V-PDB (IAEA, 1995):

$$\delta^{13}C_{sample} = \left[\frac{(^{13}C/^{12}C)_{sample}}{(^{13}C/^{12}C)_{PDB}} - 1 \right] x1000$$

All $\delta^{13}C$ chronologies (raw data) show a decreasing trend which is attributed to the rise of ^{13}C-depleted atmospheric CO_2 due to fossil fuel burning and deforestation since industrialization (Fig. 3). Since the main goal of this study was to assess the climatic signal of these series, the raw $\delta^{13}C$ chronologies were corrected for changing atmospheric $\delta^{13}C$ (non-climatic trend) using data from ice cores and direct measurements (Leuenberger, 2006). As a result, we obtained the corrected $\delta^{13}C$ chronologies ($\delta^{13}C_c$). Similar to dendrochronological procedures, an autoregressive (AR) model that removes autocorrelation was applied using the program FMT from the DPL software (Holmes, 1992) resulting in autocorrelation free $\delta^{13}C$ tree-ring chronologies ($\delta^{13}C.AR_c$). Table 3 shows the main statistics of the raw data, as well as $\delta^{13}C_c$ and $\delta^{13}C.AR_c$ data.

Comparison among sites and proxies

To assess the inter-series relationships, Pearson correlation coefficients were calculated for the 20th century (1901-1999) among the ring-width chronologies (std_c and res_c), and the corrected $\delta^{13}C$ chronologies ($\delta^{13}C_c$ and $\delta^{13}C.AR_c$). Moreover, four Principal Component Analyses (PCAs) were computed to evaluate the shared variance among the different chronologies (std_c.PCA, res_c.PCA, $\delta^{13}C_c$.PCA, $\delta^{13}C.AR_c$.PCA). Additionally, to define the relationship between both proxies, two PCAs were done among the series with autocorrelation (std_c-$\delta^{13}C_c$.PCA) and

without autocorrelation (res_c-$\delta^{13}C.AR_c.PCA$).

Climate relationships

Correlation and response function analyses were performed using the program Dendroclim2002 (Biondi and Waikul, 2004) to quantify the climate-growth and the climate-$\delta^{13}C$ relationships. The used meteorological data corresponded to mean monthly temperature and total precipitation from 1931 to 2002. These data belong to a Spanish gridded data set (25 x 25 km grid-box) created by the *Instituto Nacional de Meteorologia* (INM). The nearest data set was selected for each site, choosing the same set for *ps*Tej and *pu*Vin due to their geographical proximity.

In order to avoid the problem of multi colinearity, i.e. interdependence commonly found in multi-variable sets of meteorological data, a stepwise multiple regression was computed on principal components to assess climate-growth relationships (response function analysis; Fritts, 1976). The significance of the calculated Pearson correlation and partial regression coefficients was computed based on 1000 bootstrapped iterations obtained by random extraction with replacement from the initial data set (Guiot, 1991). The analyzed period of tree growth was from previous July to October of the current year.

Results

Relationship among chronologies

Table 4 shows Pearson correlation coefficients among std_c and $\delta^{13}C_c$ for the 20th century. Few significant relationships were found between std_c, except for the highly significant correlation between *ps*Tej and *pu*Vin ($r=0.669$; $p<0.01$), the two sites located close to each other. This was the only case where std_c reached higher values than the corresponding $\delta^{13}C_c$. All the other correlations among $\delta^{13}C_c$ were higher and significant. The correlation between *ps*Lil and *pu*Vin turned out to be a particular case because it showed non-significant values between std_c and significant negative coefficients between $\delta^{13}C_c$. The $\delta^{13}C_c$ mean correlation (0.268±0.18) was higher than the std_c (0.156±0.22).

All Pearson correlation coefficients were higher among $\delta^{13}C.AR_c$ than among res_c for the 20th century (Table 5), except for two cases. As above, correlation between *ps*Tej and *pu*Vin was higher for res_c than for $\delta^{13}C.AR_c$. The same was found between *ps*Lil and *pu*Vin. A higher mean correlation with a smaller standard deviation (SD) was also found for $\delta^{13}C.AR_c$ (0.367±0.08) in comparison with res_c (0.324±0.17).

Table 6 shows that the first and the second principal components (PC1 and PC2, respectively) were significant in std_c.PCA, res_c.PCA and $\delta^{13}C_c$.PCA, while only PC1 was significant in

$\delta^{13}C.AR_c$.PCA. On the other hand, std_c-$\delta^{13}C_c$.PCA and res_c-$\delta^{13}C.AR_c$.PCA showed four and three significant PCs, respectively. Figure 4 illustrates the relationships between both kinds of parameters depicting the scatter plot of the PC1 and PC2 loadings. The PC1 shows positive and negative loadings for std_c and $\delta^{13}C_c$, respectively (Fig. 4a). Similarly, res_c and $\delta^{13}C.AR_c$ also show positive and negative loadings with PC1 (Fig. 4b). Despite the significance of other PCs, we focussed on the PC1 as it represents the maximum percentage of common variance shared by all the involved chronologies. Table 7 summarizes the correlations between both proxies at each site. All correlations were negative except for one, with most of them being low and not significant.

Comparisons within the same proxies improved correlations after removing autocorrelations from tree-ring series. All correlations were higher among res_c (Table 5) than among std_c (Table 4), improving the mean correlation from 0.156 (std_c) to 0.324 (res_c). The std_c.PC1 explained lower variance than the res_c.PC1 (Table 6).

Correlation coefficients among $\delta^{13}C_c$ (Table 4) generally also improved after autocorrelation removal (Table 5). The mean correlation increased from 0.268 ($\delta^{13}C_c$) to 0.367 ($\delta^{13}C.AR_c$). However, the differences between $\delta^{13}C_c$ and $\delta^{13}C.AR_c$ were found to be smaller than between std_c and res_c. The $\delta^{13}C_c$.PC1 explained lower variance than the $\delta^{13}C.AR_c$.PC1 (Table 6).

Climate relationships

Significant correlation and response function partial regression (RF) coefficients were found between both tree-ring proxies and climate. For each site, similar but not identical responses were found between std_c and res_c, as well as between $\delta^{13}C_c$ and $\delta^{13}C.AR_c$ (results not shown). However, no distinct pattern was found among sites concerning which series, with (std_c/$\delta^{13}C_c$) or without autocorrelation (res_c/$\delta^{13}C.AR_c$) showed the highest correlation with meteorological data. For example, while at the site of *pn*Caz, res_c and $\delta^{13}C_c$ achieved the highest values versus temperature and precipitation, a more heterogeneous picture emerged at the site of *ps*Lil. In the latter case the highest correlations with temperature were found with std_c and $\delta^{13}C_c$, but the highest correlations with precipitation were found using res_c and $\delta^{13}C.AR_c$. *Pu*Ped, *Ps*Tej and *pu*Vin also revealed a rather mixed behaviour depending on the standardization method and the meteorological variables chosen.

For the assessment of the nature and strength of the climatic signal recorded in ring-width and $\delta^{13}C$ chronologies, considering similar frequency domain we can either use std_c and $\delta^{13}C_c$ or res_c and $\delta^{13}C.AR_c$. Although removing autocorrelation did not result in a clearer climatic signal for all the

chronologies, res_c versus $\delta^{13}C.AR_c$ were chosen for further detailed explanations because all the residual chronologies (res_c) achieved a reliable EPS for the studied period (Table 2).

Res_c-climate relationships

Figure 5 shows the significant correlation and RF coefficients found between res_c and meteorological data. Non-uniform relationships among the sites with their corresponding meteorological data sets were found. *Pn*Caz from southern Spain revealed significant RF coefficients with previous September (-0.195), current February (0.243) and June temperature (-0.190), as well as current June precipitation (0.165). However, the highest correlation (-0.425) and RF coefficients were found between ring width and current September precipitation. *Ps*Lil, in the northwest, showed significant positive correlations with June and July precipitation of the current growing period (0.343 and 0.337, respectively). *PuP*ed located in the northeast only showed significant positive correlation coefficients with temperature prior to the year of ring formation (July: 0.227; August: 0.227; October: 0.335; November: 0.343), with November also being significant in RF analysis. *Ps*Tej revealed a significant correlation with temperature of previous September (-0.238) and November (0.248), as well as with current January (0.242), August (0.247) and October (-0.271), with a significant RF coefficient only in October. Finally, *pu*Vin revealed a significant correlation with temperature of previous November (0.280), current May (0.216) and August (0.320), as well as precipitation of current May (-0.265), and also showing significant RF coefficients for temperature of previous November and current August and October.

$\delta^{13}C.AR_c$-climate relationships

Figure 6 shows correlation and RF coefficients established between the $\delta^{13}C.AR_c$ and the meteorological data. During summer months, all $\delta^{13}C$ chronologies displayed significant negative correlations with summer precipitation of the current year: *pn*Caz (July: -0.362), *ps*Lil (June: -0.306; July: -0.325), *pu*Ped (June: -0.428; July: -0.472), *ps*Tej (June: -0.311; July: -0.299; August: -0.465) and *pu*Vin (July: -0.225). Accordingly, the corresponding RF coefficients were found to be significant in many cases (Fig. 6). Besides, all $\delta^{13}C.AR_c$ showed significant positive correlation coefficients with summer temperatures of the current year: *pn*Caz (September: 0.263), *ps*Lil (July: 0.243), *pu*Ped (June: 0.341; July: 0.385; August: 0.385), *ps*Tej (June: 0.212; August: 0.266) and *pu*Vin (August: 0.272). It should be noted that the two sites, namely *ps*Tej and *pu*Vin, located only 10 km away from each other did not react evenly, showing different patterns of significance in their variables.

Discussion

Common variability

One of the main dendrochronological principles is the assumption that common information shared among trees in a stand can be regarded as climatic information (Cook and Briffa, 1990). Hence, on a broader scale, the common variability shared by the five chronologies across the Iberian Peninsula might be due to climate, as was reported using a network of thirty-eight ring-width chronologies by Andreu et al. (2007). In a similar frequency domain, correlations among the $\delta^{13}C$ chronologies were higher than between the ring width series. Accordingly, the variance explained by the PC1 showed that $\delta^{13}C$ variations at different sites presented more similarities than ring width variations. The same finding was described by Saurer et al. (1995), who also suggested climate as the main cause of the strong similarities between $\delta^{13}C$ series from two sites. According to this, the higher and more homogenous agreement found among the carbon isotope records in comparison with ring widths suggests that $\delta^{13}C$ ratios may better record large scale climatic signals than ring-width variations. Furthermore, the highest correlation was found between the two ring-width chronologies of the sites located close to each other (*ps*Tej and *pu*Vin), while between these two $\delta^{13}C$ chronologies, the correlation coefficient was lower, presenting a similar value than coefficients between the other $\delta^{13}C$ series. Therefore, our results point out that ring-width series may reflect local factors, while $\delta^{13}C$ ratios may contain a wider spatial climatic signal. Gagen et al. (2004) by examining high-frequency variability found that $\delta^{13}C$ series are less sensitive to local conditions than growth proxies. Studies by Robertson et al. (1997a, b) also demonstrated that significant climate signals are contained in isotopic proxies of tree-rings, while ring-widths contained little or no such information.

Ring width-$\delta^{13}C$ relationship

Correlations (Table 7) and the PC1s (Fig. 4) reveal a negative relationship between ring-widths and $\delta^{13}C$ values. Although the inter-annual variability of both parameters is related to climatic variations, the same climate variable can lead to opposite reactions with regard to the two proxies. This is, however, not surprising because the basic biochemical and plant physiological reactions are directly controlled by meteorological quantities such as temperature or precipitation, while the isotopic signal is only indirectly governed by these quantities. For instance, warm and dry summers normally produce narrow rings (less growth) but give rise to high $\delta^{13}C$ values due to a strong reduction of the stomatal aperture as a measure for preventing unnecessary water loss. Discrimination against the heavier stable carbon isotope (^{13}C) is lower

under dry conditions because of reduced intercellular CO_2 concentration due to which the photosynthetic apparatus cannot afford a generous selection of the lighter ^{12}C isotope, thus leading to higher $\delta^{13}C$ values in tree-rings (Francey and Farquhar, 1982; Hemming et al., 1998). Thus, long and severe droughts generally correspond to narrow rings and less negative $\delta^{13}C$ values. The assessment of the climatic signal recorded in these series confirmed that ring-width and $\delta^{13}C$ chronologies contain different climatic information (see sections below).

Climatic signal and frequency domain

The autoregressive modelling was considered by Cook and Briffa (1990) a technique that removes noise or non-climatic variability from tree-ring series. Our results highlight a higher agreement among chronologies after removing autocorrelation (due to an enhancement of the current year climatic signal), finding higher correlations among res_c than among std_c, as well as among $\delta^{13}C.AR_c$ than among $\delta^{13}C_c$. According to these facts, Robertson et al. (1997a, b) also reported that both ring-width and $\delta^{13}C_c$ indices record high-frequency common forcing better than lower-frequency forcing.

Although our chronologies showed higher similarities without autocorrelation, we did not distinguish patterns concerning which series, with or without autocorrelation, correlate better with meteorological variables, finding a wide range of responses depending on sites, frequency domain and meteorological variables chosen. Some authors (e.g. Roberston et al., 1997a,b; Treydte et al., 2001) used the same statistical treatment for meteorological series as for tree-ring chronologies to compare the same frequency domain. However, in this work, we used raw meteorological data without applying any detrending or filtering in order to preserve the original temporal structure of these series. This could be one of the reasons for the heterogeneous picture found, as each local meteorological series can provide the highest agreement with tree-ring series in different frequency domains since each chronology may record different climatic signals. Another possible explanation is that while common variance among chronologies is related to macroclimate, our meteorological variables represent local climate.

Climatic sensitivity of ring-width and $\delta^{13}C$ chronologies

*Pn*Caz growth was constrained by water stress during late summer and early autumn of the preceding year as was displayed by the negative relationship with previous September and October temperature and positive correlation with previous September precipitation. Warm late summers can prolong the growing season, limiting the formation of metabolic reserves

and consequently affecting radial growth in the following year (Fritts, 1976). Growth also showed a positive response to warm February causing an early beginning of the growing season. Due to the fact that *pn*Caz was the driest studied site, water stress seemed to start rather early, i.e. already in June, at the beginning of the summer season. Similar results were reported for *P. nigra* in the southeast of Spain (Richter and Eckstein, 1991), except for the negative relationship found with September precipitation. However, Ferrio et al. (2003) found the only significant (negative) relationship between precipitation and radial growth in *Quercus ilex* for September. *P. sylvestris* growth in the northwest of Spain (*ps*Lil) also seems to be sensitive to the lack of water during summer (June-July). The other stands did not respond to summer drought, being only sensitive to temperature. *Ps*Tej, the other *P. sylvestris* site, showed a positive response to warm August. Similarly, the nearby *P. uncinata* site (*pu*Vin) also showed a positive response to warm August, as well as a general negative response to precipitation, especially to May. This is probably related to a negative effect of late spring snow falls that can delay the starting of the growing season. Finally, *pu*Ped was not sensitive to precipitation. Nevertheless, a positive response to summer and autumn temperatures of the previous year was found. The positive response to November temperature of the preceding year shared by the two *P. uncinata* sites has also been reported in the Pyrenees (Tardif et al., 2003).

The negative response to summer rainfall detected in all $\delta^{13}C$ records showed that $\delta^{13}C$ chronologies were highly sensitive to precipitation. This tends to indicate that at no one of the sites water is available in sufficient quantities during summer season. To a lesser degree, $\delta^{13}C$ records were also sensitive to temperature, but this response was weaker and less homogenous among sites. Different results in $\delta^{13}C$ response observed between the two nearest chronologies (*ps*Tej and *pu*Vin) may be due to species-specific and/or aspect differences of the stands. However, Treydte et al. (2001) reported that site exposure influenced the absolute $\delta^{13}C$ values, but did not necessarily obscure the climatic signal of the stable isotope records.

The photosynthetic demands and needs are basically governed by climatic quantities which in turn control CO_2 diffusion into the leaves and the biochemical turn over during photosynthetic CO_2 assimilation. These two processes are, however, the key processes for the fractionation of the carbon isotopes (Francey and Farquhar, 1982). Hence, $\delta^{13}C$ is largely controlled by the relative CO_2 diffusion rates. High (less negative) $\delta^{13}C$ values reflect low concentrations of CO_2 in the stomatal chambers, including intercellular air spaces which

may be due to low stomatal conductance and/or high photosynthetic rates, or some combination of both processes (McCarroll and Pawellek, 2001). Thus, $\delta^{13}C$ values indicate most likely the balance between stomatal conductance (related to air relative humidity and antecedent rainfall) and photosynthetic rate (related to temperature and photon flux). Therefore, sensitivity to precipitation and temperature (linked to air relative humidity) suggests that the variability of $\delta^{13}C$ was mainly controlled by stomatal conductance in all the studied sites. However, it should be kept in mind, that temperature is also affecting the photosynthetic rate. The finding of a strong dependence of tree-ring $\delta^{13}C$ with water availability as a strong and consistent climatic control common among all the studied stands was in agreement with the spatially broad and homogeneous common signal shared by the $\delta^{13}C$ chronologies.

The climatic sensitivity detected for ring width was different to that recorded for isotopic ratios in all the sites. Each ring-width chronology showed its own particular relationship with climate according to the variety of stand features and local climatic conditions. In contrast, a common negative response to summer precipitation, as well as a positive response to summer temperature (though the latter less pronounced) was shared by all $\delta^{13}C$ chronologies. Therefore, drought stress during the summer season was more distinct in $\delta^{13}C$ chronologies than in ring-width series, indicating that $\delta^{13}C$ is a valuable integrator of water availability. This highlights the potential of isotopic ratios as a useful tool for climatic reconstruction when relationships between climate and ring-width are weak.

In contrast to our findings, there was no significant correlation between precipitation and $\delta^{13}C$ of cold and moist northern Eurasian chronologies, as in these regions $\delta^{13}C$ is temperature sensitive (Saurer et al., 2004). However, studies from Mediterranean or semi-arid sites showed that the $\delta^{13}C$ of Iberian *P. halepensis* was highly dependent on water availability (Ferrio and Voltas, 2005). $\delta^{13}C$ of Californian conifers (Feng and Epstein, 1995) and Australian grasstrees and conifers (Swanborough et al., 2003) were also shown to be inversely correlated with rainfall. $\delta^{13}C$ of latewood cellulose from pine trees growing in dry subalpine environments in French Alps provide a powerful proxy measure of past changes in summer moisture stress, the strongest signal being the total precipitation of July and August (Gagen et al., 2004). These results are comparable to several other tree-ring $\delta^{13}C$ studies in central Switzerland for *Fagus sylvatica* (Saurer et al., 1995), *Picea abies* (Anderson et al., 1998) or in the Swiss Alps for *Picea abies* (Treydte et al., 2001). According to that, Warren et al. (2001) remarked that $\delta^{13}C$ may be a useful indicator of

drought stress, but only in seasonally dry climates. The reported results by all these studies agreed with our findings. The observed responses indicate that $\delta^{13}C$ is strongly dependent on local conditions (i.e. dry sites; Saurer et al., 1995), but also suggest that trees growing under Mediterranean climate tend to show a strong precipitation signal.

Acknowledgements

We are very grateful to Oriol Bosch, Montse Ribas, Elena Muntán, Mariano Barriendos, Carlos Almarza, Pedro Antonio Tíscar, Marc Filot, Markus Leuenberger and Heinz Vos for their help during sampling, laboratory work and manuscript preparation. This research was funded by EU project ForMAT (Contract ENV4-CT97-0641), EU project ISONET (Contract EV K2-2001-00237) and EU FP6 project Millennium (GOCE 017008).

References

Anderson W. T., Bernasconi S. M., McKenzie J. A. and Saurer M. 1998. Oxygen and carbon isotopic record of climatic variability in tree ring cellulose (*Picea abies*): An exemple from central Switzerland (1913-1995). *J. Geophys. Res.* **103**(D24), 31625-31636.

Andreu L., Gutiérrez E., Macias M., Ribas M., Bosch O. and Camarero J. J. 2007. Climate increases regional tree growth variability in Iberian pine forests. *Global Change Biol.* **13**, 804-815, doi: 10.1111/j.1365-2486.2006.01322.x

Aniol R. W. 1983. Tree-ring analysis using CATRAS. *Dendrochronolgia* **1**: 45-53.

Biondi F. and Waikul K. 2004. DENDROCLIM2002: A C++ program for statistical calibration of climate signals in tree-ring chronologies. *Comput Geosci-UK* **30**, 303-311.

Blanco E., Casado M. A., Costa M., Escribano R., García M., Génova M., Gómez A., Gómez F., Moreno J. C., Morla C., Regato P. and Sainz H. 1997. *Los bosques ibéricos*. Editorial Planeta, Barcelona, 572 pp.

Cook E. R. 1985. A time series analysis approach to tree-ring standardization. DS thesis, University of Arizona, Tucson.

Cook E. R. and Briffa K. R. 1990. Data Analysis. In: *Methods of dendrochronology* (eds Cook ER and Kairiukstis LA), pp. 97-162. Kluwer, Boston.

Cook E. R. and Peters K. 1997. Calculating unbiased tree-ring indices for the study of climatic and environmental change. *Holocene* **7**, 359-368.

Feng X. and Epstein S. 1995. Carbon isotopes of trees from arid enviornments and implications for reconstructing atmospheric CO_2 concentration. *Geochim. Cosmochim. Acta* **59**(12), 2599-2608.

Feng X. 1998. Long-term c_i/c_a response of trees in western North America to atmospheric CO_2 concentration derived from carbon isotope chronologies. *Oecologia* **117**, 19-25.

Ferrio J. P., Florit A., Vega A., Serrano L. and Voltas J. 2003. $\Delta^{13}C$ and tree-ring width reflect different drought responses in *Quercus ilex* and *Pinus halepensis*. *Oecologia* **137**, 512-518.

Ferrio J. P. and Voltas J. 2005. Carbon and oxygen isotope ratios in wood constituents of *Pinus halepensis* as indicators of

precipitation, temperature and vapour pressure deficit. *Tellus* **57B**, 164-173.

Francey R. J. and Farquhar G. D. 1982. An explanation of $^{13}C/^{12}C$ variations in tree-rings. *Nature* **297**, 28-31.

Fritts H. C. 1976. *Tree rings and climate*. Academic Press, New York, 433 pp.

Gagen M., McCarroll D. and Edouard J.-L. 2004. Latewood width, maximum density, and stable carbon isotope ratios of pine as climate indicators in a dry subalpine environment, French Alps. *Arct. Antarct. Alp. Res.* **36**, 166-171.

Gagen M., McCarroll D. and Edouard J.-L. 2006. Combining ring width, density and stable carbon isotope proxies to enhance the climatic signal in tree-rings: an example from the southern French Alps. *Clim. Change* **78**, 363-379.

Guiot J. 1991. The bootstrapped response function. *Tree-Ring Bull*. **51**, 39–41.

Helama S., Lindholm M., Timonen M. and Eronen M. 2004. Detection of climate signal in dendrochronological data analysis: a comparison of tree-ring standardization methods. *Theor. Appl. Climatol*. **79**, 239-254.

Helle G., Schleser G. H. and Bräuning A. 2002. Climate History of the Tibetan Plateau for the last 1500 years as inferred from stable carbon isotopes in tree-rings. *IAEA CN*-**80-80**, 301-311

Helle G. and Schleser G. H. 2004. Interpreting climate proxies from tree-rings. In: *Towards a synthesis of Holocene proxy data and climate models* (eds Fischer H., Floeser G., Kumke T., Lohmann G., Miller H., Negendank J. F. W. and von Storch H.), 129-148 pp. Springer Verlag, Berlin.

Hemming D. L., Switsur V. R., Waterhouse J. S., Heaton T. H .E. and Carter A. H. C. 1998. Climate variation and the stable carbon isotope composition of tree ring cellulose: an intercomparison of *Quercus robur*, *Fagus sylvatica* and *Pinus sylvestris*. *Tellus* **50B**, 25-33.

Holmes R. L. 1983. Computer-assisted quality control in tree-ring dating and measurement. *Tree-Ring Bull.* **43**, 68-78.

Holmes R. L. 1992. Dendrochronology program library. Version 1992-1. Laboratory of Tree-Ring Research, University of Arizona, Tucson.

IAEA 1995. TECDOC-825. Reference and Intercomparison Materials for Stable Isotopes of Light Elements, Proceedings of a Consultants Meeting, 1-3 December 1993, Vienna.

IPCC 2001. Chapter 13. Europe. In: *Climate Change 2001: Impacts, Adaptation and Vulnerability. Contribution of Working Group II to the the Third Assessment Report of the Intergovernmental Panel on Climate Change* (eds. McCarthy J. J., Canziani O. F., Leary N. A., Dokken D. J. and White K. S.), pp. 643-681. Cambridge University Press, Cambridge.

Klein T., Hemming D., Lin T., Grünzweig J. M., Maseyk K., Rotenberg E. and Yakir D. 2005. Association between tree-ring and needle $\delta^{13}C$ and leaf gas exchange in *Pinus halepensis* under semi-arid conditions. *Oecologia* **144**, 45-54.

Leavitt S. W. and Long A. 1984. Sampling strategy for stable carbon isotope analysis of tree rings in pine. *Nature* **311**, 145-147.

Leuenberger M. 2006. To what extent can ice core data help to understand biological systems? In: *Isotopes as Tracers of Ecological Change.* (eds. Dawson T. and Siegwolf R.), Elsevier Academic Press.

Loader N. J., Robertson I., Barker A. C., Switsur V. R. and Waterhouse J. S. 1997. An improved method for the batch processing of small wholewood samples to α-cellulose. *Chem. Geol.* **136**(3-4), 313-317.

Macias M., Andreu L., Bosch O., Camarero J. J. and Gutiérrez E. 2006. Increasing aridity is enhancing silver fir (*Abies alba* Mill.) water stress in its south-western distribution limit. *Clim. change* **79**, 289-313, doi: 10.1007/s10584-006-9071-0

Matzner S. L., Rice K. J. and Richards J. H. 2001. Factors affecting the relationship between carbon isotope discrimination and transpiration efficiency in blue oak (*Quercus douglasii*). *Aust. J. Plant Physiol*. **28**(1), 49-56.

McCarroll D. and Pawellek F. 2001. Stable carbon isotope ratios of *Pinus sylvestris* from northern Finland and the potential for extracting a climate signal from long Fennoscandian chronologies. *Holocene* **11**(5), 517-526.

Panek J. A. 1996. Correlations between stable carbon-isotope abundance and hydraulic conductivity in Douglas-fir across a climate gradient in Oregon, USA. *Tree Physiol.* **16**, 747-755.

Panek J. A. and Goldstein A. H. 2001. Response of stomatal conductance to drought in ponderosa pine: implications for carbon and ozone uptake. *Tree Physiol.* **21**(5), 337-344

Peñuelas J., Lloret F. and Montoya R. 2001. Severe Drought Effects on Mediterranean Woody Flora in Spain. *For. Sci.* **47**(2), 214-218.

Planells O., Gutiérrez E., Helle G. and Schleser G. H. 2007. Assessment of 20th century ring width, $\delta^{13}C$ and $\delta^{18}O$ of two pine species from the Iberian System (Spain) as climate proxy series. *Clim. change*.

Ponton S., Dupouey J. L., Bréda N., Feuillat F., Bodénès C. and Dreyer E. 2001. Carbon isotope discrimination and wood anatomy variations in mixed stands of *Quercus robur* and *Quercus petraea*. *Plant Cell Environ.* **24**(8), 861-868

Richter K. and Eckstein D. 1991. The dendrochronological signal of pine trees (*Pinus* spp.) in Spain. *Tree-Ring Bull.* **51**, 1-13.

Robertson I., Rolfe J., Switsur V. R., Carter A. H. C., Hall M. A., Barker A. C. and Waterhouse J. S. 1997a. Signal strength and climate relationship in $^{13}C/^{12}C$ ratios of tree ring cellulose from oak in southwest Finland. *Geophys. Res. Lett*. **24**, 1487-1490.

Robertson I., Switsur V. R., Carter A. H. C., Barker A. C., Waterhouse J. S., Briffa K. R. and Jones P. D. 1997b. Signal strength and climate relationship in $^{13}C/^{12}C$ ratios of tree ring cellulose from oak in east England. *J. Geophys. Res*. **102**, 19507-19516.

Saurer M., Siegenthaler U. and Schweingruber F. H. 1995. The climate-carbon isotope relationship in tree rings and the significance of site conditions. *Tellus* **47B**, 320-330.

Saurer M., Siegwolf R. T. W. and Schweingruber F. H. 2004. Carbon isotope discrimination indicates improving water-use efficiency of trees in northern Eurasia over the last 100 years. *Global Change Biol.* **10**, 2109-2120.

Stokes M. A. and Smiley T. L. 1968. *An introduction to tree-ring dating*. University of Chicago Press, Chicago, 73 pp.

Swanborough P. W., Lamont B. B. and February E. C. 2003. $\delta^{13}C$ and water-use efficiency in Australian grasstrees and South African conifers over the last century. *Oecologia* **136**, 205-212.

Tang K., Feng X. and Funkhouser G. 1999. The $\delta^{13}C$ of tree rings in full-bark and strip-bark bristlecone pine trees in the White Mountains of California. *Global Change Biol.* **5**, 33-40.

Tardif J., Camarero J. J., Ribas M. and Gutiérrez E. 2003. Spatiotemporal variability in tree growth in the central Pyrenees: climatic and site influences. *Ecol. Monogr.* **73**(2), 241-257.

Treydte K., Schleser G. H., Schweingruber F. H. and Winiger M. 2001. The climatic significance of $\delta^{13}C$ in subalpine spruces (Lötschental, Swiss Alps). *Tellus* **53B**, 593-611.

Warren C. R., McGrath J. F. and Adams M. A. 2001. Water availability and carbon

isotope discrimination in conifers. *Oecologia* **127**, 476-486.

Wigley T. M. L., Briffa K. R. and Jones P. D. 1984. On the average value of correlated time series, with applications in Dendroclimatology and Hydrometeorology. *J. Clim. Appl. Meterol.* **23**, 201-213.

Williams D. G. and Ehleringer J. R. 1996. Carbon isotope discrimination in three semi-arid woodland species along a monsoon gradient. *Oecologia* **106**, 455-460.

Wilson A. T. and Grinsted M. J. 1977. $^{12}C/^{13}C$ in cellulose and lignin as palaeothermometers. *Nature* **265**, 133-135.

Yamaguchi D. K. 1991. A simple method for cross-dating increment cores from living trees. *Can. J. For. Res.* **21**, 414-416.

Table 1. Location and characteristics of the study sites.

Site	Species	Site code	Range	Latitude	Longitude	Altitude (m a.s.l.)	Aspect	Stand type
Cazorla	*Pinus nigra*	*pn*Caz	Betic	37º 48' N	02º 57' W	1800	SW	open forest
Pinar de Lillo	*P. sylvestris*	*ps*Lil	Cantabrian	43º 03' N	05º 15' W	1600	NW	mainly open forest
Pedraforca	*P. uncinata*	*pu*Ped	Pre-Pyrenees	42º 14' N	01º 42' E	2100	E	open forest
Tejeros	*P. sylvestris*	*ps*Tej	Urbión	42° 00' N	02º 49' W	1750	NE	closed forest
Vinuesa	*P. uncinata*	*pu*Vin	Urbión	41° 58' N	02º 45' W	1950	SW	closed forest

Table 2. Mean correlation of the tree-ring chronologies calculated using COFECHA software for the 1800-2002 period. Mean Sensitivity (MS_x), a measure of the inter-annual variability, first order autocorrelation (AC1) for std_c and res_c, and the expressed population signal statistic (EPS) were calculated for the 1901-1999 period using the ARSTAN software.

Site ID	Time span	Trees/ radii	Mean correlation	std_c		res_c		EPS (1901-1999)		
				MS_x	AC1	MS_x	AC1	Tree/radii	std_c	res_c
*pn*Caz	1800-2002	29/53	0.682	0.14	0.60	0.16	0.00	24/36	0.925	0.957
*ps*Lil	1800-2002	21/44	0.594	0.11	0.69	0.13	0.03	19/40	0.876	0.89
*pu*Ped	1800-2003	21/53	0.591	0.08	0.67	0.10	-0.01	19/45	0.902	0.906
*ps*Tej	1800-1999	15/25	0.579	0.09	0.73	0.11	0.07	12/20	0.764	0.854
*pu*Vin	1800-1999	17/32	0.571	0.09	0.64	0.11	0.01	9/16	0.844	0.878

Table 3. Statistics of raw, corrected ($\delta^{13}C_c$) and without autocorrelation ($\delta^{13}C.AR_c$) $\delta^{13}C$ tree-ring chronologies. Min: Minimum; Max: Maximum; PAC1: First order partial Autocorrelation (PAC1).

Site ID	Time-span	Trees/ Cores	raw $\delta^{13}C$ (‰)					$\delta^{13}C_c$ (‰)					$\delta^{13}C.AR_c$ (‰)	
			Mean ± SD	Min	Max	Range	PAC1	Mean ± SD	Min	Max	Range	PAC1	Mean ± SD	PAC1
*pn*Caz	1800-2002	4/9	-21.38 ± 0.62	-22.9	-20.4	2.46	0.81	-20.95 ± 0.35	-22.0	-20.2	1.75	0.43	0.98 ± 0.32	0.06
*ps*Lil	1800-2002	4/10	-22.53 ± 0.63	-24.2	-21.1	3.05	0.51	-22.11 ± 0.52	-23.5	-21.0	2.46	0.32	0.92 ± 0.49	-0.05
*pu*Ped	1800-2002	4/8	-22.35 ± 0.56	-24.3	-21.0	3.32	0.47	-21.93 ± 0.45	-23.2	-20.6	2.64	0.15	0.94 ± 0.45	-0.13
*ps*Tej	1900-1999	8/8	-23.55 ± 0.58	-24.9	-22.5	2.36	0.66	-22.86 ± 0.37	-24.0	-21.9	2.05	0.21	1 ± 0.36	0.01
*pu*Vin	1800-1999	8/8	-21.91 ± 0.82	-24.5	-20.3	4.27	0.83	-21.5 ± 0.5	-23.0	-20.2	2.85	0.57	1 ± 0.39	-0.02

Table 4. Pearson correlation coefficients among std_c (left within each column) and $\delta^{13}C_c$ (right) of different sites. * p<0.05; ** p<0.01; numbers in bold indicates the highest or more significant coefficients between each pair of correlation.

std_c mean ± SD 0.156 ± 0.22	$\delta^{13}C_c$ mean ± SD **0.268** ± 0.18	*pn*Caz	*ps*Lil		*pu*Ped		*ps*Tej		*pu*Vin	
*pn*Caz		1	0.037	**0.250***	-0.022	**0.325****	0.244*	**0.346****	0.218*	**0.223***
*ps*Lil			1		-0.129	**0.364****	0.203*	**0.374****	0.012	-0.204*
*pu*Ped					1		0.136	**0.360****	0.188	**0.255***
*ps*Tej							1		**0.669****	0.384**
*pu*Vin									1	

Table 5. Pearson correlation coefficients among res_c (left within each column) and $\delta^{13}C.AR_c$ (right) of different sites. * p<0.05; ** p<0.01; numbers in bold indicates the highest or more significant coefficients between each pair of correlation.

res_c mean ± SD 0.324 ± 0.17	$\delta^{13}C.AR_c$ mean ± SD **0.367** ± 0.08	*pn*Caz	*ps*Lil		*pu*Ped		*ps*Tej		*pu*Vin	
*pn*Caz		1	0.278**	**0.310****	0.013	**0.309****	0.296**	**0.321****	0.223*	**0.303****
*ps*Lil			1		0.188	**0.349****	0.388**	**0.456****	**0.343****	0.251*
*pu*Ped					1		0.361**	**0.439****	0.442**	**0.465****
*ps*Tej							1		**0.680****	0.466**
*pu*Vin									1	

Table 6. Number of chronologies involved in each PCA performed among chronologies and the variance explained by each significant PC. ns: non significant.

		Variance (%)			
PCAs	Nº chronologies	PC1	PC2	PC3	PC4
std_c	5	37.4	23.2	ns	ns
res_c	5	47.5	20.6	ns	ns
$\delta^{13}C_c$	5	42.4	24.1	ns	ns
$\delta^{13}C.AR_c$	5	49.4	ns	ns	ns
std_c - $\delta^{13}C_c$	10	25.3	17.6	16.9	10.0
res_c – $\delta^{13}C.AR_c$	10	29.3	21.1	10.1	ns

Table 7. Pearson correlation coefficients between ring-width (std_c or res_c) and $\delta^{13}C$ chronologies ($\delta^{13}C_c$ or $\delta^{13}C.AR_c$) at each site. * p<0.05; ** p<0.01.

	*pn*Caz	*ps*Lil	*pu*Ped	*ps*Tej	*pu*Vin	Mean ± SD
std_c vs $\delta^{13}C_c$	0.050	-0.026	-0.183	-0.169	-0.394**	-0.144 ± 0.17
res_c vs $\delta^{13}C.AR_c$	-0.016	-0.126	-0.205*	-0.130	-0.274**	-0.150 ± -0.07

Figure 1

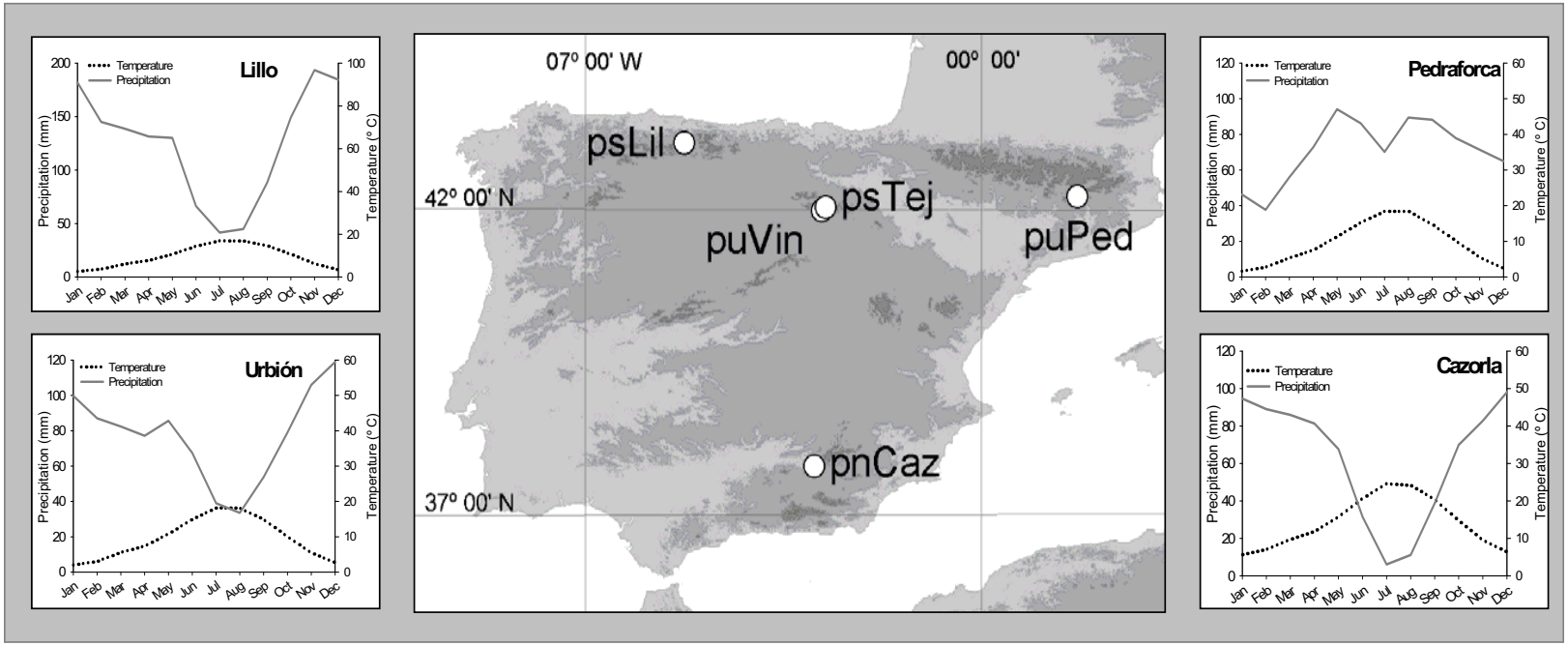

Geographical location of the studied sites in the Iberian Peninsula and ombrotermic climate diagrams of each region.

Figure 2

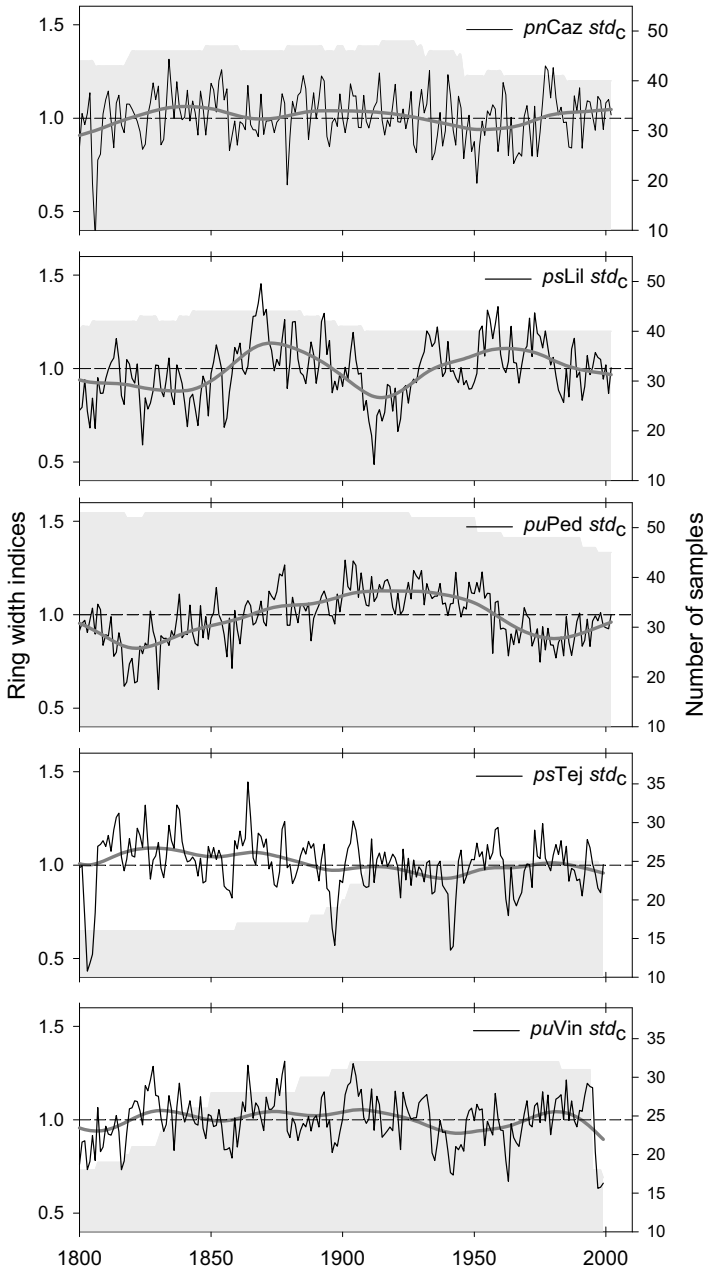

Standard ring-width chronologies "std_c" (black lines). Just to show long-term fluctuations, 50-year smoothing splines fitted on std_c (thick grey lines) are depicted. Sample depths are shown as grey areas (right axis).

Figure 3

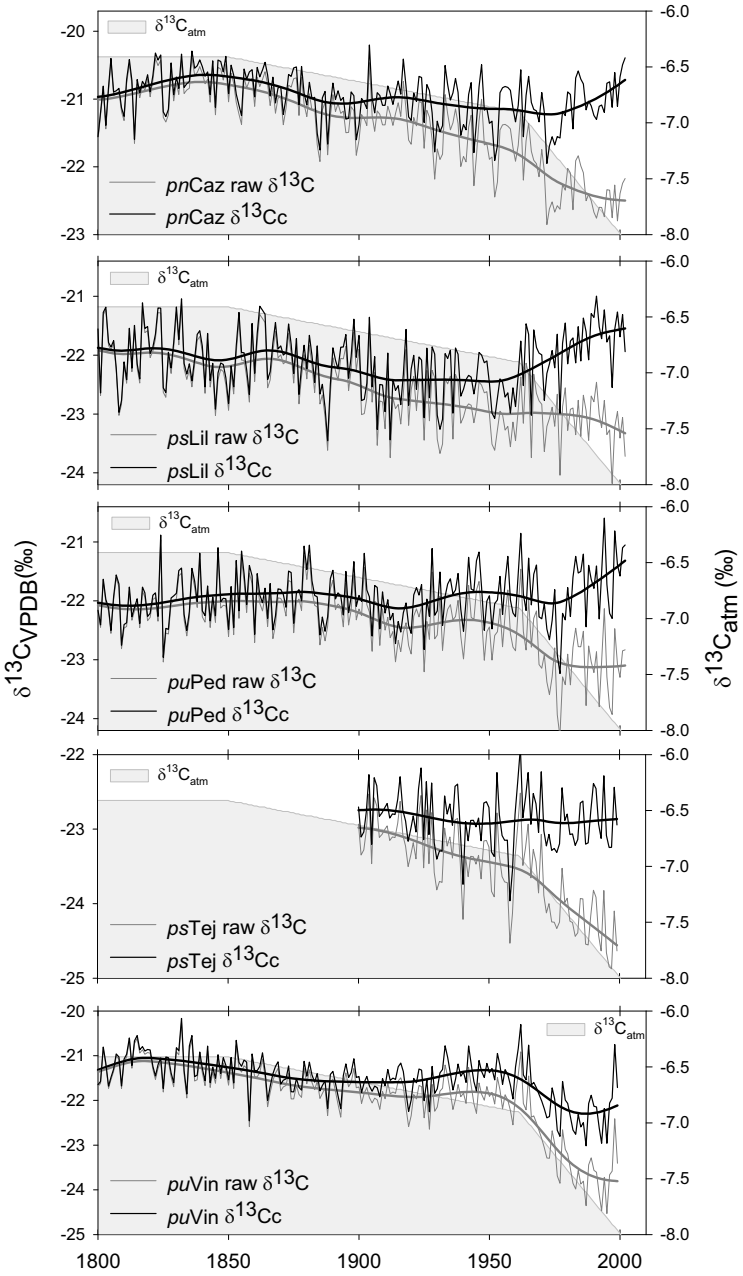

Raw $\delta^{13}C$ chronologies (grey lines) and corrected $\delta^{13}C$ chronologies "$\delta^{13}C_c$" (black lines), see methodology for details. Just to show long-term fluctuations, 50-year smoothing splines fitted on the raw $\delta^{13}C$ chronologies (thick grey lines) and $\delta^{13}C_c$ (thick black lines) are depicted. The $\delta^{13}C_{atm}$ decrease is shown by the grey area (right axis).

Figure 4

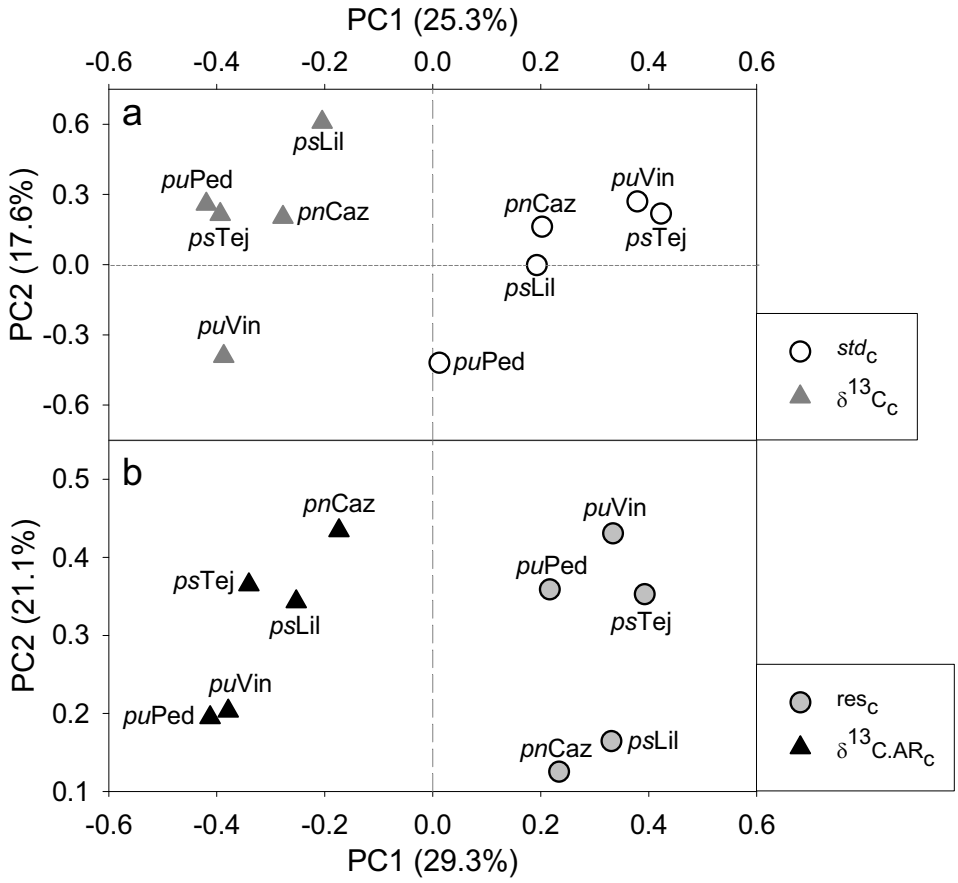

Scatter plot of PC1 and PC2 loadings of the PCA performed for the ring-width and $\delta^{13}C$ chronologies for the 20th century: a) with autocorrelation (std_c and $\delta^{13}C_c$); b) without autocorrelation (res_c and $\delta^{13}C.AR_c$).

Figure 5

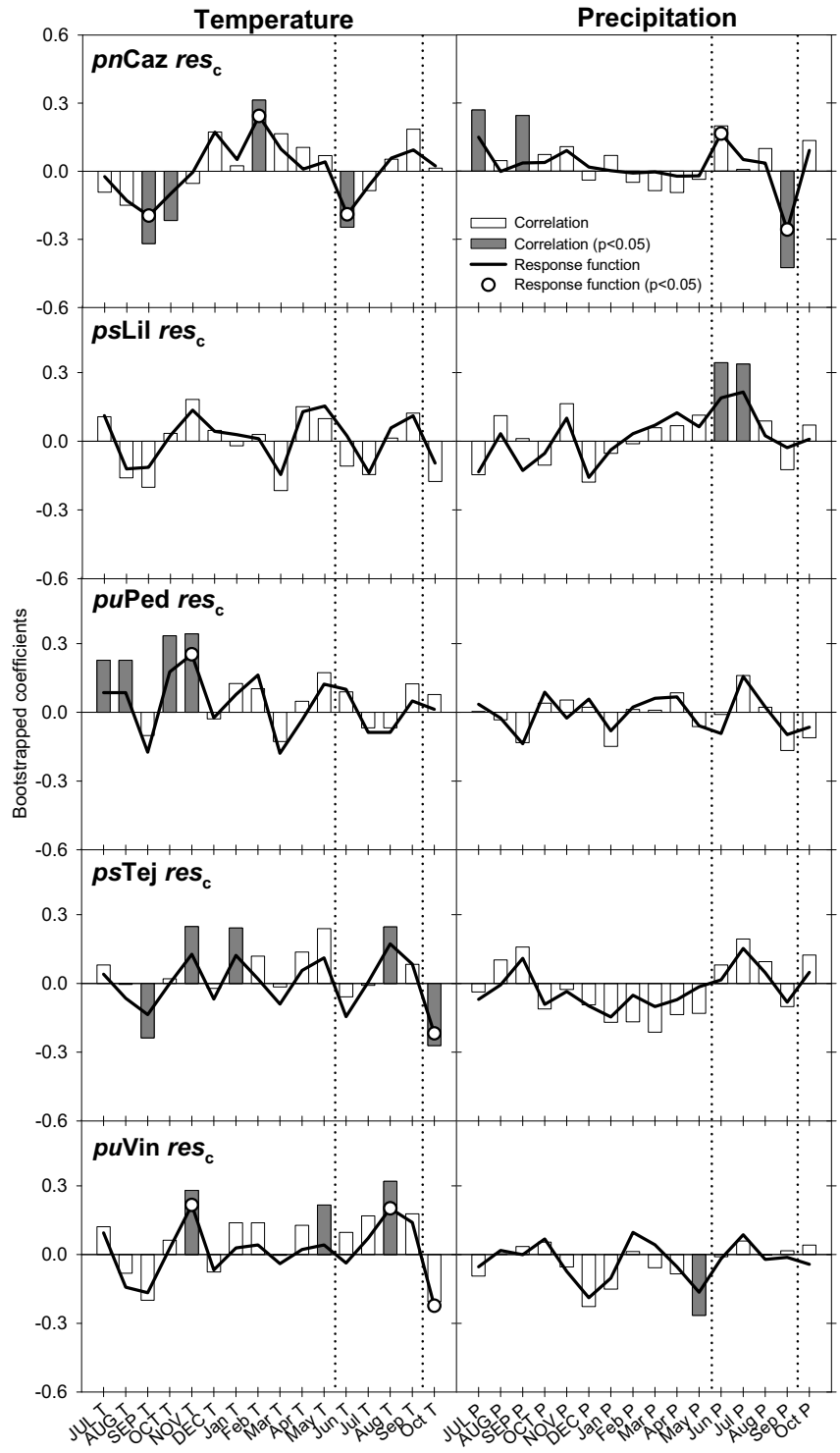

Bootstrapped correlations (bars) and response functions (lines) performed between res_c and meteorological data. Capitals: prior year months; lowercase: current year months. Significant correlation and response function coefficients ($p < 0.05$) are indicated with grey bars and white circles, respectively.

Figure 6

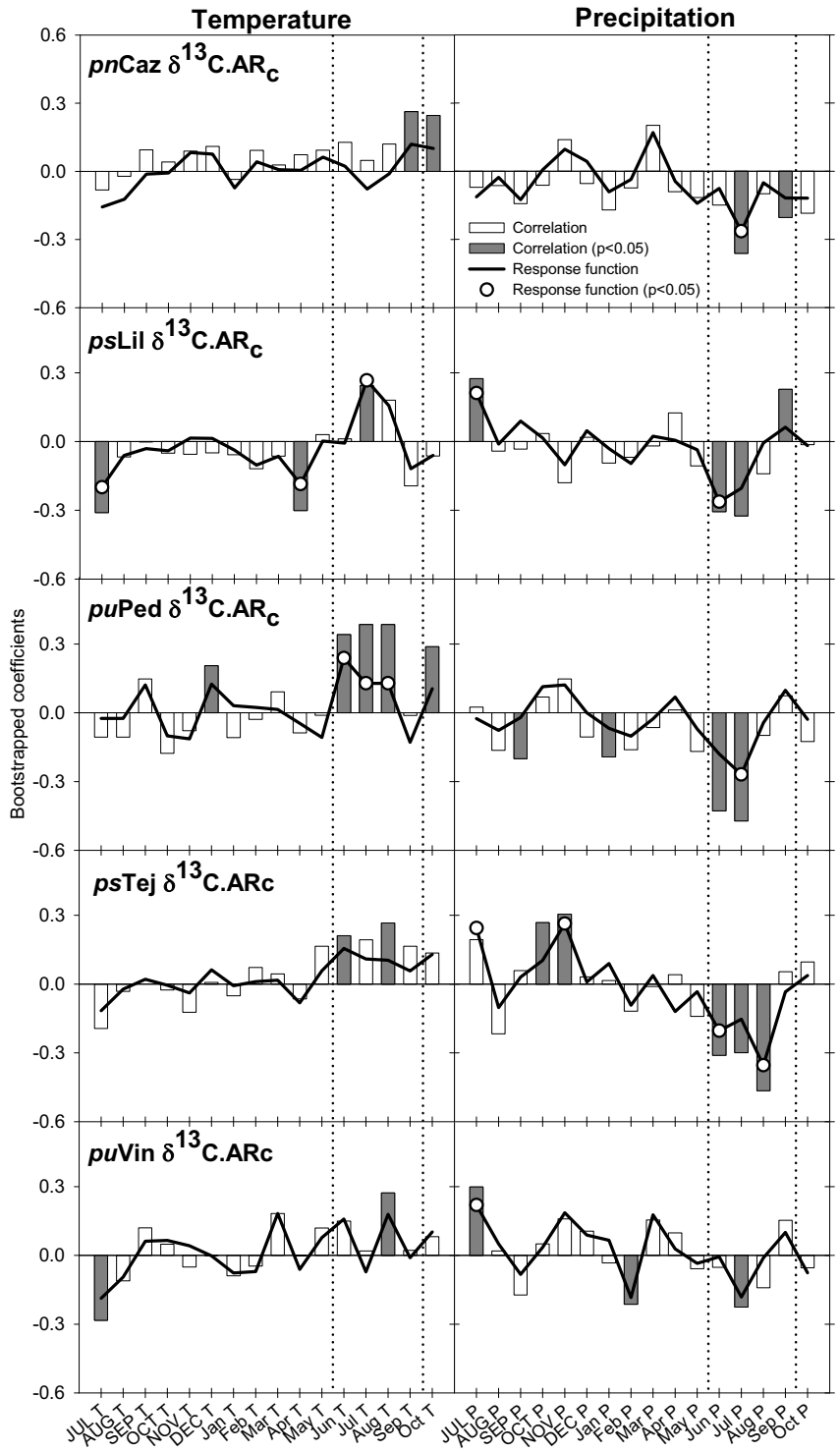

Bootstrapped correlations (bars) and response functions (lines) performed between $\delta^{13}C.AR_c$ and meteorological data. Capitals: prior year months; lowercase: current year months. Significant correlation and response function coefficients ($p < 0.05$) are indicated with grey bars and white circles, respectively.

CHAPTER 4

Paper to be submitted to *International Journal of climatology*

Title: **RECONSTRUCTION OF SUMMER PRECIPITATION IN SPAIN FOR THE LAST 400 YEARS FROM WIDTH AND $\delta^{13}C$ TREE-RING CHRONOLOGIES.**

Authors: Laia Andreu[1,2], Octavi Planells[1], Emilia Gutiérrez[1], Gerhard Helle[2], Marc Filot[3], Markus Leuenberger[3], Gerhard H. Schleser[2]

(1) Departament d'Ecologia, Universitat de Barcelona. Avinguda Diagonal, 645. 08028. Barcelona. Spain. (2) Institute for Chemistry and Dynamics of the Geosphere, Institute 5: Sedimentary Systems, Forschungszentrum Jülich GmbH (FZJ), Leo-Brandt Strasse, D-52425 Jülich, Germany. (3) Climate and Environmenal Physics, Physics Institute, University of Bern, Sidlerstrasses 5, CH-3012 Bern, Switzerland.

RECONSTRUCTIONS OF SUMMER PRECIPITATION IN SPAIN FOR THE LAST 400 YEARS FROM WIDTH AND $\delta^{13}C$ TREE-RING CHRONOLOGIES

Laia Andreu[1,2], Octavi Planells[1], Emilia Gutiérrez[1], Gerhard Helle[2], Marc Filot[3], Markus Leuenberger[3], Gerhard H. Schleser[2]

(1) Departament d'Ecologia, Universitat de Barcelona. Avinguda Diagonal, 645. 08028. Barcelona. Spain. (2) Institute for Chemistry and Dynamics of the Geosphere, Institute 5: Sedimentary Systems, Forschungszentrum Jülich GmbH (FZJ), Leo-Brandt Strasse, D-52425 Jülich, Germany. (3) Climate and Environmenal Physics, Physics Institute, University of Bern, Sidlerstrasses 5, CH-3012 Bern, Switzerland

Correspondence author: Laia Andreu Hayles. Departament d'Ecologia, Universitat de Barcelona. Avinguda Diagonal, 645 08028. Barcelona, Spain. Phone: +34.93.402.15.08. Fax number: ++34.93.411.14.38. E-mail: laiandreu@ub.edu

Abstract

Reconstructions of June-July precipitation (P0607) in Spain are made back to AD. 1600 using width and $\delta^{13}C$ tree-ring chronologies established at three different locations. The $\delta^{13}C$ of tree-ring cellulose was analyzed by two different methods, combustion and pyrolysis, obtaining two $\delta^{13}C$ chronologies per each site. Principal component analyses (PCA) were performed using combinations of the tree-ring chronologies, resulting in different tree-ring proxy sets composed by principal components (PCs). P0607 was obtained from two different sets of monthly precipitation: *Instituto Nacional de Meteorologia* (INM) and *Climatic Research Unit* (CRU). The best correlations in the calibration period were achieved combining both kinds of tree-ring series. Thus, the transfer functions used to estimate P0607 INM or P0607 CRU were stepwise multiple regressions based on three different sets of tree-ring proxies: (a) standard and $\delta^{13}C$ series; (b) standard and $\delta^{13}C$ series without autocorrelation; (c) standard and $\delta^{13}C$ series with temporal lags. Strong similarities were found between reconstructions based on INM and CRU data, although their agreement was lower between the two reconstructions based on $\delta^{13}C$ series without autocorrelation, and even lower when proxies with temporal lags were used. Larger similarities were observed among reconstructions based on INM data than on CRU data. Non-stability between tree-ring proxies and climate was detected, as well as discrepancies among reconstructions in the low frequency domain, introducing questions about the reliability of our reconstructions. However, agreements found with several historical documentary reconstructions during the 17th and 18th century validated somehow our results. In addition, there were significant relationships between our reconstructions and NAO and SOI

indices, indicating a link between our series and general atmospheric phenomena, as well as their influence over Iberian precipitation.

Introduction

Although there are many natural archives of palaeoclimatic information (e.g. ice cores, ocean and sediments, etc), tree-rings are the ones having these two advantages: perfect annual resolution with exact dating of each ring and possibility to define confidence limits (McCarroll and Loader 2004). Several high resolution millennial-length reconstructions of past temperatures based on ring width or density measurements of annual tree-rings have been published (Jones et al. 1998; Mann et al. 1999; Briffa 2000; Esper et al. 2002). Even though similar variations from multi-decadal to centennial scales were detected after removing the lowest frequency trends from these large-scale temperature reconstructions (Esper et al. 2004), strong discrepancies have been detected in the range of amplitude among these reconstructions (Briffa and Osborn 2002; Esper et al. 2004; D'Arrigo et al. 2006). These differences at the low frequency domain highlight the difficulty in establishing the true range of temperature change during the last millennium (Gagen et al. 2007). The different degree of low-frequency signal retained related to the application of statistical detrending methods to remove age trends (Cook et al. 1995; Helama et al. 2004; Esper et al. 2002) is a problem associated with the use of width and density tree-ring series. The measurements of stable carbon isotope ratios in tree rings can provide a relevant advantage to reconstruct past climate since they may not contain any long-term age-related trends; thus, if none statistical detrending is required, stable isotopes can retain climatic information at all frequency domains (McCarroll and Loader 2004; Gagen et al. 2007).

Isotope ratios ($\delta^{13}C$) in tree rings have the added advantage that physiological controls on their variation are reasonably well understood and relatively simple in comparison to the numerous factors controlling annual growth increment (McCarroll and Loader 2004). $\delta^{13}C$ reflects the internal concentration of CO_2 and therefore the balance between stomatal conductance and photosynthetic rate: while in dry environments, $\delta^{13}C$ will be dominated by stomatal conductance being related to air relative humidity and antecedent rainfall; in wet environments, $\delta^{13}C$ will be controlled by photosynthetic rate being related to photon flux and temperature (McCarroll and Pawellek 2001). Isotope time-series have been widely used for palaeoenvironmental research, being a summary of related publications in McCarroll and Loader (2004). Some reconstructions were done for temperature (e.g. Gagen et al. 2007), precipitation (e.g. Treydte et al. 2006), summer drought (e.g. Raffalli-Delerce et al. 2004) or local summer temperature

and water stress (Masson-Delmotte et al. 2005) using $\delta^{13}C$ and $\delta^{18}O$ chronologies.

Tree-ring chronologies at boreal and alpine zones have been extensively used for climatic reconstructions, being found temperature as the predominant limiting factor for tree growth, while precipitation plays usually an insignificant role (Tranquillini 1979). According to this, there are many other publications in addition to the millennial reconstructions cited above that reconstruct past temperature covering the last centuries in the northern hemisphere (Briffa et al. 1990; D'Arrigo et al. 2000; Cook et al. 2003; Wilson and Luckman 2003; Büntgen et al. 2006). However, other authors reconstructed past precipitation in more xeric sites where tree growth can be also limited by precipitation (Till and Guiot 1990; Díaz et al. 2001; Oberhuber and Kofler 2002; Cleaveland et al. 2003; Touchan et al. 2003; Wilson et al. 2005). The Iberian Peninsula is a suitable area for precipitation reconstruction as drought stress is present during summer season (Andreu et al. 2007). There are several temperature and precipitation reconstructions based on tree ring-width in Spain (Creus 1991-92, 1995, 1996; Fernández et al. 1996; Manrique and Fernández-Cancio 2000) and even some attempt have done to reconstruct local summer precipitation using tree-ring stable isotope (Planells et al. 2006). Here, we reconstruct regional precipitation in Spain based on a combination of width and $\delta^{13}C$ tree-ring proxies.

The objectives of this paper were three: (a) to develop preliminary summer precipitation reconstructions in Spain over the past 400 years based on width and $\delta^{13}C$ chronologies; (b) to compare different statistical treatments of the tree-ring proxies used as predictors in the transfer functions, as well as reconstructions obtained from two different meteorological data sets (INM and CRU); and (c) to conduct a preliminary examination of links between large-scale climate and reconstructed climate.

Materials and methods

Three forest stands with trees older than 400 years were sampled in the Iberian Peninsula (Fig 1): a *Pinus nigra* stand in the south-east (*pn*Caz), a *P. sylvestris* stand in the north-west (*ps*Lil) and a *P. uncinata* stand in the north-east (*pu*Ped). Sampling was focused on the oldest trees of the stand. Site characteristics are described in Table 1. At each site, more than fifteen trees were cored with an increment borer at around 1.30 m stem height. At least four cores were taken from each tree: two for ring-width chronology building and the rest for isotope analyses.

Ring-width chronologies

Cores were mounted, sanded until wood cells were clearly visible under microscope (Stokes and Smiley 1968) and visually cross-dated (Yamaguchi 1991). Afterwards, ring widths were measured with an accuracy of 0.01 mm

using an ANIOL semi-automatic device (Aniol 1983) and underwent a cross-dating quality control with the software Cofecha (Holmes 1983).

Standardization was done using the program TurboArstan, the windows version of Arstan (Cook 1985), to make the individual raw ring width series comparable (Fritts 1976). First, a power transformation of raw series was applied to stabilize variance (Cook and Peters 1997; Helama et al. 2004). Second, the series were detrended by negative exponential or linear fitting, considered conservative methods applied only for removing age related trends. Third, an autoregressive model was applied to remove autocorrelation. A robust mean, which reduces the variance and bias caused by extreme values, was computed at the end of each step (Cook and Briffa 1990). As a result, the standard chronologies "*std*" (detrended; Fig. 2) and the residual chronologies "*res*" (detrended without autocorrelation) were obtained. The reliable time span of the chronologies was determined by the Expressed Population Signal criteria (EPS > 0.85, Wigley et al. 1984). Table 2 shows the descriptive statistics calculated using Cofecha (Holmes 1983) and Arstan (Cook 1985) software.

Isotope chronologies

Eight cross-dated samples from four different trees were selected at each site (at least two cores per tree: Table 3). Tree-rings were split up and pooled year by year (Leavitt and Long 1984; Treydte et al. 2001). α-cellulose was extracted to avoid isotope variations due to varying compositions of wood components such as lignin (Wilson and Grinsted 1977) or resins which show a systematically different isotopic signature. The extraction method used sodium hydroxide, sodium chlorite and acetic acid to remove the extractives (Loader et al. 1997). The α-cellulose was homogenized with an ultrasonic device developed at the Forschungszentrum Jülich GmbH, Germany. Carbon isotopes were measured as CO_2 by combusting the α-cellulose samples in an elemental analyzer (Fisons NA 1500 NC) coupled via an open split to an isotope ratio mass spectrometer (Micromass Optima) operating in continuous flow mode. The precision was up to 0.1‰. The isotope signature is expressed in the delta notation, relative to the standard VPDB (IAEA 1995):

$$\delta^{13}C_{sample} = \left[\frac{(^{13}C/^{12}C)_{sample}}{(^{13}C/^{12}C)_{PDB}} - 1 \right] x1000$$

The traditional method to measure $\delta^{13}C$ is based on combustion (described above), where the 45/44 mass ratio reflects the $^{13}C/^{12}C$ ratio. Saurer et al. (1998) showed that the 29/28 mass ratio of produced CO by pyrolysis of cellulose also reflect the $^{13}C/^{12}C$ ratio. This was confirmed and enhanced by Knöller et al. (2005) and Leuenberger and Filot (2007). Combustion and pyrolysis were used to analyze the cellulose, resulting into two types of $\delta^{13}C$ chronologies: $\delta^{13}C.c$ and $\delta^{13}C.p$, respectively.

All raw $\delta^{13}C$ chronologies show a decreasing trend that is attributed to the increase in ^{13}C-depleted CO_2 due to fossil fuel burning and deforestation since industrialization. As this study is focused on extracting the climatic signal, this decreasing non-climatic trend was removed from the series, obtaining the corrected $\delta^{13}C.c$ (Fig. 3A-C) and $\delta^{13}C.p$ (Fig. 3D-F) chronologies used in further analyses. The applied correction based on data from ice cores and direct measurements was described by Leuenberger (2006). Main statistics of raw and corrected $\delta^{13}C$ chronologies are shown in Table 3.

An autoregressive (AR) modelling that removes autocorrelation was applied, similarly to dendrochronological procedures using the program FMT from the DPL software (Holmes 1992). As a result, the $\delta^{13}C$ tree-ring chronologies without autocorrelation ($\delta^{13}C.AR$) were obtained.

The meteorological data

The used meteorological data comprised the total precipitation from 1931 to 2002. This data belongs to a Spanish gridded data set (25 x 25 Km grid-box) created by the *Instituto Nacional de Meteorologia* (INM). Once the nearest data was selected for each site, a Principal Component Analyses (PCA) was done with the series of monthly precipitation of the three sites together. The first Principal Component (PC1) was selected as an estimation of the precipitation over all the sites for each monthly variable.

Total precipitation of Spain from TYN CY 1.1 data set (Mitchell et al. 2003) also was used. The country aggregation is based on the CRU TS 2.0 gridded data set. The gridded data were aggregated into countries using political boundaries (Mitchell et al. 2002).

Therefore, we have two sets of monthly precipitation data: INM and CRU. A total of 66 combinations were obtained as a result of grouping monthly meteorological variables bi-monthly, tri-monthly, etc. to annually.

Dendroclimatic reconstruction

As a preliminary step, the relationship between tree-ring indices and monthly/ seasonal grouping of meteorological data (66 combinations) was investigated for the calibration period (1931-2002) by means of response functions (Fritts 1976) and Pearson correlations, respectively. June-July precipitation from INM data set (P0607 INM) was selected as an appropriate predictand for reconstruction as it achieved the highest values for most of the chronologies.

Different sets of tree-ring chronologies were transformed to uncorrelated predictors by PCA prior to developing a regression equation. This transformation emphasizes the variance in common among the original chronologies (Fritts 1976; D'Arrigo and Jacoby 1991; Touchan et al. 2003). PCAs were done with: the 3 *std* chronologies (*std*.PCA); the 3 $\delta^{13}C.c$ and the 3 $\delta^{13}C.p$

chronologies (δ^{13}C.PCA); and finally these 9 series together ($\mathbf{A_t}$: *std*.δ^{13}C.PCA). The same procedure was done using the series without autocorrelation (*res* and δ^{13}C.AR chronologies). An additional PCA with the 3 *std* chronologies and the 6 δ^{13}C.AR chronologies was calculated ($\mathbf{B_t}$:. *std*.δ^{13}C.PCA). Table 4 shows a diagram of the PCAs performed and the number of PCs obtained for each PCA.

Following the model of the statistical calibration proposed by Fritts (1976), we lagged the 9 PCs of *std*.δ^{13}C.PCA ($\mathbf{A_t}$), one year back ($\mathbf{A_{t-1}}$) and one year forward in time ($\mathbf{A_{t+1}}$), because these series showed significant correlations with precipitation. Afterwards, we performed a new PCA ($\mathbf{A_{tt-1}}$) with the 9 PCs of A_t and the 9 PCs of A_{t-1}, obtaining 18 PCs. A second PCA combining A_t and A_{t+1} was done ($\mathbf{A_{tt+1}}$), as well as a third one combining A_t, A_{t-1} and A_{t+1} ($\mathbf{A_{ttt+1-1}}$). A diagram of the PCAs performed and the number of PCs obtained is shown in Table 5. These new PCAs were performed in order to distribute again the variance among PCs, avoiding redundancy among the new PCs obtained.

The PCs obtained were used as predictors in the regression model/equation to reconstruct P0607 INM, selecting the predictors for the final reconstruction by a forward stepwise regression procedure. Calibration model/equations used precipitation data for the period 1931-2002 in order to maximize the number of observations and the degrees of freedom used to calculate model significance in the final regression equation (Touchan et al. 2003). Model reliability and stability were also verified using a split-sample procedure (Snee 1977; Touchan et al. 2003) that divided the full period into two subsets of equal length (1931-1966 and 1967-2002), allowing determinations of verification statistics as correlation coefficient, sign test, reduction of error (RE) or coefficient of efficiency (CE) (Fritts 1976; Fritts et al. 1990). The sign test is a simple non-parametric test which evaluates the number of agreements and disagreements between the actual and the estimated data necessary to obtain significance as a function of the total number of cases (Fritts 1976). RE compares the sum of square differences between observations and regression estimates and the sum of square differences between observations and mean of observation data used for calibration, ranging from negative infinity to a maximum value of 1, which indicates a perfect estimation (Fritts et al. 1990). CE is calculated in the same way, but using the mean of the observation data from the verification period. To check the reliability of our reconstructions, we use the same predictors to reconstruct P0607 CRU.

Links with the NAO and ENSO

In order to establish whether our summer precipitation reconstructions exhibited links with large-scale atmospheric circulation in the Northern Hemisphere by means of relationship with the North Atlantic oscillation (NAO), as well as in

the Southern Hemisphere by means of relationship with the El Niño-Southern Oscillation (ENSO), we analyzed correlations between our P0607 reconstructions and monthly variables of NAO index and Southern Oscillation Index (SOI) with various temporal lags (t-1, t-2, t-3).

Results

Dendroclimatic reconstructions

Since *res*.PCs (R=0.422) achieved lower correlation values than *std*.PCs (R=0.492), *res*.PCs were not shown in Tables 4 and 6 as it was not used for further analyses. For the same reason, we do not present results of δ^{13}C.c.PCs (R=0.663) and δ^{13}C.p.PCs (R=0.653) separately, as they showed lower correlation than when we considered all these series together (δ^{13}C.PCs R=0.678). Table 6 shows the results of statistical calibration between P0607 INM as predictand and the transformed tree-ring data as predictors. The best results were obtained combining ring-width and δ^{13}C data ($\mathbf{A_t}$: *std*.δ^{13}C.PCs; R=0.738), being even still improved when the δ^{13}C series without autocorrelation were used ($\mathbf{B_t}$: *std*.δ^{13}C.AR.PCs R=0.758). Combination of one year lagged back in time ($\mathbf{A_{tt-1}}$ R=0.789) gave slightly better results than forward in time ($\mathbf{A_{tt+1}}$ R=0.781), achieving the best results when both back and forward series were used ($\mathbf{A_{ttt-1+1}}$ R=0.816). When P0607 CRU was used as a predictand with the same predictors than above (Table 6), very similar correlations, although a bit lower, were obtained.

As an example of calibration, Figure 4 shows the three sets of proxies (A_t, B_t and $A_{ttt-1+1}$) selected as potential predictors to estimate P0607 from INM data, which are defined by the following equations or transfer functions (main statistics of these stepwise regressions are described in Table 6):

P0607 INM = 0.01 + 0.2PC1.$\mathbf{A_t}$ – 0.3PC4.$\mathbf{A_t}$ – 0.22PC5.$\mathbf{A_t}$ + 0.27PC6.$\mathbf{A_t}$ – 0.35PC9.$\mathbf{A_t}$ (Fig. 4a)

P0607 INM = 0.04 + 0.26PC1.$\mathbf{B_t}$ – 0.29PC4.$\mathbf{B_t}$ + 0.24PC6.$\mathbf{B_t}$ – 0.42PC9.$\mathbf{B_t}$ (Fig. 4b)

P0607 INM = -0.2 + 0.20PC1.$\mathbf{A_{ttt-1+1}}$ + 0.16PC4.$\mathbf{A_{ttt-1+1}}$ + 0.16PC7.$\mathbf{A_{ttt-1+1}}$ – 0.18PC9.$\mathbf{A_{ttt-1+1}}$– 0.15PC10.$\mathbf{A_{ttt-1+1}}$ + 0.15PC12.$\mathbf{A_{ttt-1+1}}$ – 0.16PC14.$\mathbf{A_{ttt-1+1}}$ – 0.16PC17.$\mathbf{A_{ttt-1+1}}$ – 0.33PC18.$\mathbf{A_{ttt-1+1}}$ + 0.33PC19.$\mathbf{A_{ttt-1+1}}$ (Fig. 4c)

The transfer function equations that estimated P0607 from CRU data for the calibration period with the same set of proxies are:

P0607 CRU = 59.7 + 6.4PC1.$\mathbf{A_t}$ – 4.3PC4.$\mathbf{A_t}$ – 7.8PC9.$\mathbf{A_t}$

P0607 CRU = 60.3 + 7.4PC1.$\mathbf{B_t}$ – 5.9PC5.$\mathbf{B_t}$ – 12.5PC9.$\mathbf{B_t}$

P0607 CRU = 60.1 + 6.8PC7.$\mathbf{A_{ttt-1+1}}$ – 3.8PC9.$\mathbf{A_{ttt-1+1}}$ – 4.2PC10.$\mathbf{A_{ttt-1+1}}$ + 5.3PC12.$\mathbf{A_{ttt-1+1}}$ – 4.2PC13.$\mathbf{A_{ttt-1+1}}$ + 7.7PC16.$\mathbf{A_{ttt-1+1}}$ – 5.8PC18.$\mathbf{A_{ttt-1+1}}$

Prior to reconstruction of P0607 INM and P0607 CRU using A_t, B_t and $A_{ttt-1+1}$ data proxy, the reliability and stability of the models were assessed, calculating verification statistics using a split-sample procedure. All correlation coefficients and sign tests were significant for all predictors and periods, except the sign

test for B_t calibration/verification (C/V) period (1967-2002/1931-66) when estimating P0607 INM (Table 7). Moreover, RE and CE also were significant for all the cases, with the exception of A_t C/V period (1967-2002/1931-66) for P0607 INM and CRU estimations. This fact indicates a non-stability of these models, but a reconstruction using the A_t proxy as well, will provide information about the potential of different kinds of proxy data (A_t, B_t and $A_{ttt-1+1}$) to be predictors in the transfer function to reconstruct precipitation. It is noteworthy to point out that all reconstructions show higher correlation values in the C period 1967-2002 together with lower values of RE and CE for the V period 1931-66 in comparison with statistics obtained for the C/V period (1931-66/1967-2002). Additionally, we calculated verification statistics for longer C/V period (1951-2000/1901-50) with CRU series as the time-span of this data set was from 1901, obtaining the following statistics (C period: R=0.63; R^2=0.48; Adjusted R^2=0.46; V period: R=0.61; sign test=40/9***; RE=0.24; CE=0.22).

Reconstructions of P0607 INM and P0607 CRU for the last 400 years were done with the regression equations described above that were calculated for the full calibration period from 1931 to 2000, 2001 or 2002 (Table 6). Figure 5 shows a comparison between P0607 INM and P0607 CRU reconstructions built with the three different sets of proxies. Correlations coefficients between series indicate that P0607 INM and the P0607 CRU reconstructed based on A_t were more similar than based on B_t or $A_{ttt-1+1}$ (Table 8). For the common calibration period (1931-2000) correlation coefficients between reconstructions were 0.908, 0.775 and 0.732, respectively, while for the complete period (1604-2001) correlations were a little bit lower: 0.789, 0.734 and 0.526, respectively. Correlations among INM reconstruction were higher than among CRU reconstructions (Table 8). This fact could also be detected observing the trends of these series (Fig. 5).

Links with the NAO and ENSO

The most relevant and significant Pearson correlation between our summer precipitation reconstructions and monthly NAO indices (Fig. 6) were: negative with January of the current year (NAO_t); negative with February, March and September, but positive with November of prior year (NAO_{t-1}); and positive with October of two years before (NAO_{t-2}). Almost any significant correlations were found between reconstructions and NAO indices of three years before (NAO_{t-3}). Although there are some discrepancies between INM and CRU reconstructions, patterns of correlations with NAO indices are rather similar.

Pearson correlation between our summer precipitation reconstructions and monthly SOI are illustrated in Figure 7. Significant correlations with monthly SOI were not common among the different reconstructions, making difficult to select a specific month as the

most relevant for all the cases. However, while negative correlations were observed with SOI of the current year (SOI_t), positive correlations were found with SOI of one, two and three years before (SOI_{t-1}, SOI_{t-2}, SOI_{t-3}, respectively).

Discussion

Combination of proxies

The use of tree-ring width series together with $\delta^{13}C$ chronologies as predictors of the regression equations to estimate summer precipitation, gave the best results achieving the highest correlations values for the calibration period, highlighting the enormous potential of combining both kind of tree-ring proxies for palaeoclimatic reconstructions. By combining proxies, the strength of the climate correlations increases and the range of extractable parameters extended (McCarroll et al. 2003). However, only when proxies have the same dominant climate control their combination enhances the climatic signal (Gagen et al. 2006).

Instability between tree-ring proxies and climate

Although almost all verification statistics calculated for our reconstructions were significant, we detected lower RE and CE values for the V period 1931-66/67 in all reconstructions, and even a failure of these statistics in P0607 INM and CRU reconstructions based on A_t predictors, indicating a non-stability in these models. Even though, these two reconstructions were good for the rest of verification statistics, showing the highest similarities between INM and CRU reconstructions (Fig. 5A). When statistics were calculated for longer C/V period using CRU data (1951-2000/1901-50), correlation for the C period was lower, while RE and CE were significant. Therefore, the non-significant or lower values of RE and CE for the V period 1931-66/67 were linked with higher correlation for the C period 1967/66-2002. The high relationship found between tree-ring proxies and climate during the end of the second half of the 20th century could not be representative of the climatic signal registered by trees during the first half of the century. Instability of the relationship between tree growth and climate along the 20th century was already detected in the Iberian Peninsula using networks of tree ring width chronologies (Tardif et. al. 2003; Macias et al. 2006; Andreu et al. 2007). Similarly, Oberhuber and Kofler's reconstruction (2002) presented significant statistics for both C/V split periods, but higher correlation for the C period (1954-97) together with lower RE and CE values for their corresponding V period (1911-53) were found in comparison with statistics values of C/V (1911-53/1954-97).

Verification statistics

Verification statistics measure the degree of similarity between independent estimates of climate made from the model and the corresponding instrumental data for time periods

independent for calibration (Gordon 1982; Fritts et al. 1990). The sign test indicates that the sign of the estimate is more often correct than would be expected from random numbers (Fritts 1976), while the correlation coefficient measures the relative variation (covariance) that is common to two data sets, reflecting the entire spectrum of variation (high and low frequencies) (Fritts et al. 1990). RE and CE provide a highly sensitive measure of the reconstruction reliability (Fritts et al. 1990), assessing that differences between observations and estimations are lower than differences between observations and their mean for the C and V period, respectively. However, this statistic has the disadvantage that one extremely bad estimate can completely offset the effect of several very good estimates. McIntyre and McKitrick (2005) alerted that although RE statistic is widely used for evaluation skill in palaeoclimatic studies, it lacks a theoretical distribution and can be affected by prior transformation of the data before performing PCA. Therefore, other C/V methodologies to estimate models parameters independently from the temporal structure of the data as bootstrapped (Guiot et al. 2005) or jackknife (Gagen et al. 2007) could be a solution to validate reliability of our reconstructions in the future since non stability between tree-ring proxies and climate has been assessed. Other tree ring variables as oxygen and deuterium stable isotopes, that can be also measured from tree ring cellulose, could be added to improve our current sets of tree-ring proxies composed by width and $\delta^{13}C$ tree-ring chronologies, probably enhancing the stability of the relationship of our predictors with climate.

Reliability of P0607 reconstructions

To reconstruct Turkish spring precipitation, Touchan et al. (2003) used tree-ring series pre-whitened with low-order autoregressive models to remove persistence, as this persistence was presumed to be unrelated to precipitation variability because precipitation series were not significantly autocorrelated. Since our precipitation series did not present autocorrelation values (results not shown), we also decided to use our tree-ring series without autocorrelation (B_t). Although correlations in the calibration period were higher than when we used $\delta^{13}C$ with autocorrelation (Table 6), very low relationship were obtained between CRU and INM reconstructions (Fig. 5B; Table 8). Briffa et al. (1990) included lagged ring-width variables in the regression model because significant one-year-lag autocorrelation was found in their response function analyses. Accordingly, the highest correlations in the calibration periods also were achieved using tree-ring proxy data with temporal lags ($A_{ttt-1+1}$). However, even stronger differences than using B_t as predictors were found when comparing INM and CRU reconstructions based on $A_{ttt-1+1}$, showing a very different behaviour of these series in the low-frequency domain (Fig. 5C; Table 8). Despite A_t proxy did not present the highest correlations over the calibration

period, the highest similarities between INM and CRU were found when using this proxy. This result may indicate that more realistic results were obtained when less statistical treatments were applied to the series, recommending special caution if autocorrelation is remove or temporal lags are incorporated to the tree-ring proxies. Concerning comparison between the two set of meteorological data, similarities among INM reconstructions were larger than among CRU reconstructions, especially in the low-frequency fluctuations.

Discrepancies found among our reconstructions in the low-frequency domain introduce a huge uncertainty to identify dry and humid periods throughout time, making difficult to validate the results. However, general comparison with other Iberian precipitation reconstructions based on historical documentary sources can be performed to validate our reconstructions with independent proxies. Our results show a rainy 17th century in agreement with Rodrigo et al. (1999) and Vicente-Serrano and Cuadrat (2007) whom described for the same period moist conditions at the beginning and normal precipitation until the end of the century. Drier periods appear during the 18th century accordingly to other authors that described the most intense droughts in the first half in the south of the Iberian Peninsula (Rodrigo et al. 1999) or in the last quarter in the middle Ebro Valley (Vicente-Serrano and Cuadrat 2007) and in Catalonia (Martín-Vide and Barriendos 1995; Barriendos 1997). During the 19th century, we detected a high variability in our reconstructions, but we did not perform validations with historical reconstructions based on rogations during this period because, as was reported by Vicente-Serrano and Cuadrat (2007), the number of this documentary sources decrease during the second half of the 19th century.

Teleconnections with general atmospheric phenomena

The NAO is a climatic phenomenon in the North Atlantic Ocean of fluctuations difference of sea-level pressure between Iceland and Azores. A permanent low-pressure system over Iceland (the Icelandic Low) and a permanent high-pressure system over the Azores (the Azores High) control the direction and strength of westerly winds into Europe. The relative strengths and positions of these systems vary from year to year and this variation is known as the NAO. A large difference in the pressure and the two stations (a high index year, denoted NAO+) leads to increased westerlies, resulting in warm and wet winters in Central Europe, but cold and dry in Southern Europe. In contrast, if the index is low (NAO-), westerlies are suppressed, most storms goes southerly toward the Mediterranean sea, resulting in cold and dry winters in Central Europe. Summers in Central Europe are cool in years when westerlies are strong, but if westerlies are suppressed, temperature is more extreme in summer and winter leading to heatwaves, deep freezes and reduced rainfalls. Therefore, January NAO_t and

February-March NAO_{t-1} established a negative relationship with our summer precipitation reconstructions, indicating that when westerlies are strong (NAO+) less precipitation is present in Spain, while when westerlies are weak (NAO-) rainfall increase. Accordingly, Zorita et al. (1992) reported less precipitation during winter for NAO+. Nevertheless, a positive relationship with October NAO_{t-2} and non-significant relationship with monthly NAO_{t-3} indicate that although NAO preserve its influence until two years forward in time, these relationships are not stable throughout time.

ENSO is a global coupled ocean-atmosphere phenomenon. SOI, their atmospheric signature, reflects the monthly or seasonal fluctuations in the air pressure difference between Tahiti and Darwin. ENSO is the most prominent known source of inter-annual variability in weather and climate around the world, though not all areas are affected. Even though, significant relationships were found between our summer precipitation reconstructions for Spain and SOI indices until three years forward in time. Some authors have already detected correlations between SOI indices and precipitation data from the Iberian Peninsula (Rodó et al. 1997; Rodríguez-Puebla et al. 1998), and even register this signal in lake sediments (Rodó et al. 1997).

Different relationships were found between NAO and SOI indices and our summer precipitation reconstructions depending on temporal lags, predictands (CRU or INM) and/or predictors used, indicating that complexity of the climatic system sometimes make these teleconnections difficult to interpret. However, the influence of NAO and ENSO over Iberian precipitation has been validated.

Conclusions

Summer precipitation reconstructions based on ring width and $\delta^{13}C$ appear to be more reliable than the ones based only on proxies taken separately. Agreements found among ours and other several historical Iberian reconstructions, as well as their significant links with large-scale atmospheric phenomena (NAO and ENSO) validate somehow the reliability of our reconstructions. However, non-stability between tree-ring proxies and climate, as well as discrepancies among reconstructions in the low frequency domain, alert about the need to discuss more about the different standardization methods and the reliability of the verification statistics. A multiproxy approach for palaeoclimatic reconstructions appears as a useful way to solve the particular problems of each kind of proxy (Mann 2002), increasing the reliability of future reconstructions. Climatic reconstructions as the ones presented here could contribute in a near future to perform studies with this multidisciplinary approach in the Iberian Peninsula.

Acknowledgements

We are very grateful to Oriol Bosch, Enric Batllori, Elena Muntán, Mariano Barriendos, Roberto Rodríguez, Carlos Almarza, Pedro Antonio Tíscar and Heinz Vos for their help during sampling, laboratory work and manuscript preparation. This research was funded by EU project ForMAT (Contract ENV4-CT97-0641), EU project ISONET (Contract EV K2-2001-00237) and EU FP6 project Millennium (GOCE 017008).

References

Andreu L, Gutiérrez E, Macias M, Ribas M, Bosch O, Camarero JJ (2007) Climate increases regional tree growth variability in Iberian pine forests. *Global Change Biology* **13**: 804-815, doi: 10.1111/j.1365-2486.2006.01322.x

Aniol RW (1983) Tree-ring analysis using CATRAS. *Dendrochronolgia* **1**: 45-53.

Barriendos M (1997) Climatic variations in the Iberian Peninsula during the late Maunder Minimum (AD 1675-1715): an analysis of data from rogation ceremonies. *The Holocene* **7**(1): 105-111.

Briffa KR, Bartholin TS, Ekstein D, Jones PD, Karlén W, Schweingruber FH, Zetterberg P (1990) A 1400 year tree-ring record of summer temperatures in Fennoscandia. *Nature* **346**: 434-439.

Briffa KR (2000) Annual climate variability in the Holocene: interpreting the message of ancient trees. *Quaternary Science Reviews* **19**: 87-105.

Briffa KR, Osborn TJ (2002) Blowing hot and cold. *Science* **295**: 2227-2228.

Büntgen U, Frank DC, Nievergelt D, Esper J (2006) Summer temperature variations in the European Alps, AD. 755-2004. *Journal of climate* **19**: 5606-5623.

Cleaveland MK, Stahle DW, Therrell MD, Villanueva-Diaz J, Burns BT (2003) Tree-ring reconstructed winter precipitation and tropical teleconnections in Durango, Mexico. *Climatic Change* **59**: 369-388.

Cook ER (1985) A time series analysis approach to tree-ring standardization. DS thesis, University of Arizona, Tucson.

Cook ER, Briffa KR (1990) Data Analysis. In: *Methods of dendrochronology* (eds Cook ER and Kairiukstis LA), pp. 97-162. Kluwer, Boston. 394 pp.

Cook ER, Briffa KR, Meko DM, Graybill DA, Funkhouser G (1995) The 'segment length curse' in long tree-ring chronology development for palaeoclimatic studies. *Holocene* **5**: 229-237.

Cook ER, Peters K (1997) Calculating unbiased tree-ring indices for the study of climatic and environmental change. *Holocene* **7**: 359-368.

Cook ER, Krusic PJ, Jones PD (2003) Dendroclimatic signals in long tree-ring chronologies from the Himalayas of Nepal. *International Journal of Climatology* **23**: 707-732.

Creus J (1991-92) Tendencia secular de la temperatura de mayo en el Pirineo oriental. *Notes de Geografía Física* **20-21**: 41-49.

Creus J, Beorlegui M, Fernández-Cancio A (1995) Reconstrucciones climáticas en Galicia durante las últimas centurias. Estudio dendrocronológico. *Xunta de Galicia*, Serie monografías **5**. Jaca.

Creus J, Fernández-Cancio A, Manrique E (1996) Evolución de la temperatura y precipitación anuales desde el año 1400 en el sector central de la depresión del Ebro. *Lucas Mallada. Revista de Ciencias*, Instituto de Estudios Altoaragoneses **8**: 9-27.

D'Arrigo RD, Jacoby GC (1991) A 1000-year record of winter precipitation from northwestern New Mexico, USA: a reconstruction from tree-rings and its relation

to El Niño and the southern oscillation. *The Holocene* **1**(2): 95-101.

D'Arrigo R, Jacoby G, Pederson N, Frank D, Buckley B, Nachin B, Mijiddorj R, Dugarjav C (2000) Mongolian tree-rings, temperature sensitivity and reconstructions of Northern Hemisphere temperature. *Holocene* **10**(6): 669-672.

D'Arrigo R, Wilson R, Jacoby G (2006) On the long-term context for late twentieth century warming. *Journal of Geophysical Research* **111**: D03103. doi:10.1029/2005JD006352.

Díaz SC, Touchan R, Swetnam TW (2001) A tree-ring reconstruction of past precipitation for Baja California sur, Mexico. *International Journal of Climatology* **21**: 1007-1019.

Esper J, Cook ER, Schweingruber FH (2002) Low-frequency signals in long tree-ring chronologies for reconstructing past temperature variability. *Science* **295**: 2250-2253.

Esper J, Frank DC, Wilson RJS (2004) Climate Reconstructions: Low-frequency Ambition and High-Frequency Ratification. *EOS Trans. AGU* **85**(12):113.

Fernández A, Génova M, Creus J, Gutiérrez E (1996) Dendroclimatological investigations covering the last 300 years in Central Spain. In: *Tree Rings, Environment and Humanity* (eds. Dean JS, Meko DM, Swetman TW), pp. 181-190 *RADIOCARBON*. 889 pp.

Fritts HC (1976) *Tree rings and climate*. Academic Press, New York, 433 pp.

Fritts HC, Guiot J, Gordon GA, Schweingruber F (1990) Methods of calibration, verification, and reconstruction. In: *Methods of dendrochronology* (eds Cook ER and Kairiukstis LA), pp. 163-217. Kluwer, Boston. 394 pp.

Gagen M, McCarroll D, Edouard J-L (2006) Combining ring width, density and stable carbon isotope proxies to enhance the climatic signal in tree-rings: an example from the southern French Alps. *Climatic Change* **78**: 363-379.

Gagen M, McCarroll D, Loader NJ, Robertson I, Jalkanen R, Anchukaitis KJ (2007) Exorcising the "segment length curse": summer temperature reconstruction since AD 1640 using non-detrended stable carbon isotope ratios from pine trees in northern Finland. *The Holocene* **17**(4): 435-446.

Gordon GA (1982) Verification of Dendroclimatic Reconstructions. In: *Climate from Tree Rings* (eds. Hughes MK, Kelly PM, Pilcher JR, Lamarche VC). Cambridge University Press, Cambridge. 223 pp.

Guiot J, Nicault A, Rathgeber C, Edourd JL, Guibal F, Pichard G, Till C (2005) Last-millennium summer-temperature variations in western Europe based on proxy data. *The Holocene* **15**(4): 489-500.

Helama S, Lindholm M, Timonen M, Eronen M (2004) Detection of climate signal in dendrochronological data analysis: a comparison of tree-ring standardization methods. *Theoretical and Applied Climatology* **79**: 239-254.

Holmes RL (1983) Computer-assisted quality control in tree-ring dating and measurement. *Tree-Ring Bulletin* **43**: 68-78.

Holmes RL (1992) Dendrochronology program library. Version 1992-1. Laboratory of Tree-Ring Research, University of Arizona, Tucson.

IAEA (1995) TECDOC-825. Reference and Intercomparison Materials for Stable Isotopes of Light Elements, Proceedings of a Consultants Meeting, 1-3 December 1993, Vienna.

Jones PD, Briffa KR, Barnett TP, Tett SFB (1998) High-resolution palaeoclimatic records for the last millennium: integration, interpretation and comparison with general circulation model control run temperatures. *Holocene* **8**: 455-471.

Knöller K, Boettger T, Weise SM, Gehre M (2005) Carbon isotope analyses of cellulose using two different on-line techniques (elemental analysis and high-temperature pyrolysis)- a comparison. *Rapid Communications in Mass Spectrometry* **19**: 343-348.

Leavitt SW, Long A (1984) Sampling strategy for stable carbon isotope analysis of tree rings in pine. *Nature* **311**: 145-147.

Leuenberger M (2006) To what extent can ice core data help to understand biological systems? In: *Isotopes as Tracers of Ecological Change.* (eds. Dawson T. and Siegwolf R.), Elsevier Academic Press.

Leuenberger M, Filot M (2007) Temperature dependencies of high-temperature reduction on conversion products and their isotopic signatures. *Rapid Communications in Mass Spectrometry* **21**: 1587-1598.

Loader NJ, Robertson I, Barker AC, Switsur VR, Waterhouse JS (1997) An improved method for the batch processing of small wholewood samples to a-cellulose. *Chemical Geology* **136**(3-4): 313-317.

Macias M, Andreu L, Bosch O, Camarero JJ, Gutiérrez E (2006) Increasing aridity is enhancing silver fir (*Abies alba* Mill.) water stress in its south-western distribution limit. *Climatic change* **79**: 289-313, doi: 10.1007/s10584-006-9071-0

Mann ME, Bradley RS, Hughes MK (1999) Northern Hemisphere temperatures during the past millennium: inferences, uncertainties and limitations. *Geophysical Research Letters* **26**: 759-762.

Mann ME (2002) The value of multiple proxies. *Science* **297**: 1481-1482.

Manrique E, Fernández-Cancio A (2000) Extreme climatic events in dendroclimatic reconstructions from Spain. *Climatic Change* **44**: 123-138.

Martín-Vide J, Barriendos M (1995) The use of rogation ceremony records in climatic reconstructions: a case study from Catalonia (Spain). *Climatic change* **30**: 201-221.

Masson-Delmotte V, Raffalli-Delerce G, Danis PA, Yiou P, Stievenard M, Guibal F, Mestre O, Bernard V, Goose H, Hoffman G, Jouzel J (2005) Changes in European precipitation seasonality and in drought frequencies revealed by a four-century-long tree-ring isotopic record from Brittany, western France. *Climate Dynamics* **24**: 57-69.

McCarroll D, Pawellek F (2001) Stable carbon isotope ratios of *Pinus sylvestris* from northern Finland and the potential for extracting a climate signal from long Fennoscandian chronologies. *The Holocene* **11**(5): 517-526.

McCarroll D, Jalkanen R, Hicks S, Tuovinen M, Gagen M, Pawellek F, Eckstein D, Schmitt U, Autio J, Heikkinen O (2003) Multiproxy dendroclimatology: a pilot study in northern Finland. *The Holocene* **13**(6): 829-838.

McCarroll D, Loader NJ (2004) Stable isotopes in tree rings. *Quaternary Science Review* **23**: 771-801.

McIntyre S, McKitrick R (2005) Hockey sticks, principal component, and supurious significance. *Geophysical Research Letters* **32**: L03710, doi:10.1029/2004GL21750.

Mitchell TD, Hulme M, New M (2002) Climate data for political areas. *Area* **34**: 109-112.

Mitchell TD, Carter TR, Jones PD, Hulme M, New M (2003) A comprehensive set of high-resolution grids of monthly climate for Europe and the globe: the observed record (1901-2000) and 16 scenarios (2001-2100). Tyndall Working Paper 55, Tyndall Centre, UEA, Norwich, UK. hhtp://www.tyndall.ac.uk

Oberhuber W, Kofler W (2002) Dendroclimatological spring rainfall reconstruction for an inner Alpine dry valley. *Theoretical and Applied Climatology* **71**: 97-106.

Planells O, Andreu L, Bosch O, Gutiérrez E, Filot M, Leuenberger M, Helle G, Schleser GH (2006) The potential of stable isotopes to record aridity conditions in a low-sensitive ring width forest from the eastern Pre-Pyrenees. 2005-*TRACE Proceedings*, 266-272.

Raffalli-Delerce G, Masson-Delmotte V, Dupouey JL, Stievenard M, Breda N, Moisselin JM (2004) Reconstruction of summer droughts using tree-ring cellulose isotopes: a calibration study with living oaks from Brittany (western France). *Tellus* **56B**: 160-174.

Rodó X, Baert E, Comin FA (1997) Variations in seasonal rainfall in Southern Europe during the present century: relationships with the North Atlantic Oscillation and the El Niño-Southern Oscillation. *Climate Dynamics* **13**: 275-284.

Rodrigo FS, Esteban-Parra MJ, Pozo-Vázquez D, Castro-Díez Y (1999) A 500-year precipitation record in southern Spain. *International Journal of Climatology* **19**: 1233-1253.

Rodríguez-Puebla C, Encinas AH, Nieto S, Garmendia J (1998) Spatial and temporal patterns of annual precipitation variability over the Iberian Peninsula. *International Journal of Climatology* **18**: 299-316.

Saurer M, Robertson I, Siegwolf R, Leuenberger M (1998) Oxygen isotope analysis of cellulose: an interlaboratory comparison. *Analytical Chemistry* **70**: 2074-2080.

Snee RD (1977) Validation of regression models: methods and examples. *Technometrics* **19**: 415-428.

Stokes MA, Smiley TL (1968) An introduction to tree-ring dating. University of Chicago Press, Chicago.

Tardif J, Camarero JJ, Ribas M, Gutiérrez E (2003) Spatiotemporal variability in tree growth in the central Pyrenees: climatic and site influences. *Ecological Monographs* **73**(2): 241-257.

Till C, Guiot J (1990) Reconstruction of precipitation in Morocco since 1100 AD. Based on *Cedrus atlantica* tree ring widths. *Quaternary Research* **33**: 337-351.

Touchan R, Garfin GM, Meko DM, Funkhouser G, Erkan N, Hughes MK, Wallin BS (2003) Preliminary reconstructions of spring precipitation in southwestern Turkey from tree-ring width. *International Journal of Climatology* **23**: 157-171.

Tranquillini W (1979) Physiological ecology of the alpine timberline. Tree existence in high altitudes with special reference to the European Alps. *Ecological Studies* **31**. Berlin, Heidelberg, New York. Springer, 137 pp.

Treydte K, Schleser GH, Schweingruber FH, Winiger M (2001) The climatic significance of $\delta^{13}C$ in subalpine spruces (Lötschental, Swiss Alps). *Tellus* **53B**: 593-611.

Treydte KS, Schleser GH, Helle G, Frank DC, Winiger M, Haug GH, Esper J (2006) The twentieth century was the wettest period in northern Pakistan over the past millennium. *Nature* **440**: 1179-1182.

Vicente-Serrano SM, Cuadrat JM (2007) North Atlantic oscillation control of droughts in north-east Spain: evaluation since 1600 AD. *Climatic Change* DOI 10.1007/s10584-007-9285-9.

Wigley TML, Briffa KR, Jones PD (1984) On the average value of correlated time series, with applications in Dendroclimatology and Hydrometeorology. *Journal of Climate and Applied Meterology* **23**: 201-213.

Wilson AT, Grinsted MJ (1977) $^{12}C/^{13}C$ in cellulose and lignin as palaeothermometers. *Nature* **265**: 133-135.

Wilson RJS, Luckman BH (2003) Dendroclimatic reconstruction of maximum summer temperatures from upper treeline sites in Interior British Columbia, Canada. *Holocene* **13**(6): 851-861.

Wilson RJS, Luckman BH, Esper J (2005) A 500 year dendroclimatic reconstruction of spring-summer precipitation from the lower Bavarian forest region, Germany. *International Journal of Climatology* **25**: 611-630.

Yamaguchi DK (1991) A simple method for cross-dating increment cores from living trees. *Canadian Journal of Forest Research* **21**: 414-416.

Zorita E, Kharin V, von Storch H (1992) The atmospheric circulation and sea surface temperature in the North-Atlantic area in winter: their interaction and relevance for Iberian precipitation. *Journal of Climate* **5**: 1097-1108.

Table 1 Location and characteristics of the study sites.

Site	Species	Site code	Range	Latitude	Longitude	Altitude (m a.s.l.)	Aspect
Cazorla	*Pinus nigra*	*pn*Caz	Betic	37º 48' N	02º 57' W	1800	SW
Pinar de Lillo	*P. sylvestris*	*ps*Lil	Cantabrian	43º 03' N	05º 15' W	1600	NW
Pedraforca	*P. uncinata*	*pu*Ped	Pre-Pyrenees	42º 14' N	01º 42' E	2100	E

Table 2 Mean correlation, Mean Sensitivity defined as a measure of the inter-annual variability (MS_x), and first order autocorrelation (AC1) of the standard (*std*) and residual (*res*) tree-ring width chronologies (calculated using COFECHA software) for each site. The time-span in which the expressed population signal statistic (EPS) shows values higher than 0.85 (calculated using ARSTAN software).

Site ID	Time span	Trees/ radii	Mean correlation	MSx	AC1	Reliable time span (EPS>0.85)	
						std	*res*
*pn*Caz	1125-2002	33/68	0.676	0.253	0.823	1373-2002	1324-2002
*ps*Lil	1511-2002	21/45	0.595	0.258	0.842	1670-2002	1654-2002
*pu*Ped	1269-2003	23/57	0.565	0.175	0.876	1767-2002	1550-2002

Table 3 Statistics of raw and corrected $\delta^{13}C$ tree-ring chronologies per each site (where $\delta^{13}C$.c was analyzed by combustion and $\delta^{13}C$.p by pyrolysis). MS_x: Mean Sensitivity; Min: Minimum; Max: Maximum; PAC1: First order partial autocorrelation.

Site ID	Time-span	Trees/ Cores	MS_x	Raw $\delta^{13}C$					Corrected $\delta^{13}C$				
				Mean ± SD	Min	Max	Range	PAC1	Mean ± SD	Min	Max	Range	PAC1
*pn*Caz $\delta^{13}C$.c	1600-2002	4/9	0.015	-21.05 ± 0.60	-22.9	-19.9	2.99	0.781	-20.88 ± 0.36	-22.0	-19.9	2.06	0.406
*ps*Lil $\delta^{13}C$.c	1600-2002	4/10	0.022	-22.13 ± 0.69	-24.2	-20.6	3.54	0.612	-21.96 ± 0.52	-23.5	-20.7	2.77	0.333
*pu*Ped $\delta^{13}C$.c	1600-2002	4/8	0.02	-22.01 ± 0.61	-24.3	-20.5	3.82	0.612	-21.84 ± 0.45	-23.2	-20.6	2.68	0.277
*pn*Caz $\delta^{13}C$.p	idem	idem	0.013	-22.11 ± 0.47	-23.7	-20.9	2.79	0.707	-21.94 ± 0.32	-22.9	-21.0	1.93	0.359
*ps*Lil $\delta^{13}C$.p	idem	idem	0.019	-22.91 ± 0.56	-24.8	-21.5	3.32	0.536	-22.74 ± 0.46	-23.9	-21.4	2.52	0.309
*pu*Ped $\delta^{13}C$.p	idem	idem	0.017	-23 ± 0.51	-24.8	-21.5	3.34	0.529	-22.83 ± 0.43	-23.9	-21.4	2.50	0.321

Table 4 Different combinations of tree-ring proxies involved in the PCAs that will be use as predictors of the reconstructions and their number of PCs (see terminology description in methodology).

tre-ring width	*pn* Caz *std* *ps* Lil *std* *pu* Ped *std*	*std* .PCA (3 PCs)	**A_t** *std.* δ^{13}C PCA (9PCs)	**B_t** *std.* δ^{13}C.AR PCA (9PCs)
tree-ring cellulose	*pn* Caz δ^{13}C.c *ps* Lil δ^{13}C.c *pu* Ped δ^{13}C.c *pn* Caz δ^{13}C.p *ps* Lil δ^{13}C.p *pu* Ped δ^{13}C.p	δ^{13}C.PCA (6 PCs)		

Table 5 PCA done with the 9 PCs of the *std.*δ^{13}C.PCA (**A_t**) and: A_{t-1} (**A_{tt-1}**); A_{t+1} (**A_{tt+1}**); A_{t-1} and A_{t+1} (**$A_{ttt-1+1}$**) (see terminology description in methodology).

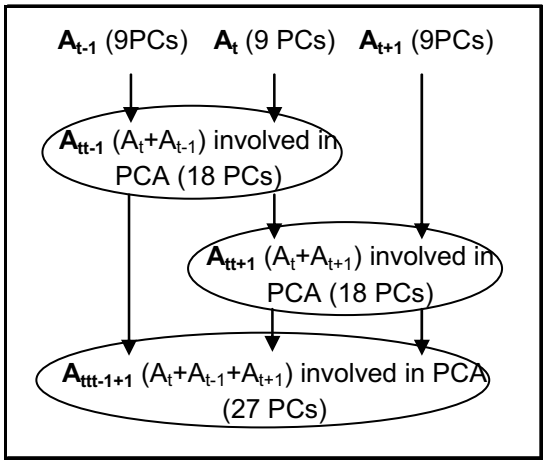

Table 6 Statistics of the stepwise multiple regressions to estimate P0607 from INM and CRU data (predictand) based on the different selected sets of tree-ring proxy data (predictors) for the calibration (C) period: correlation (R), coefficient of determination (R^2) and adjusted R^2 (Aj.R^2).

Predictors	P0607 INM				P0607 CRU			
	C period	R	R^2	Aj. R^2	C period	R	R^2	Aj. R^2
std.PCs	1931-2002	0.492	0.242	0.220	1931-2000	0.533	0.284	0.262
δ^{13}C.PCs		0.678	0.460	0.444		0.642	0.412	0.404
$\mathbf{A_t}$: *std*.δ^{13}C.PCs		0.738	0.544	0.510		0.701	0.491	0.468
$\mathbf{B_t}$: *std*.δ^{13}C.AR.PCs		0.758	0.575	0.549		0.735	0.540	0.520
$\mathbf{A_{tt\text{-}1}}$.PCs	1931-2001	0.789	0.622	0.580	1931-2000	0.740	0.548	0.513
$\mathbf{A_{tt+1}}$.PCs		0.781	0.610	0.567		0.721	0.520	0.498
$\mathbf{A_{ttt\text{-}1+1}}$.PCs		0.816	0.665	0.609		0.771	0.595	0.549

Table 7 Summary of verification statistics using as predictors A_t, B_t, $A_{ttt-1+1}$ and as predictands P0607 from INM and CRU data. Calibration (C) period: correlation (R) and ajusted R^2 (Aj. R^2) of the stepwise regression. Verification (V) period: correlation (R), sign test, Reduction Error (RE) and Coefficient of Efficiency (CE) between observations and estimates. Significance levels of sign test: * p<0.10, ** p<0.05; *** p<0.01.

Predictors	P0607 INM								P0607 CRU							
	C period	R	Aj. R^2	V period	R	Sign test	RE	CE	C period	R	Aj. R^2	V period	R	Sign test	RE	CE
A_t	1931-66	0.64	0.31	1967-2002	0.80	28/7***	0.60	0.60	1931-65	0.74	0.51	1966-2000	0.66	23/11*	0.40	0.40
	1967-2002	0.86	0.70	1931-66	0.49	23/12*	-1.68	-1.69	1966-2000	0.76	0.53	1931-65	0.61	25/9***	-0.60	-0.60
B_t	1931-66	0.65	0.35	1967-2002	0.83	25/10**	0.68	0.67	1931-65	0.69	0.43	1966-2000	0.77	25/9***	0.57	0.57
	1967-2002	0.85	0.69	1931-66	0.54	20/15	0.13	0.13	1966-2000	0.78	0.56	1931-65	0.68	29/5***	0.42	0.42
$A_{ttt-1+1}$	1931-66	0.81	0.51	1967-2001	0.66	25/9***	0.41	0.41	1931-65	0.78	0.50	1966-2000	0.73	25/9***	0.47	0.47
	1967-2001	0.894	0.72	1931-66	0.64	26/9***	0.30	0.30	1966-2000	0.82	0.58	1931-65	0.64	27/7***	0.36	0.36

Table 8 Pearson correlations among P0607 reconstructions based on INM and CRU data from 1604 to 2001.

Reconstructions		INM			CRU		
		A_t	B_t	$A_{ttt-1+1}$	A_t	B_t	$A_{ttt-1+1}$
INM	A_t	1	0.918	0.828	0.789	0.596	0.547
	B_t		1	0.839	0.807	0.734	0.586
	$A_{ttt-1+1}$			1	0.699	0.626	0.526
CRU	A_t				1	0.888	0.661
	B_t					1	0.644
	$A_{ttt-1+1}$						1

Figure 1

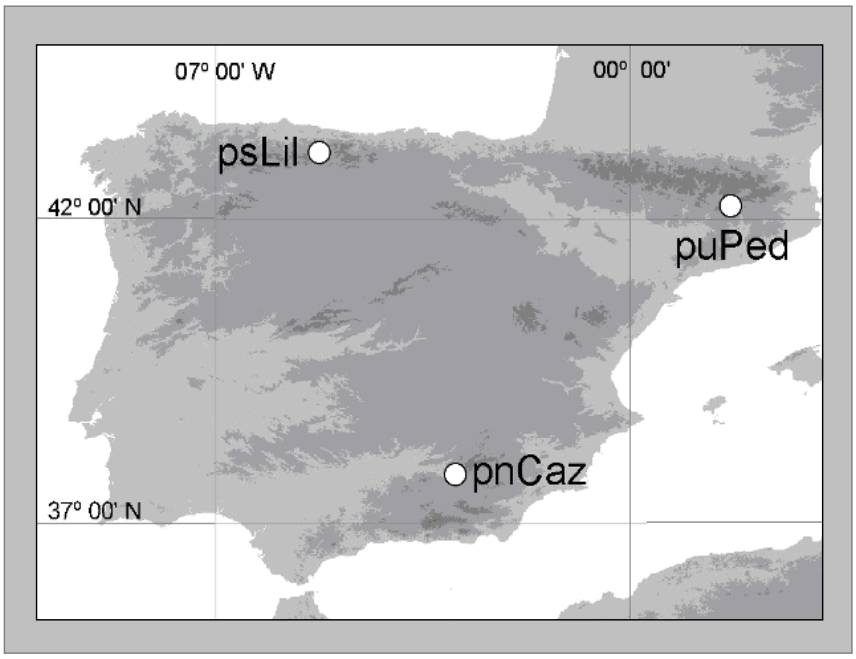

Location of the three selected sites in the Iberian Peninsula.

Figure 2

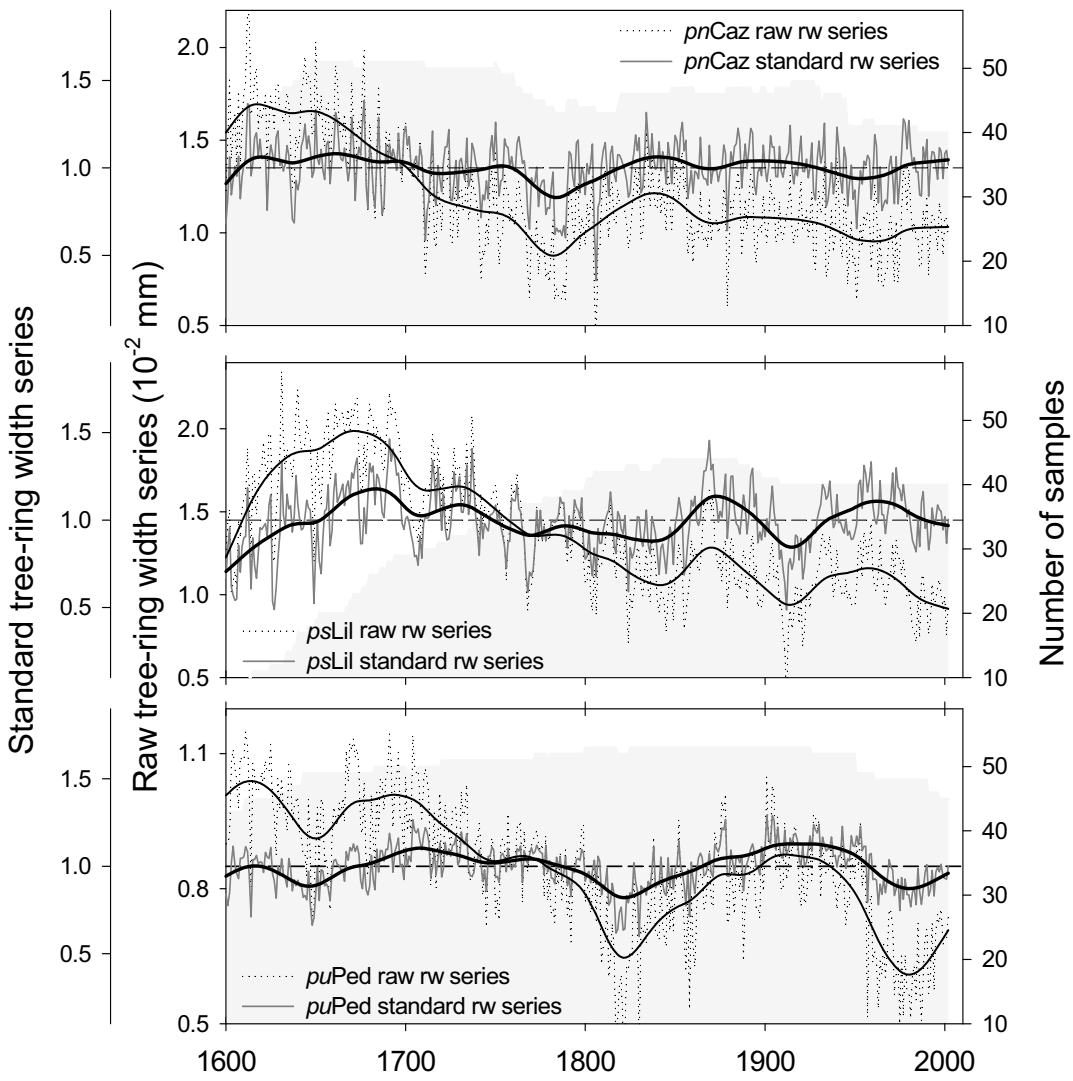

Raw (dotted) and standard (grey lines) ring-width chronologies built at the three studied sites. Just to show long-term fluctuations, 50-year smoothing splines fitted on raw (thin black lines) and standard (thick black lines) are depicted. Sample depths are shown as grey areas (right axis).

Figure 3

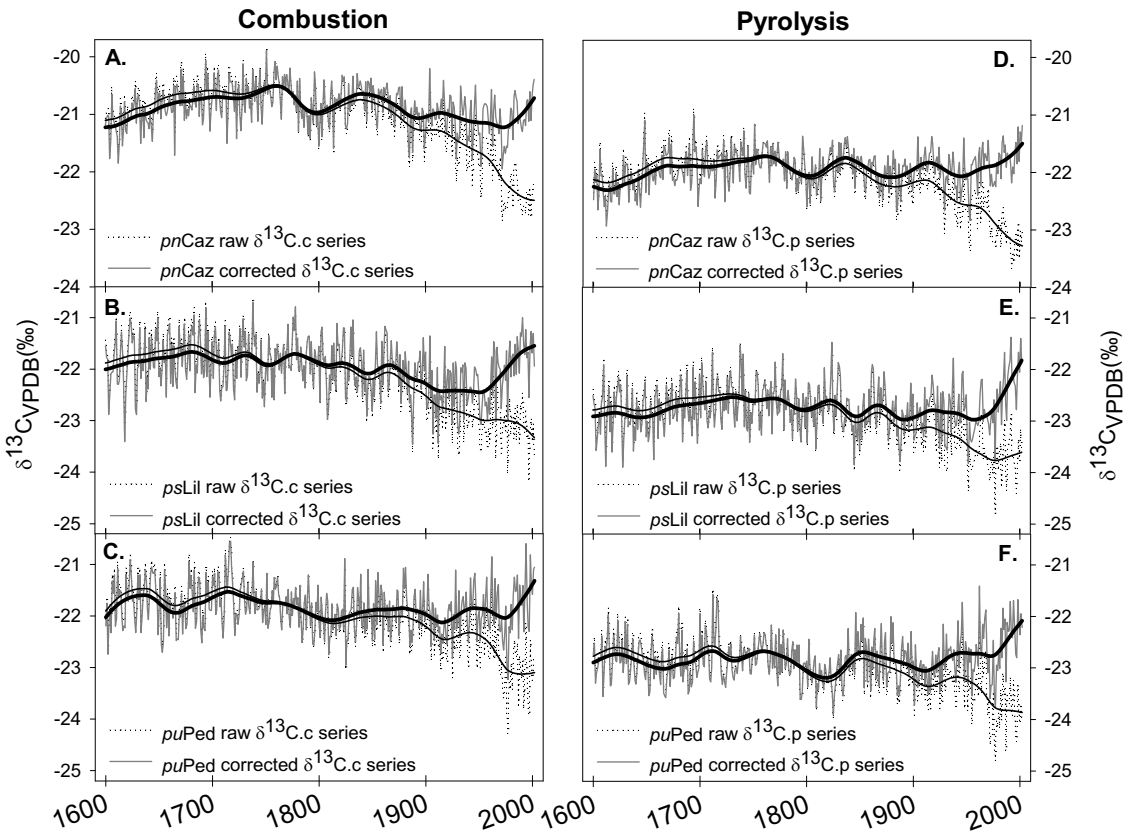

Raw (dotted) and corrected (grey lines) $\delta^{13}C$ tree-ring chronologies built at the three studied sites. Just to show long-term fluctuations, 50-year smoothing splines fitted on raw (thin black lines) and corrected (thick black lines) $\delta^{13}C$ series are depicted. $\delta^{13}C$ tree-ring chronologies analyzed by combustion are noted by $\delta^{13}C.c$ (A-C) and by pyrolysis by $\delta^{13}C.p$ (D-F).

Figure 4

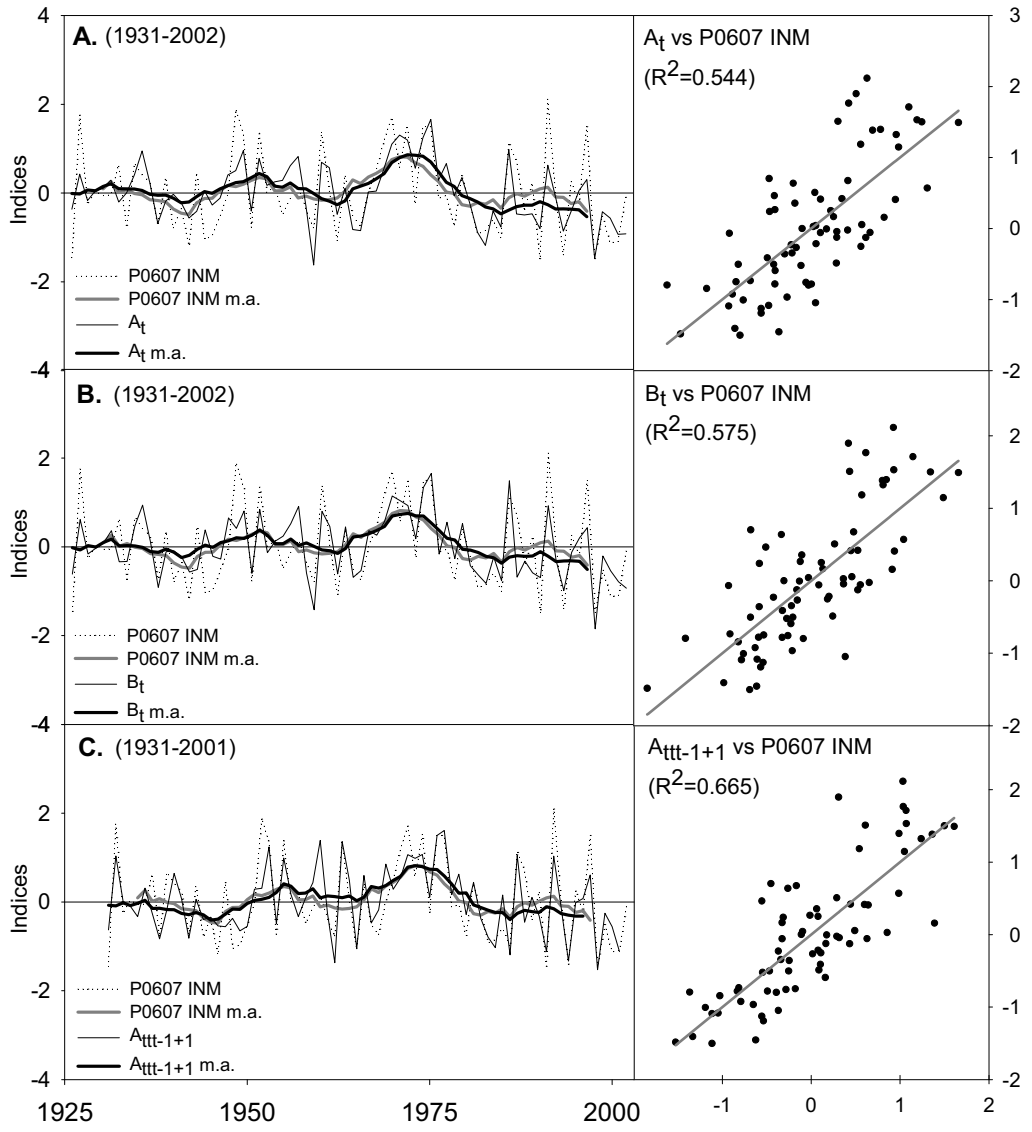

Trends and R^2 of P0607 INM data versus the three different set of proxies: A_t (A) B_t (B) and $A_{ttt-1+1}$ (C) for the calibration period. A moving average of 10-years (m.a.) was applied to highlight the trends of these series.

Figure 5

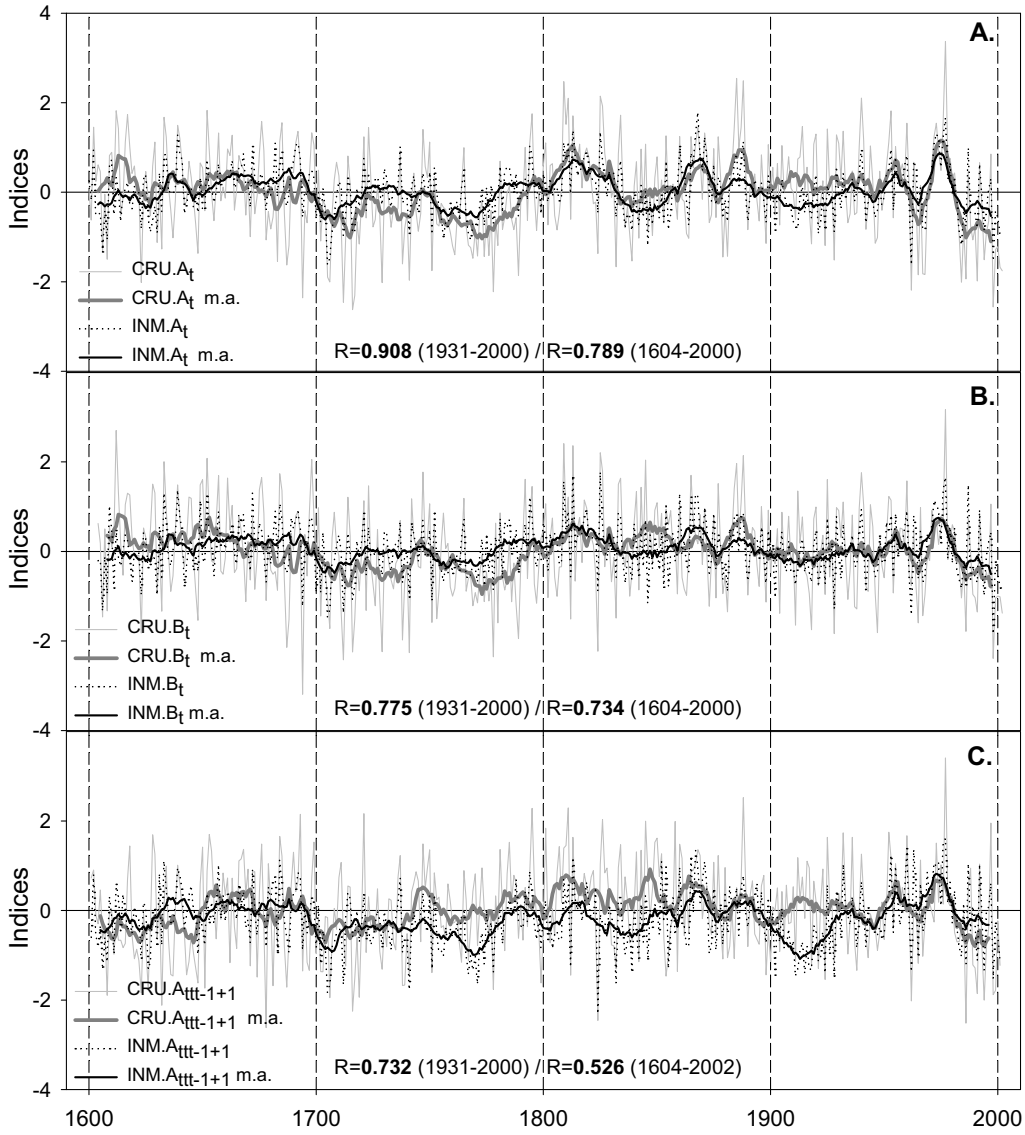

Reconstructions of P0607 INM and P0607 CRU built with the three different set of proxies A_t (A) B_t (B) and $A_{ttt-1+1}$ (C). A moving average of 10-years (m.a.) was applied to highlight the trends of these series. Correlations between both reconstructions for two different periods are indicated.

Figure 6

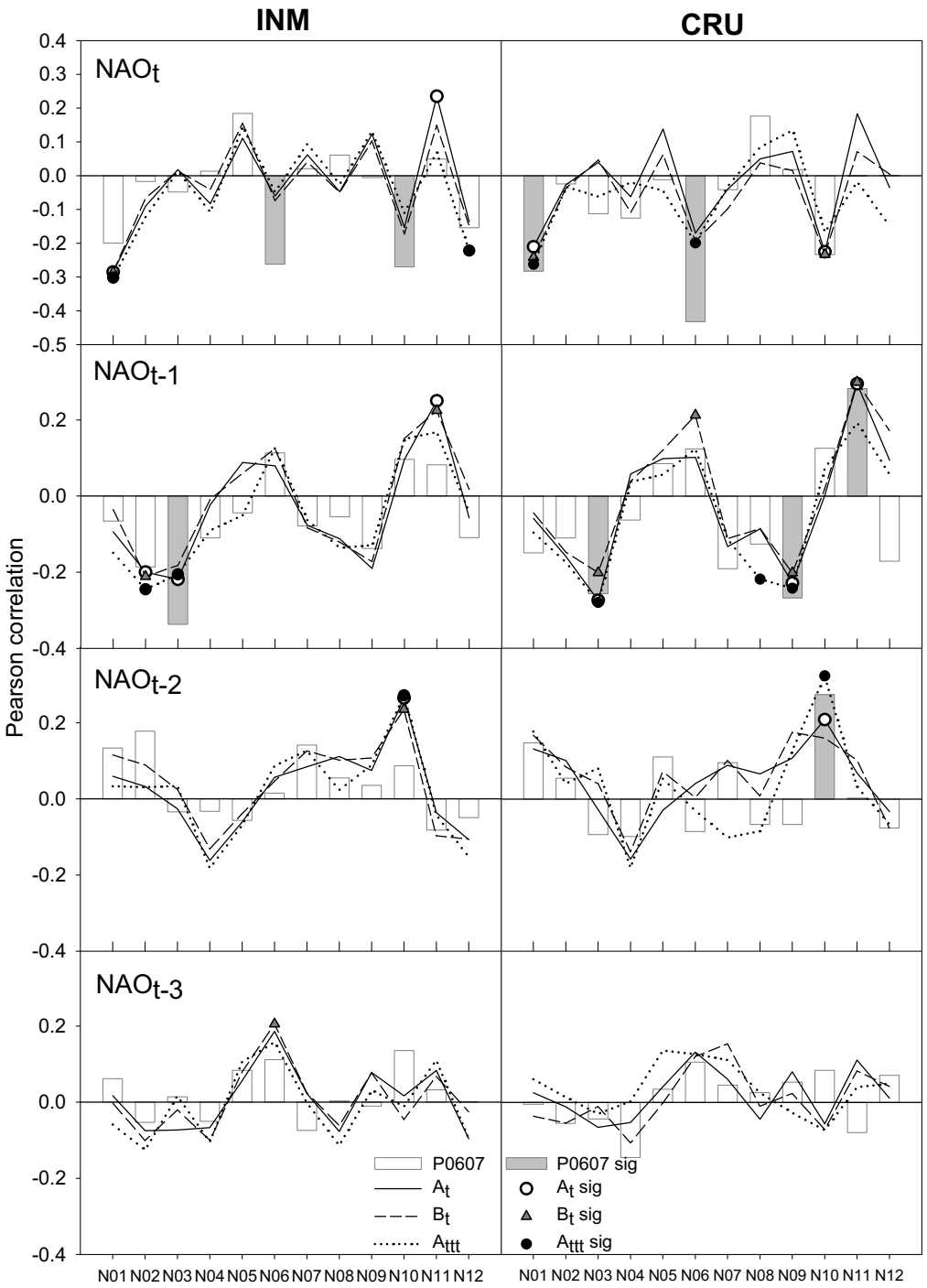

Pearson correlation between monthly NAO indices using several temporal lags (t-1, t-2, t-3) versus P0607 instrumental data from 1931 to 2000 (bars) and P0607 reconstructions from 1900 to 2000 (lines). Significant Pearson correlations ($p<0.05$) are indicated with grey bars and symbols.

Figure 7

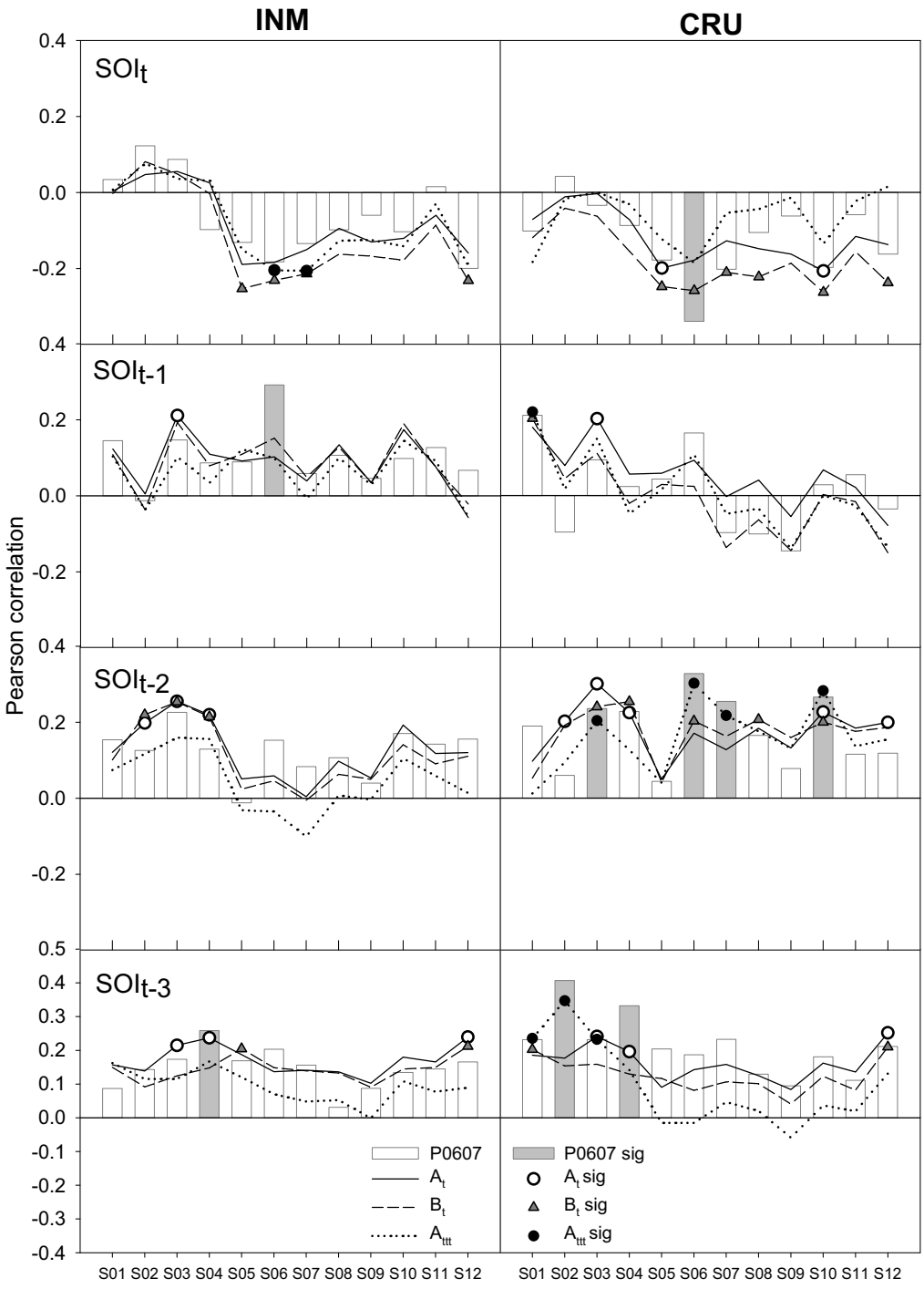

Pearson correlation between monthly SOI using several temporal lags (t-1, t-2, t-3) versus P0607 instrumental data from 1931 to 2000 (bars) and P0607 reconstructions from 1900 to 2000 (lines). Significant Pearson correlations ($p<0.05$) are indicated with grey bars and symbols.